To Mom and Dad

Foamer evaluation by the sparging test method for application to gas well deliquification

MSc THESIS

Author:
Shrey Joshi (4331672)
Track:
Solid and Fluid Mechanics

Supervisors:
Ir. Pejman Shoeibi Omrani (TNO)
Prof. dr. ir. R.A.W.M. Henkes

27th October 2014 - 8th July 2015

Faculty of Mechanical, Maritime and Materials Engineering (3mE)
Delft University of Technology

Contents

List of figures

List of tables

Abstract

Natural gas wells produce small amount of liquids along with the gas. During the initial part of the reservoir life, the gas velocity in the well tubing is large enough to drag the liquid upwards. As the well matures, the reservoir pressure starts to decline leading to a decline in the gas velocity in the tubing; here the gas momentum is not enough to carry the liquid to the top and the liquid starts to accumulate at the bottom of the well. One of the ways to remove the liquid is the use of foam assisted lift technique where surfactant is injected downhole and turbulent mixing between the gas and the liquid generates foam which can easily be transported by the gas to the surface.

However, the liquid produced in a gas well may differ from well to well. Depending on the fluid composition (gas, condensate, water) and the physical conditions of the well, a surfactant may or may not be able to remove the liquid from the bottom of the well. Hence it is imperative to evaluate the surfactant before its use. There are various methods available to evaluate a surfactant; one of the prominent methods is a small scale sparger test, where gas is injected into a surfactant solution to generate foam. We attempt to understand the foam behaviour in the small scale setup and we will use the insights to possibly standardize surfactant evaluation.

The present work focusses on understanding the effect of three parameters on the foam generated in a small scale sparger setup, namely: gas velocity, surfactant concentration and pressure. We conduct three tests for each variation of the above three parameters, namely: build-up test, collapse test and carryover test. Two commercial surfactants: Foamatron and Trifoam Block 820 have been studied in the present work. In addition to these measurements, the characteristics of the dynamic surface tension of the surfactants are measured by using the maximum bubble pressure method.

Increasing the pressure (in the range of our measurement) is found to have a stabilizing effect on the foam but it does not seem to directly affect the ability of the surfactant to unload liquid. The amount of foam formed in the small scale test strongly correlates with the gas velocity but is found to have a weak correlation with the surfactant concentration. Even though the hydrodynamics of the flow differ between the test scale and the flow loop scale, the small scale tests can still give important information which can help in evaluating surfactants. To be more specific, the carryover test is found to have similar trends as with data from intermediate scale tests (i.e. flow loop test) in context of ability of surfactant in unloading liquid. However the

results from the flow loop scale suggest that the small scale sparger setup is not a good predictor in terms of pressure drop.

We find that for an increasing velocity in the small scale setup, we operate within two flow regimes: bubble flow and slug flow. We recommend conducting the test in the slug flow regime which is closer to the actual hydrodynamics in the gas wells during liquid loading (churn flow). However, there are certain limitations to conducting the test in the slug flow: since the gas velocities are high the limit of carryover could affect the interpretation of results.

Chapter 1 Introduction

Liquid loading is one of the prominent issues in matured gas wells and its relevance will even increase in the near future as more and more gas wells will reach their end of field life stage. Simply put, the inability of the produced gas to remove the produced liquid from a well is called liquid loading. However, the actual problem is fairly complicated. If the produced liquid cannot be removed naturally by the produced gas, it starts to accumulate in the wellbore which either reduces the gas production or at times even completely halts it. To understand the problem of liquid loading it is imperative to understand the interaction of the liquid and the gas phase in a vertical conduit under flowing conditions. This chapter will give an overview of flow regimes in a vertical conduit, a brief description of liquid loading problem with present solutions and the scope of the present work.

1.1 Multiphase flows in vertical conduits

There are broadly four regimes which have been identified in a vertical conduit with liquid and gas flowing together. The demarcation between various regimes is ultimately based on two factors: the velocity of the two phases and the relative amount of each phase in the conduit (holdup). Figure 1 shows the four different regimes of a two-phase flow in a vertical conduit:

1) **Bubble flow:** This regime will occur when the liquid holdup is high (liquid is the continuous phase) and the gas flows through the liquid in form of bubbles at low velocity. This situation would be encountered when liquids fill the bottom of the well, and the production in such condition will be difficult.
2) **Slug flow:** When the gas throughput increases, there are more bubbles in the liquid and they coalesce to form large bubbles in between liquid slug bodies; this is called slug flow. Both the liquid slug body and the gas bubble (with surrounding liquid film) contribute to the pressure drop. This condition is also indicative of liquid accumulation at the lower part of the well bore but the production rate of gas is higher than that of bubble flow.
3) **Churn flow (slug-annular transition):** The continuous phase in this regime changes from liquid to gas. The liquid is mostly accumulated at the wall with chunks of liquid entrained in the gas phase. The pressure drop can majorly be attributed to the hydrostatic

component, but the gas phase also has some contribution. This condition indicates the onset of liquid loading in the gas well; this can decrease the production significantly.

4) **Annular-mist flow:** The gas phase is the continuous phase; significant amount of the liquid is entrained in the gas in form of mist (small liquid droplets). Some of the liquid forms a thin layer at the wall and the pressure gradient is determined predominantly from the gas phase. This condition is mostly observed when the gas well is in its early phases and liquid does not accumulate in such conditions.

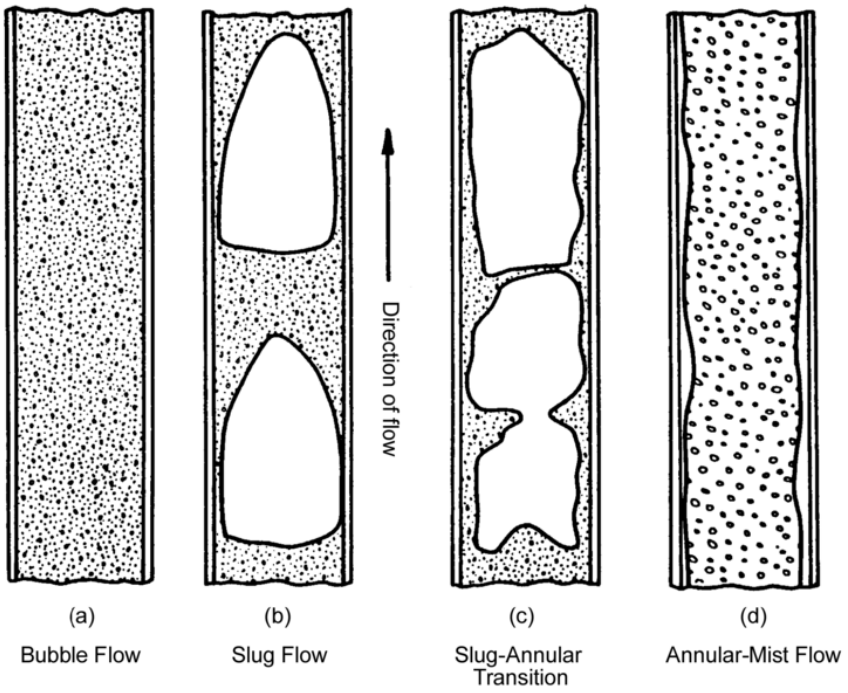

Figure 1: Various multiphase flow regimes in a vertical conduit.

1.2 Liquid loading in wells

A natural gas reservoir produces wet gas (wet refers to some liquid, condensate/water, along with gas). As the reservoir becomes older, the reservoir pressure declines and the gas velocity in the production tubing in the well is not sufficient enough anymore to carry the liquid to the top. Thus liquid is unable to go to the top and it starts accumulating in the well; this can affect the reservoir production and may at times lead to shut down of the well.

A high gas velocity generates a mist flow pattern with liquid droplets finely dispersed in the gas. This results in a low percent by volume of liquids present in the tubing (i.e., low liquid "holdup")

and, as a result, there is a low pressure drop due to the hydrostatic component of the flowing fluids. A well flowing at a high gas velocity can have a high pressure drop due to friction but the component of the pressure drop due to accumulated liquids in the conduit is relatively low. As the velocity of the gas in the production conduit drops with time, the velocity of the liquids carried by the gas decreases even faster. As a result, liquids begin to collect on the walls of the conduit, liquid slugs begin to form, and eventually liquids accumulate in the bottom of the well, adding to the percent of liquids in the conduit while the well is still flowing. The presence of more liquids in the production conduit while the well is flowing can slow or even stop gas production altogether.

Liquids can accumulate in a well through a variety of mechanisms. Often gas wells produce liquids directly into the wellbore. In some cases, both hydrocarbons (condensate) and water can condense from the gas stream as the temperature and pressure change during travel to the surface. Liquids can also come into the wellbore as a result of coning water from an underlying zone as well.

1.3 Present solutions for liquid loading

There are a number of methods used to deliquify a well. As mentioned in [1] some of them are: gas lift, plunger lift, Hydraulic pumps, methods like electrical submersible pumps, gas lift, or other pumps might be effective in tackling the problem, the cost aspects are not very appealing. On the other hand use of foams has proved to be effective in terms of cost as well as effectiveness in deliquifying wells. The present study is focused on the use of surfactants to create foam in order to deliquify the well. The next section briefly describes the method of using foam for deliquification of wells.

1.4 Deliquification using foams

Foams have several applications in oil field operations. They are used as a circulation medium for drilling wells, well cleanouts, and as fracturing fluids. These applications differ slightly from the application of foam as a means of removing liquid from producing gas wells. The former applications involve generating the foam at the surface with controlled mixing and using only water. In gas well liquid removal applications, the liquid-gas-surfactant mixing must be

accomplished downhole and often in the presence of both water and liquid hydrocarbons. The principal benefit of foam as a gas well dewatering method is that liquid is held in the bubble film and exposed to more surface area resulting in less gas slippage and a low-density mixture. The foam is effective in transporting the liquid to the surface in wells with very low gas rates when liquid holdup would otherwise result in sizable liquid accumulation and/or high pressure loses. Surface active agents (surfactants) generally are employed to reduce the surface tension of the liquid to enable more gas-liquid dispersion.

In recent years, foaming agents have been applied broadly with success as a means of artificial lift and for unloading loaded wells. Foam-Assisted Lift (FAL) has become an integral part of extended production plans for many wells considered to be marginal producers. Foaming agents have been used globally for removal of liquid from loaded wellbores for many years. In some areas, liquid and/or powdered detergents also have been utilized to create foam for liquid removal from a wellbore. Recent applications indicate that FAL can not only be an integral part of mature production, it can also be utilized on adolescent producers to improve production rates by returning wells to their unconstrained production potential. With gas consumption becoming an increasingly more important part of global energy supply, producers are focusing on efforts to support the demand by increasing production from all wells.

An effective FAL program must have a foaming agent suitable for completion of the task. Testing must be conducted on fluid from each well in order for a program to achieve a sustainable and/or substantial increase in production. Foaming agents are not all the same, they will perform differently on fluid of varying compositions. Surfactant that works on given well may or may not be effective when used in other wells. The mechanism of foam formations and the flow of foams itself might as well differ from well to well. In order to effectively use FAL it becomes imperative to conduct detailed studies on performance of foamers under different conditions and compositions. Understanding the mechanism of foam formation and its stability under different flow regimes could prove handy in deciding the best FAL program for each well. For this purpose various tests can be conducted at different scale to understand the behavior of foam. These tests can be conducted at different scales and one the common test to evaluate foamer is the sparger test where gas is sparged through a column of liquid in order to produce foam.

1.5 Scope of the present study

The present work is part of a joint industry project on "experimental evaluation foam" at TNO in collaboration with industrial partner: EBN, NAM, TOTAL, GDF SUEZ, ONE and TAQA. The objective of the work at TNO is to standardize methodology to evaluate different foamers, improve the link between selection and field quantification of the deliquification measure of foamers. The present thesis is a part of the project and is focused on using small scale foam evaluation setup (sparger test) to study effects of various physical parameters. This section will describe the research questions and the objective of the thesis.

Research question:

- How do different parameters (gas velocity, pressure, concentration of surfactant) affect the foamer evaluation method for deliquifying gas wells?
- How can these results contribute to standardizing foamer evaluation methods?

Objectives:

Understanding the effect of dynamic conditions on foamability (i.e. foam density) and foam stability in small scale setup by:

- Investigating the effect of following parameters on the foam behavior
    - Sparging gas velocity
    - Pressure
    - Surfactant (composition and concentration)
- Identifying the relevance of these parameters in context of foam quality and stability.
- Using the insights obtained with the study to make recommendations regarding standardizing foamer evaluation methods.

Chapter 2 Literature review

This chapter will present an overview of the scientific literature relevant to the thesis. This chapter is divided into three sections. The first section describes the surface chemistry which includes a brief description of different types of surfactants, mechanisms of surface tension reduction and relevance of equilibrium and dynamic surface tension. The second section emphasizes on the following aspects of foams: morphology, coarsening, coalescence and drainage in aqueous foams. The formation of foam in gas wells is a result of complex hydrodynamics between gas and liquid flowing together through the well. While studying foams in lab conditions there are various methods used to generate foams. The third section would focus on the use of foam for deliquifying gas wells, various methods of foam generation and the different methods presently in use to evaluate foamers.

2.1 Surface chemistry

A surfactant is a substance that when added in small amounts to liquid, tends to adsorb at the interfaces or surfaces and reduces the surface tension, thus also reducing surface energies of the surface by a marked value. To understand foams it is important to understand the concept of characteristics of a surfactant, surface tension and the mechanisms behind surface tension reduction by a surfactant.

2.1.1 Characteristics of surfactant and surfactant solution

As mentioned above addition of small amounts of surfactants to liquid introduces a completely new dimension to properties of such solutions. It is hence important to understand the properties of these surfactants and also the surfactant solutions.

A surfactant molecule consists of a hydrophilic and a hydrophobic part as shown in Figure 2. The hydrophobic part or tail is generally a long-chained hydrocarbon residue and less often a halogenated or oxygenated hydrocarbon or siloxane chain; the hydrophilic group or the head is an ionic or highly polar group. Depending on nature of hydrophilic part, surfactants are classified as mentioned in [1]:

1) **Anionic**: The surface active portion of the molecule bears a negative charge, for example, $RCOO^-Na^+$ (soap), $RC_6H_4SO_3^-Na^+$ (alkyl benzene sulfonate).

2) **Cationic**: The surface-active portion bears a positive charge, for example, $RNH_3^+Cl^-$ (salt of a long chain amine), $RN(CH_3)_3^+Cl^-$ (quaternary ammonium chloride).
3) **Zwitterionic**: Both positive and negative charges may be present in the surface active portion, for example, $RN^+H_2CH_2COO^-$ (long chain amino acid), $RH^+(CH_3)_2CH_2CH_2SO_3^-$ (sulfobetaine).
4) **Nonionic:** The surface-active portion bears no apparent ionic charges, for example, $RCOOCH_2CHOHCH_2OH$ (monoglyceride of long chain fatty acid), $RC_6H_4(OC_2H_4)_xOH$ (polyoxyethylenated alkylphenol), $R(OC_2H_4)_xOH$ (polyoxyethylenated alcohol).

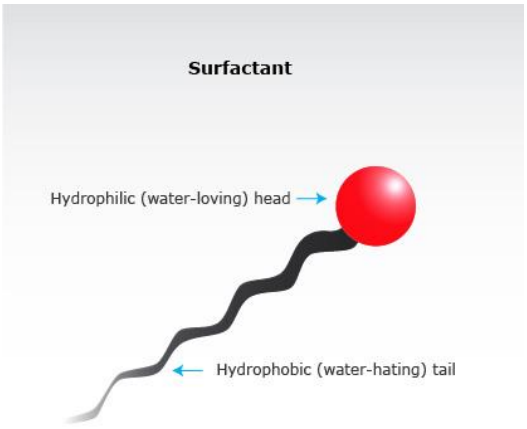

Figure 2: A typical surfactant molecule with a hydrophilic head and hydrophobic tail.

The question still is how does this surfactant molecule help in reducing surface tension of a solution and improving its stability? The stability of an isolated film is defined by the concept of disjoining pressure. A film consists of two interfaces; the interaction between the two due to electrostatic forces, the van der Waals forces etc. dictate the force between the two interfaces. For thin films the interaction leads to a repulsive force between the two interfaces and the external pressure counters this force. The disjoint pressure is thus defined as $\Pi = P(h) - P(\infty)$, where $P(h)$ is the repulsive force for a film thickness h and $P(\infty)$ is the external pressure. The film is stable if the disjoint pressure is greater than zero and unstable if it is less than zero. When this surfactant molecule adsorbs at the interface, the interaction between the surfactant molecules leads to a higher repulsive force $P(h)$, hence a more stable film is formed with lower surface tension. The reduction in surface tension is in general a dynamic process involved while the formation of a new surface occurs. When a fresh interface is created, say in water, it consists

only of water molecules and $\gamma = \gamma_{pure}$, pure solvent (for water, 72.8 mN/m). In time, surfactant molecules get adsorbed on the surface, which reduces the surface tension.

2.1.2 Equilibrium surface tension

The surface tension of a newly formed surface in a surfactant solution depends on a number of factors, one important factor being the number of surfactant molecules that attach to the surface. The attachment of the molecules has two stages, one where it travels through the liquid to the surface: diffusion and the other where it gets attached to the surface: adsorption as shown in Figure 3. If the time scale of bubble formation plus residence in the liquid (amount of time the new surface stays in the solution) of a surface is greater than the time taken for diffusion and adsorption, the surface would adsorb the maximum number of surfactant molecule and will experience a maximum reduction in surface tension and that value is called the equilibrium surface tension.

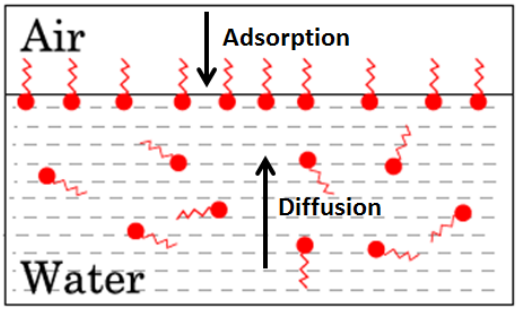

Figure 3: Schematic showing diffusion and adsorption of surfactant molecules (source: [2]).

Hence in order to theoretically quantify such a value we need to quantify the adsorption to the surface under a given condition. Adsorption can be quantified by using an isotherm which is an equation relating the bulk concentration to the corresponding surface excess concentration (Γ). It is derived from fundamental thermodynamic principles. However, in order to obtain surface excess concentration from experimentally accessible parameters, surface tension (γ) and bulk concentration (c), a surface equation of state is required in addition to the isotherm such as Gibbs isotherms. A surface equation of state can be conceptually compared with an equation of state for gasses as shown in [3], such as the ideal gas law. A monolayer of surfactants exhibit surface pressure, Π (mN/m), with the dimension of force per length, one length dimension less than the bulk pressure. A 3D equation of state relates the bulk gas pressure and the concentration;

similarly, a 2D surface equation of state for surfactants is a relation between their surface pressure, $\Pi = \gamma_0 - \gamma$ and surface excess concentration (i. e. Γ), γ_0 is the surface tension of water devoid of any surfactants. The adsorption isotherms and the surface equations of states can be derived from thermodynamics as given in [4].

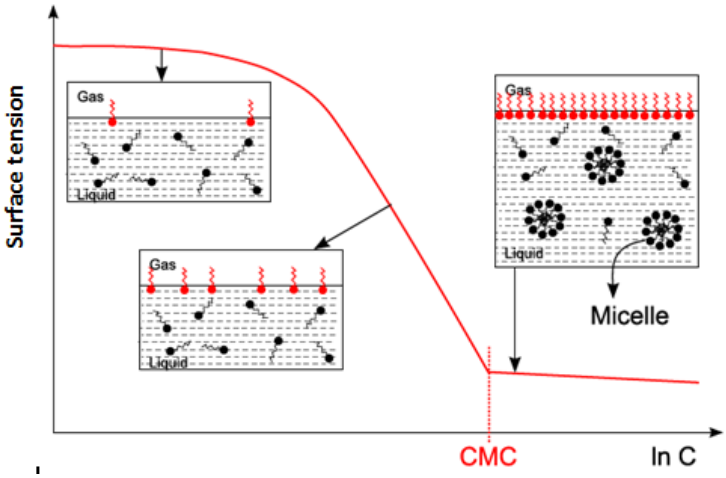

Figure 4: Sketch of equilibrium surface tension as a function of surfactant concentration with schematic of molecular phenomenon (source: [2])

Critical micelle concentration (CMC)

The micelle formation property of surfactants means that a surface active solute forms colloidal-sized clusters in solutions as shown in Figure 4. This is interpreted as a point of formation of micelle from the unassociated molecules of surfactant, with part of the charge of the micelle neutralized by associated counter-ions. The concentration at which this phenomenon occurs is called critical micelle concentration (CMC). In context of the present study CMC is important in regards to the surface tension. As shown in Figure 4 increasing the concentration decreases the equilibrium surface tension, but after the CMC the change in surface tension is observed to be slow compared to before CMC.

Figure 5 (a-d) depicts how surfactant helps in forming and stabilizing an interface. Figure 5 (a) shows a typical foam structure. The extent of gas-liquid surface area per unit volume possible in foam is greater than that in comparison to most two-phase systems. Thus the foam films are thermodynamically unstable as the free surface energy is large and hence do not sustain for a long period of time as suggested by [5]. However the presence of surfactants stabilizes the foam films, making them metastable. The adsorption of surfactant molecules as shown in Figure 5 increases the stability of films. As noticed by [6] that for an interface with adsorbed surfactant, a

change in its surface area causes a change in its surface tension. If an interface expands, the surface concentration of surfactant decreases, consequently the surface tension increases. This is known as the Gibbs effect. A perturbed interface will relax over time to its equilibrium surfactant surface coverage. During the relaxation period the surfactant will be transported to or from the perturbed surface.

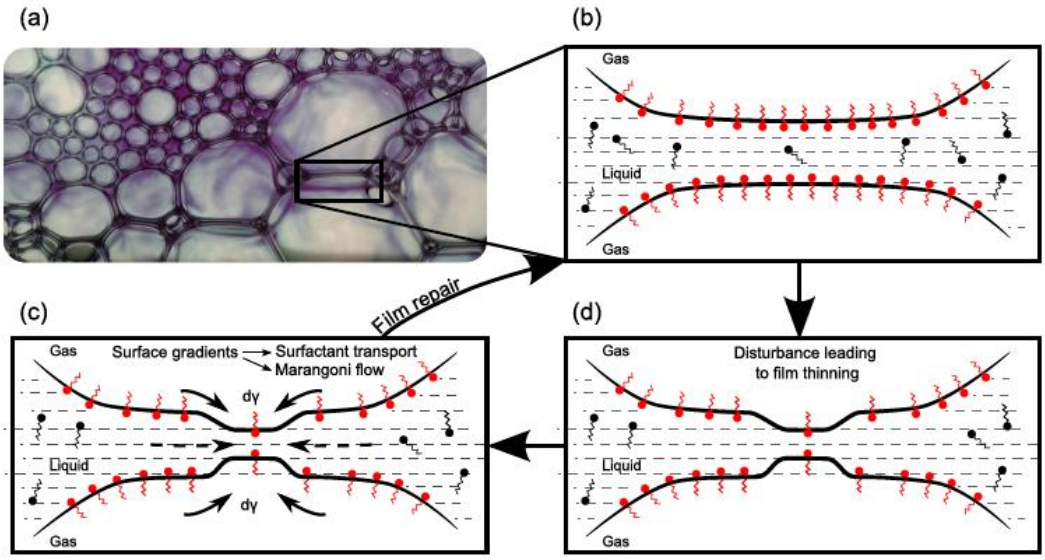

Figure 5: Film repair mechanism by Marangoni effect (source: [2]).

A foam film (Figure 5 (b)) subjected to disturbance leading to film thinning is seen in Figure 5 (d). Film thinning leads to an increase in the local surface area. As explained in [6] the surface tension at the locally thinned region is higher than at the surrounding regions. These surface tension gradients over the thinned region causes Marangoni flows from the region of low surface tension (or a region with higher concentration of surfactant molecule at the surface) to high surface tension (thinned film region with low concentration of surfactant molecule). These Marangoni flows transport liquid mass to the thinned film, thus stabilizing it. Thus these Gibbs-Marangoni effects assist in repairing the thinned film. In the case of local thinning within foam films, the Gibbs effect is followed by the relaxation period. The relaxation period includes transport of surfactant molecules due to concentration gradient, and the transport of surfactant via the Marangoni flows. Adsorption of new surfactants from the bulk to the part of the interface with increasing surface tension should be sufficiently slow, to allow Marangoni flow to repair the film. Very fast surfactant adsorption does not allow the creation of surface tension gradients.

Successful film repair requires that sufficient liquid mass is transported to the thinned region before the surface tension gradients disappear.

2.1.3 Dynamic surface tension

The reduction in surface tension reduction is directly proportional to the number of surfactant molecule that occupies the newly formed surface. If the time scale of diffusion to the surface and adsorption is larger than the time scale of the formation plus residence of a new surface, the maximum number of molecules adsorbed at the surface is less than the maximum number of molecule that can adsorb under equilibrium. This does not let the surface tension drop down to its equilibrium value and hence is termed as dynamic surface tension (DST). The dynamic surface tension of a newly formed surface is dependent on the surface excess concentration of the surfactant. Figure 6 show the variation of surface tension with time, a typical plot contains four regions:

I. Induction region
II. Rapid fall region
III. Meso-equilibrium region
IV. Equilibrium.

The following equation fits the first three regions of the plots (Figure 6) as shown by [7]:

$$\gamma_t = \gamma_m + \frac{\gamma_0 + \gamma_m}{[1 + (t/\,t^*)^n]}$$

Where γ_t is the surface tension of the surfactant solution at time t, γ_m is the meso-equilibrium surface tension, after this the surface tension shows only a small change with respect to time. γ_0 is the surface tension of a pure solvent. The value of t^* is the time required for γ_t to reach half of the difference between γ_0 and γ_m. Here n is a constant related to the molecular structure of the surfactant, as suggested by [8] that n is related to difference between the energies of adsorption and desorption of the surfactant.

The time scale (t_i) for the induction period is an important characteristic of a surfactant since the surface tension would drop only after this time scale. As shown by [8] and [9] t_i is related to the surface coverage of air-aqueous solution interface and to the apparent diffusion coefficient, D_{ap} of the surfactant, calculated using short time approximation of the Ward-Tordai equation for diffusion-controlled adsorption. An important aspect of surfactant solutions is their property to

form micelle and hence provides a CMC where after the surface tension decrease at a low pace on increasing surfactant concentration. This is true when the surface is under equilibrium (slow process of surface formation). However under more dynamic condition when DST plays important role the CMC value is not always the concentration after which surface tension decreases at a slow pace on increasing surfactant concentration. As reported by [10] the critical concentration at which surface tension starts to decrease relatively slowly will increase with decreasing time scale of surface formation. To understand the effect, $\gamma_{1\text{-}s}$ was defined which means the reduction of surface tension when surface forms in 1 second. The data with surface time corresponding to equilibrium and meso-equilibrium time scales was plotted. Figure 7 shows a plot from [10] that shows the critical concentration increases with decreasing time scales.

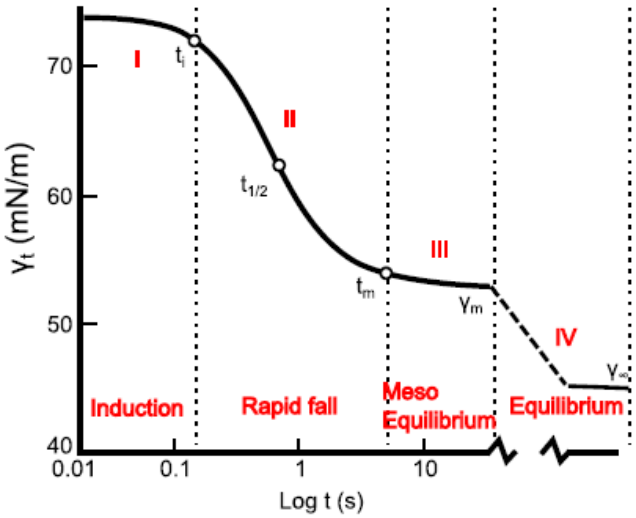

Figure 6: Typical dynamic surface tension curve with respect to time (source: [2]).

This increasing critical concentration becomes important in applications such as gas well deliquification because the time scale of bubble formation is generally small and DST plays an important role. The higher the bubble frequency the higher is the concentration required to observe a certain drop in surface tension. This becomes helpful in deciding what bulk concentration of the surfactant is required in order to optimize surfactant performance.

2.1.4 Rosen parameter

Rosen and co-authors have published a series of eight papers on dynamic surface tension and related topics ([8], [7], [9], [10], [11], [12], [13] & [14]). As mentioned in section 2.1.2 a typical DST curve can be fitted in a certain equation. The time gradient of that equation is as follows:

$$\frac{d\gamma}{dt} = \frac{(\gamma_0 - \gamma_m)[n(t/t^*)^{n-1}]}{t^*[1+(t/t^*)^2]^2}$$

As shown in [11] the gradient of dynamic surface tension with respect to time is maximum at $t = t^*$, and the maximum value of the gradient is given by:

$$\frac{d\gamma}{dt} = \frac{n(\gamma_0 - \gamma_m)}{4t^*}$$

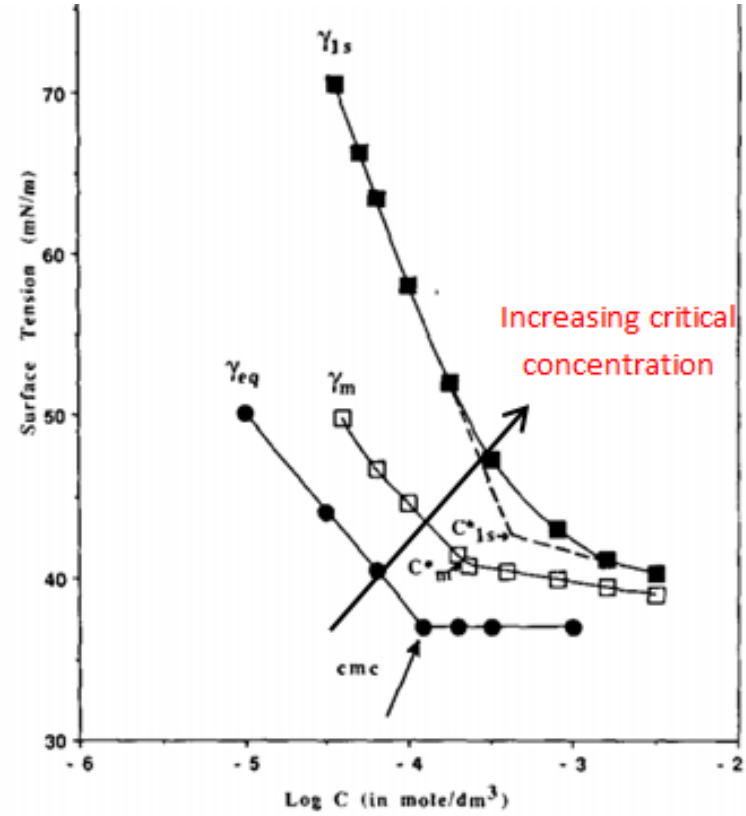

Figure 7: Plots of $\gamma_{1\text{-}s}$, γ_{eq} and γ_m vs log of surfactant concentration in bulk.

The expression on the right hand side of the above equation is supposed to correlate with the foamability and the strongest correlation was shown by [11]. This parameter was further studied in Refs [15] and [16] to understand its relation with foamability. An increase in the Rosen parameter was shown to be inversely proportional to the maximum weight of foam produced by [15] and the initial foam height in the Ross-Miles test by [16]. This is contradictory to the results

found by [11]. It was suggested that an increase surface tension reduction rate, decreases the foamability because a rapid surfactant transfer to interface does not allow creation of sufficient magnitude and duration of surface tension gradients for the healing action by the Marangoni effect.

2.2 Foam

This section describes the important characteristics of foams: foam morphology, coarsening and coalescence, drainage and events that lead to foam collapse. But it is important to understand what makes foams fundamentally different from most multi-phase systems and how that is useful for certain applications.

Aqueous foams are concentrated dispersions of gas bubbles in a surfactant solution. Their structures are organized over a large range of length scales, from the size of a bubble down to the scale of the surfactant molecules adsorbed on liquid-gas interfaces. Surfactants confer specific rheological properties to the interfaces that are coupled to the flow of the underlying bulk liquid. The interplay between capillary and gravitational forces plays an important role in defining the stability of these foams at the scale of the liquid channels (plateau border) formed due to the meeting of these films. Aqueous foam such as the one from shampoo or in beer is a multiphase mixture that generally exhibits several physical properties that makes it appropriate to be used in diverse industrial applications. Some of these properties of foam as mentioned in [17] are listed below:

- **High specific surface area**: The extent of gas-liquid surface area per unit volume possible in foam is greater than that in comparison to other two-phase systems. This property makes aqueous foam attractive for interphase mass transfer operations. Examples of such processes are froth floatation, where valuably hydrophobic particles are recovered from slurry, the recovery of oil sands and the stripping of gases from effluent by absorption into the liquid phase.
- **Low interphase slip velocity**: The slip velocity between gas and liquid phase is the relative velocity between the two phases and this is typically much smaller in foam then in a bubbly gas liquid mixture. The larger specific area in foam is able to impart a relatively larger amount of shear stress on the liquid phase, thereby limiting the slip velocities between phases (phases mean the liquid and the gas in the foam). A high contact time between the two phases

can be engendered, which can also enhance amount of mass transfer from liquid to gas, gas to liquid or liquid to interface.

- **Large expansion ratio**: Because the volumetric liquid fraction of foam can be very low, the expansion ratio (i.e. the quotient of total volume and the volume of liquid used to create that foam) can be very high. The property is harnessed in the use of the material for fighting fires and to displace hydrocarbon from reservoirs
- **Finite yield stress**: Because gas-liquid foams can support a finite shear stress, they are effective for use in delivering active agents contained in liquid in household and personal care products (such as bathroom cleaner and shaving foam), as well as in topical pharmaceutical treatment.

Thus, the geometric, hydrodynamic and rheological properties of gas-liquid foam can be harnesses to make it a uniquely versatile multiphase mixture for a variety of process applications and product design. One such application of aqueous foam is to avoid production decline from gas wells in case of liquid loading.

2.2.1 Foam morphology

Foams in terms of morphology are basically divided into dry and wet foams. The classification is based on the liquid content per unit volume of foam and quantified as liquid volume fraction (ϕ). As shown in Figure 8, wet foam typically consists of spherical gas bubbles suspended in a liquid (closely packed spheres). The liquid volume fraction generally varies from 20-30% for wet foam.

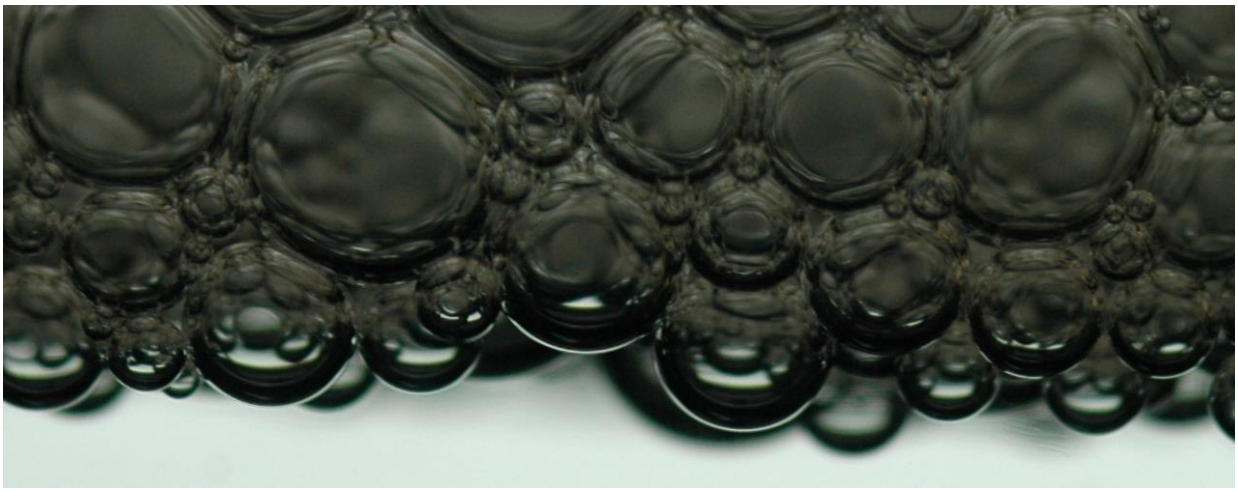

Figure 8: Typical wet foam with spherical gas bubbles suspended in liquid.

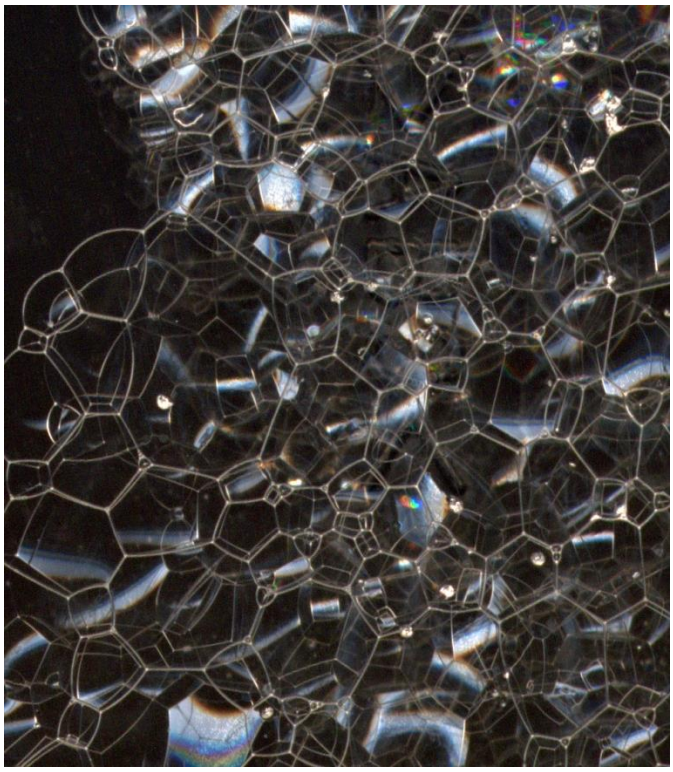

Figure 9: Structure of typical dry foam.

On the other hand, dry foam has an entirely different structure and resembles a classic paradigm's of nature's morphology: the division of space into cells. In dry foam the liquid film between two bubbles can be idealized as infinitesimally thin curved surfaces. These surfaces are not simply spherical but constitute faces of a polyhedral cell. These surfaces are subject to the following important rules, first stated by [18]:

- Faces must meet three at a time. The angles they meet must be 120 everywhere such that three cells are joined symmetrically at a cell edge.
- Edges must meet four at a time. The angles between edges are 109.43 degrees, the Maraldi angle, where six cells meet symmetrically at every corner.

In Figure 9 white lines can be observed to follow the first rule that the faces meet three at a time. These lines are channels formed by three faces meeting and are called plateau borders. A schematic of a plateau border is shown in Figure 10; these channels are where most of the flow inside foam occurs and hence are important in deciding the stability of foam.

2.2.2 Drainage in foams

Foam drainage is a complex physio-chemical hydrodynamic process governed by many simultaneous factors; it is the flow of liquid through the interstitial spaces between bubbles. The flow at the scale of interstitial spaces is a result of the capillary, gravity and viscous forces acting on the liquid. The interstitial space can be divided into three categories:

1. Films that form between two bubble and are bounded by almost flat bubble surfaces
2. The plateau borders that are channels formed wherever the films meet in configuration of three by three
3. The nodes or junctions which form where four plateau borders meet.

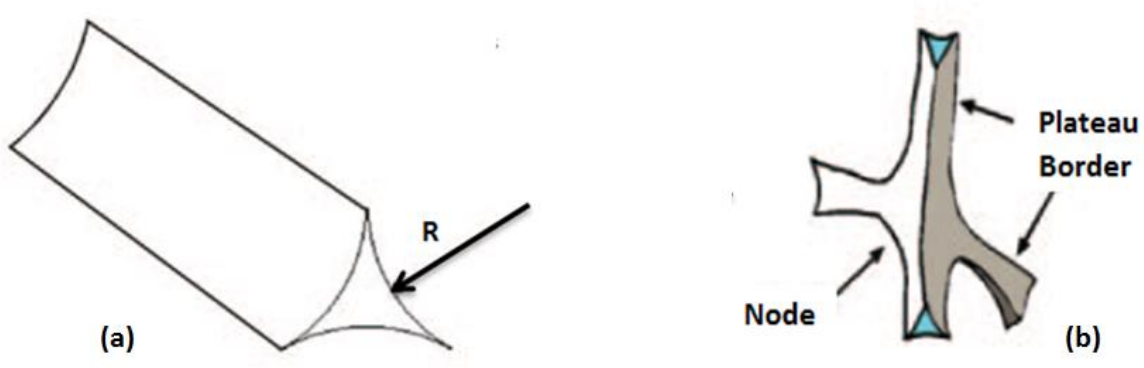

Figure 10: Schematic showing the plateau border in foam. (Source: [19]).

Figure 10 shows a typical plateau border found in foams. Drainage in foams is one of the most important phenomena which affect the stability of the foam: the larger the drainage rate, the lower the liquid volume fraction of liquid in foam and the higher the probability of the foam rupture. It was observed by [20] that liquid flows mainly through plateau borders in dry foams. The flow of fluid through the network of plateau border consists of two resistances: one through the plateau border which resembles flow through a pipe (although the cross-section of pipe is not cylindrical) and the other is the resistance at nodes where the flow behaves like a plug flow. A criterion was suggested in [21] for the transition between the two regimes of drainage dissipation, the plug flow and the pipe flow regime in the plateau borders. A surface mobility parameter was introduced as $M = 2R\left(\frac{\mu}{\mu_s}\right)$, where μ is the bulk viscosity, μ_s is the surface

viscosity, R is the radius of curvature of the plateau borders and can be estimated by $R \approx a\sqrt{\phi}$, a is the radius of bubble and ϕ is the liquid volume fraction of the foam. Kraynik's model was obtained by neglecting the capillary forces and gave a simple analytical solution for flow through plateau borders keeping the surface mobility factor low (for higher mobility factor the flow transits from pipe flow to plug flow). The model was generalized by including capillary forces mentioned in [22] which are popularly known as the trinity model, eventually [23] included dissipation through nodes as well into the model.

2.2.3 Coarsening and coalescence in foams

The evolution of foam from surfactant solutions is a complicated process but more or less there are two events responsible for evolution of foams. The first process is coarsening where the gas phase is diffused from smaller bubbles to larger ones driven by the difference in Laplace pressure between the smaller and larger bubbles. The other process is the rupturing process where the film between the bubbles starts to break due to reasons which would be discussed in this chapter.

The stability of foam is said to have a direct dependence on the average bubble size in the foam. For example, [24] gave a relation between the bubble-size distribution and the rate of drainage. The enhanced stability of foams with smaller bubbles was explained by a decrease of drainage. It was reported in [25] that a more uniform bubble size distribution and high initial gas volume fraction gave more stable foams. Hence, the discernment of the bubble-size distribution in foam is essential for an improved understanding of the foam properties and the stability of those properties. Moreover, changes in the bubble size distribution can be used to distinguish between the physical processes that contribute to the transformation of foam properties. Consider a set of bubbles of varying sizes in foam. The pressure inside the bubble has an inverse proportionality to the bubble radius. Therefore the pressure inside the smaller bubbles would be higher than that of the larger ones. This leads to diffusion of gas between the bubble and is an important step for the foam to evolve towards a thermodynamic equilibrium. The process leads to shrinkage of bubble less than the average size and growth of bubble above the average size. This leads to the overall increase in the average size of the bubble and it is called coarsening of the foam. The coarsening process is highly dependent on the volume fraction of liquid inside the foam; the increase in average bubble size with respect to time has different formulations in the dry and wet regimes.

For dry foam (typically toward a limit of liquid volume fraction less than 0.1), [26] proposed a 2D solution to the coarsening process; however the analogous to the general equation in 2D foam, the 3D foam equation is as follows:

$$\frac{dV_i}{dt} = -2\sigma k_f \sum_{j=1}^{n} S_{ij}\left(\frac{1}{R_{1,ij}} + \frac{1}{R_{2,ij}}\right)$$

Here gas diffuses through film (i,j), S_{ij}, $R_{1,ij}$ and $R_{2,ij}$ are respectively the area and the two principal radii of curvature of a film (i,j) between two neighboring bubbles i and j, k_f is the effective permeability of a film and is defined as follows:

$$\frac{1}{k_f} = \frac{1}{k_{bulk}} + \frac{1}{k_{ml}}$$

Where, the effective permeability comes from the permeability of the central bulk liquid in the film (k_{bulk}) and the permeability of the two monolayers (k_{ml}).

The analogue of von Neumann's rule has been proposed only very recently by [27] and is as follows:

$$\sum_{j=1}^{n} S_{ij}\left(\frac{1}{R_{1,ij}} + \frac{1}{R_{2,ij}}\right) = 2\pi l_i - \frac{\pi}{3}E_i$$

Where, l_i and E_i are respectively the linear size and total length of edges of bubble i. The von Neumann's law extended to 3D as of now does not have any experimental validity but high speed X-ray tomography studies could allow comparisons as shown in [28].

For wet foams (toward the higher side of liquid volume fraction 0.2), the radius of the bubble is the only important information required to determine the coarsening which is contrary to dry foams where bubble shape (number of edges, length of edges etc.) and size both play an important role. It was shown in [29] that in wet foam a reasonably well defined curve exist when average bubble growth rate is plotted against bubble size and is given in the following form:

$$\frac{dV}{dt} = V^{1/3}.G_V$$

Where, G_V has dimensions of diffusivity and is an average value over the bubbles with volume V. When G_V is greater than zero, the bubble grows and has a volume greater than $\langle V \rangle$, whereas

bubble shrink if it's size is less than $\langle V \rangle$. The average rate of change of bubble radius is given by the following equation:

$$\frac{dR}{dt} = K_2 \left(\frac{1}{\langle R \rangle} - \frac{1}{R} \right)$$

Where, $K_2 = 2\sigma \bar{k}_f$ and $\bar{k}_f$ is the effective film permeability taking into account the non-uniform film thickness in wet foam. Alternatively G_V can also be expressed by the following:

$$G_V = K_2' \left[\left(\frac{V}{\langle V \rangle} \right)^{1/3} - 1 \right]$$

With, $K_2' = 3^{1/3}(4\pi)^{2/3} K_2$.

On further analysis the equations suggests that wet foam are expected to follow the same scaling behavior as the dry ones. The evolution of bubble size can be written as:

$$\frac{R(t)}{R} = \left[1 + \frac{K_2}{2R_0^{\,2}} t \right]^{1/2}$$

$2R_0^{\,2} / K_2$ is sometimes referred to as the coarsening time. This scaling behavior was ascertained by [30], [31] and [32] using experimental data. The coarsening of foam is an important phenomenon since bubble size play crucial role in foam stability.

Additionally, it is important to discuss the collapse mechanisms of foam bubbles. The broad notion is that spontaneous growth of thermal fluctuations causes film rupture. The increase of film area leads to positive contribution to the free energy of the surface and effect of disjoining pressure leads to rupture of film. An intuitive argument then suggests that the stability of a bubble is dependent on the bubble size, the larger the size of the bubble the more fragile it was considered. Since the disjoining pressure is inversely proportional to the surface area of a film, this in fact also suggests, the larger bubble are less stable and as in case of isolated thin films.

But there are experimental data which suggest that the disjoining pressure is important in isolated thin film stability but it does not apply in case of foams. Experiments were conducted in [33] to determine the mechanism behind foam collapse. To understand the role of film size and bubble radius in the destruction of foam, dielectric experiments and visual observations were used to measure evolution of liquid fraction during collapse in the setup shown in Figure 11. The first

observation cited is that when bubbling is halted, first the height of foam remains constant. Secondly the foam dries due to drainage and bubble starts to rupture. Thirdly the rupture front propagates in the foam and the height of foam decreases. To determine whether the rupture depends upon the size of the bubble, they used different bubble sizes and found that for all bubble sizes there is a critical volume fraction at which the collapse occurs. They concluded that the threshold of the liquid fraction is independent of the bubble size and since rupture is completely dependent on the threshold volume fraction hence the rupture is independent of the bubble size. If the disjoining pressure theory was applicable then the disjoining pressure depends on the bubble size and bubble size should have influenced the rupture which is contradictory to the results in [33].

It was suggested by [34] that the rupture of foam that occurs at a critical liquid fraction is the consequence of topological rearrangements in the films. It was observed that two events namely T1 and T2 events are responsible for the rupture of foam. During this event the plateau border rearranges from films meeting in three by three into an arrangement of films meeting in four by four and then back to three by three. At a certain critical liquid fraction the amount of liquid is not enough for such a process and hence the foam collapses.

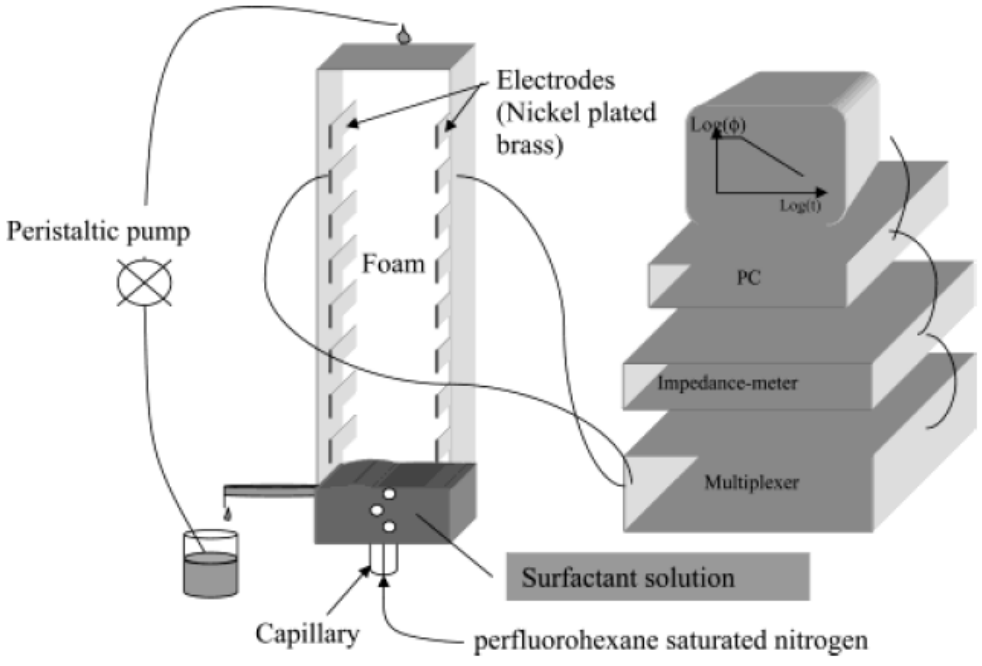

Figure 11: Experimental setup from [33] to measure the volume fraction of liquid in a foam column.

2.3 Foamer evaluation method for gas well deliquification

This section will focus on various methods for evaluating foamers used for deliquifying gas wells. The use of foam for gas well deliquification has been discussed in Chapter 11.4. The important step for such an FAL (foam assisted lift) operation is the selection of the right foamer depending on the operating conditions of the well. There are various methods available to test foamers, these methods can be at different scales depending on the type of test and the relevant ones are discussed below.

2.3.1 Flow loop test

The flow loop test are generally conducted to mimic the flow regime in an actual gas well so as to understand the foam formation and changes in regime transition due to surfactant in such flows. The scales of the test apparatus varies from order of an inch to few inches in diameter and of the order of around 10 m in length. Most studies in past have conducted tests with U_{SL} ranging from a few mm/s to a few cm/s and U_{SG} ranging from few m/s to around 30-40 m/s. Air-water flow was studied by [35] in a 2.54 cm diameter vertical pipe. The experiment were conducted with and without surfactant, they found that the gas velocity required to lift the liquid upwards without surfactant as 3.1 m/s whereas 0.8 m/s with surfactant.

Similar experiments were conducted by [36] on a 19 mm diameter vertical pipe. Experiments conducted at all flow regimes indicated in Figure 1. The authors found no significant shift in annular-churn flow transition with and without surfactant. This was contradictory to the intuitive understanding that liquid loading is related to annular-churn transition and that generally adding surfactant reduces the transition gas velocity. However they noticed a significant reduction in pressure gradient with surfactant in the churn-slug flow regime.

Experimental results in [37] and [38] also show that the surfactant reduces the transition velocity for annular-churn flow, which is consistent with the liquid loading behavior of surfactant. Overall most researchers have focused on change in transition velocities with surfactant and not much research has been performed on the actual flow with surfactants in gas wells. The only model that is available assumes a plug flow of foam, which is not consistent with the flow observed in an actual gas well.

Recently [39] studied in detail the effect of different gas and liquid flow rates at different concentration of surfactants, also varying the pipe diameter and pipe inclination. Pressure drop

and liquid hold-up data were collected to develop an engineering model in order to quantify the effect of using foamers under different conditions. According to the research, to develop such a model three important inputs should be obtained through experiments:

1. The relation between interfacial friction and the liquid film thickness at the wall.
2. The amount of foam formed per unit liquid introduced into the tube which has a large role in determining liquid film thickness.
3. The rheological properties of foam.

The first input can only be obtained through experiments on a flow loop test and the last requirement would require rheological measurements. The second input i.e. the amount of foam created depends on a number of factors such as composition of the surfactant solution, pressure, temperature etc. The flow loop tests are conducted at atmospheric temperature and pressure which limits the usage of such a model. Moreover, before using surfactant solution in a gas well it is important to study the composition of the liquid produced to use the right type and quantity of the surfactant. Hence small scale setups are used to study foam formation on site and to estimate the effect of the foamer on the gas well performance. The next section would focus on the small scale tests presently in use in the oil and gas industry for the foamer evaluation.

2.3.2 Small scale tests for foamer evaluation

The flow loop setup is generally used to study the hydrodynamics of the flow with surfactants but an essential part of the complete study should also include the study of the quality and quantity of the foam itself. Small scale setups are hence used to study foams separate from the complex hydrodynamics of the air-liquid flows. The behaviour of foam in any setup is dependent on the physio-chemical properties of the surfactant and on the methods through which the foam is generated. There are several methods for foam generation and some of them are:

- The Ross-Miler test in which a volume of surfactant solution is dropped on another volume of surfactant solution and the mixing generates foam.
- A sparging setup where gas is blown though a certain amount of surfactant solution to produce which produces foam. The gas blown is passed through either a sparging stone or a porous plate.
- Foam generation by shaking an apparatus which contains both surfactant solution and gas.

- By stirring the gas and surfactant solution mixture rigorously entrains the gas into the liquid causing foam production.
- Foam can also be generated by nucleation of dissolved gas, such as the one occurring in a beer glass.

Earlier researchers have investigated the effect of dynamics surface tension on foamability on different setup. The effect of dynamic surface tension on foam generated in a rotor test (vigorous stirring of the surfactant solution in presence of gas) was studied by [40]. They found that a lower surface tension leads to increase in amount of foam created. The relation of $R_{1/2}$ on the amount of foam created was studied by [41], [12] and [16]. Where $R_{1/2}$ is defined as:

$$R_{1/2} = \frac{\gamma_0 - \gamma_m}{2t^*}$$

Their results show an increase in foam formation when $R_{1/2}$ increases. However there were significant deviations and that suggests that there are parameters other than DST that effect the foam formation. Recently, [2] studied various surfactants on a sparging setup in order to find a similar correlation of $R_{1/2}$ and the rosen parameter with foamability, where foamability was defined as foam density. They found that for their setup the relation between foamability and rosen parameter holds a weak relationship.

There have been various studies on foam formation in a sparging setup but the question still exists whether the sparging test can be representative of the foam formation in larger scales. So far no study in the open literature has focused on the effect of changing the sparging velocity in the setup. Moreover, the pressure and temperature downhole are much higher than the condition at which these tests are conducted and hence the developed model might be futile unless the pressure and temperature effects are considered. Therefore the present study hence targets at bridging the gaps mentioned above and the research question has been discussed in Chapter 11.5. As mentioned in Chapter 11.5 an important aspect of this study will be the effect of gas velocity on foam formation. Since we will vary the gas velocity in a certain range, it becomes important to consider the various flow regimes that can occur in a bubble column before foam is formed as shown in Figure 12. To understand the formation of foam it is important to understand various flow regimes in bubble column.

2.4 Flow regimes in bubble column

There are four basic flows observed in bubble column: homogenous bubble flow, heterogeneous bubble flow, churn-turbulent bubble flow and slug flow, as mentioned in [42] and shown in Figure **13**. Homogenous bubble flows occur at relatively low superficial gas velocity; this regime consists of homogenous sized bubbles flowing through a liquid column. As the gas velocity increases the bubbles start to coalesce with each other and different sized bubble occur in the column giving rise to a heterogeneous bubble flow. When increasing the velocity even further the bubble coalescence increases to an extent where slugs of gas could be observed. For larger bubble column with high velocity a typical regime called churn-turbulent is observed. This flow pattern includes a wavy flow with pockets of gas in the liquid.

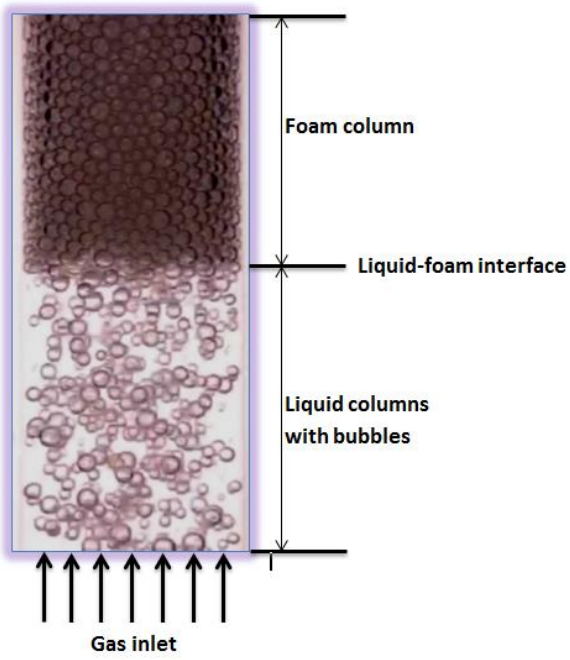

Figure 12: Typical foam column comprises of a liquid column at bottom and a foam column on top.

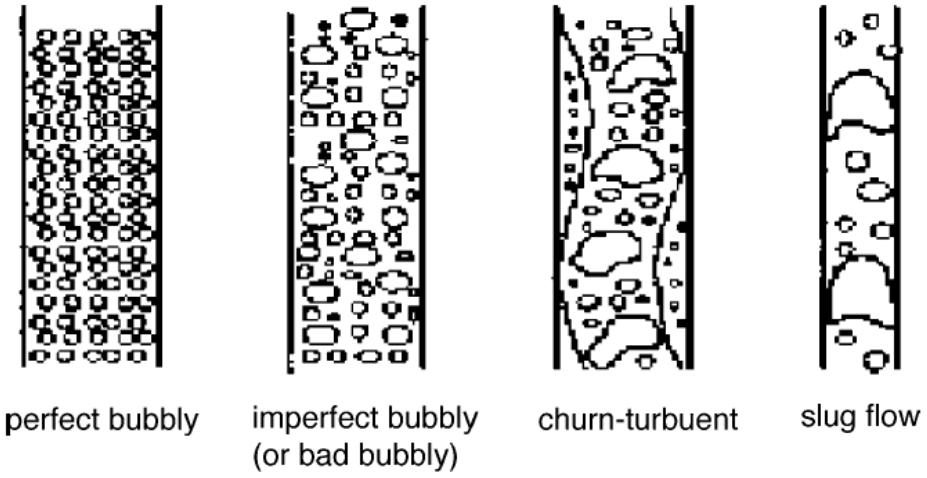

Figure 13: Various flow regimes in a bubble column.

The change of flow regime has been extensively studied in the past and one such flow regime map is shown in Figure 14 as reported by [43]. The regime map shown in Figure 14 is an average representation of flow patterns; the values in the map might not represent the exact values of regime change in specific cases as it may depend on factors other than column diameter. Various parameters that may affect the regime change velocity were listed in [44]. Some of the important parameters are: pressure, temperature, viscosity, surface tension, sparger hole size, liquid height etc. as shown in **Table 1**.

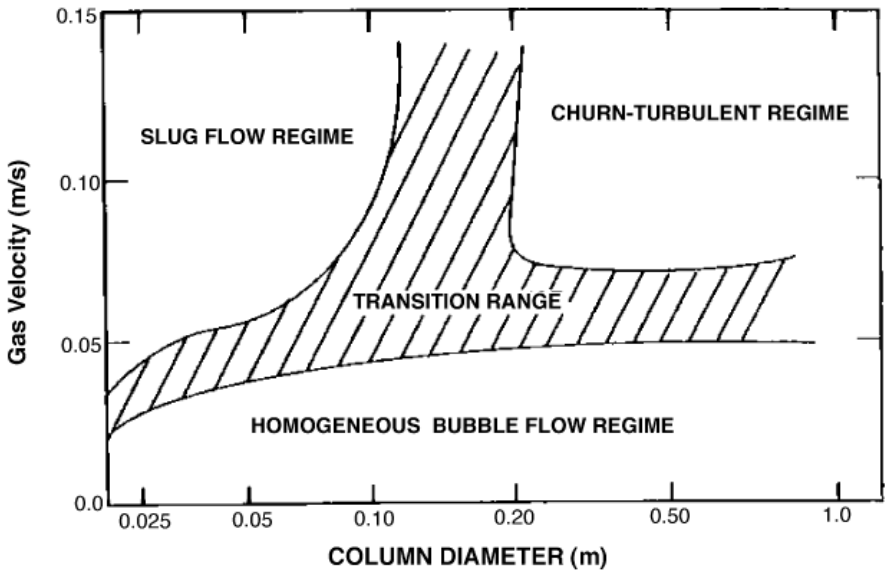

Figure 14: Bubble column flow regime map.

Table 1: Effect of various parameters on bubble flow to slug flow regime transition in a bubble column, reported in [44].

Parameter	Effect on flow regime transition	Reference
Pressure	In general, an increase in pressure results in an increase in transition velocity	[45], [46], [47], [48], [49]
Temperature	An increase in temperature increases the transition velocity and delays flow regime transition	[50], [48]
Viscosity	An increase in viscosity, in general, advances flow regime transition	[51], [52]
Surface tension	Reduction in surface tension increases transition velocity	[53]
Sparger hole size	Transition velocity decreases with an increase in hole size up to certain hole size.	[54], [55]
Liquid height	An increase in liquid height reduces the transition velocity	[54], [56]

Chapter 3 Experimental setup

The present work has been carried out on a sparger test setup at TNO in Delft with additional surfactant characterization tests on maximum bubble pressure tensiometer at the Materials Department of TNO in Eindhoven. Foam visualization techniques used to capture the formation and breakup of foam are reported in this chapter. Moreover some high speed camera measurements were conducted in order to understand the flow of gas bubbles in the liquid column.

3.1 Foam setup

The purpose of the proposed setup is to analyze the behaviour of different foamers. N_2 is sparged from below in the setup to create bubbles and hence to create foam inside the foam column. The uniqueness of the setup is that it can operate under high pressure and temperature, which is a more representative condition for gas wells than the ambient pressure and moderate temperatures used in current standard tests in the industry. In this section, a description of the experimental setup with a schematic diagram and a short description of the test procedure will be given. Surfactants are currently tested in column tests, by sparging N_2 gas through a foamer-liquid mixture at low flow rates. This test method also forms the basis for the proposed setup, although at a wider range of flows, pressures and temperatures. The foamer performance will be analyzed by using three different tests: Foam build-up test, collapse test and carryover test. A double-walled glass vessel is used in which foam will be generated. The vessel is capable of handling pressures up to 17.4 bar and temperatures up to 150 °C. A summary of the setup specifications are given in **Table 2**. The column will be temperature-controlled by using an oil bath. Foam generation will be tracked visually by using camera observation. Carryover vessel is made of steel with the inner diameter of 12.6 cm and is mounted on a scale for the liquid carryover weight measurements.

Description of the setup

The setup is shown in Figure 15.There are two columns: the foamer test column (left) and the carryover test column (right). The detailed description is given below.

- N_2 is supplied from a bottle and its mass flow rate is controlled by a Bronkhorst mass flow controller shown on the top left part of Figure 15.

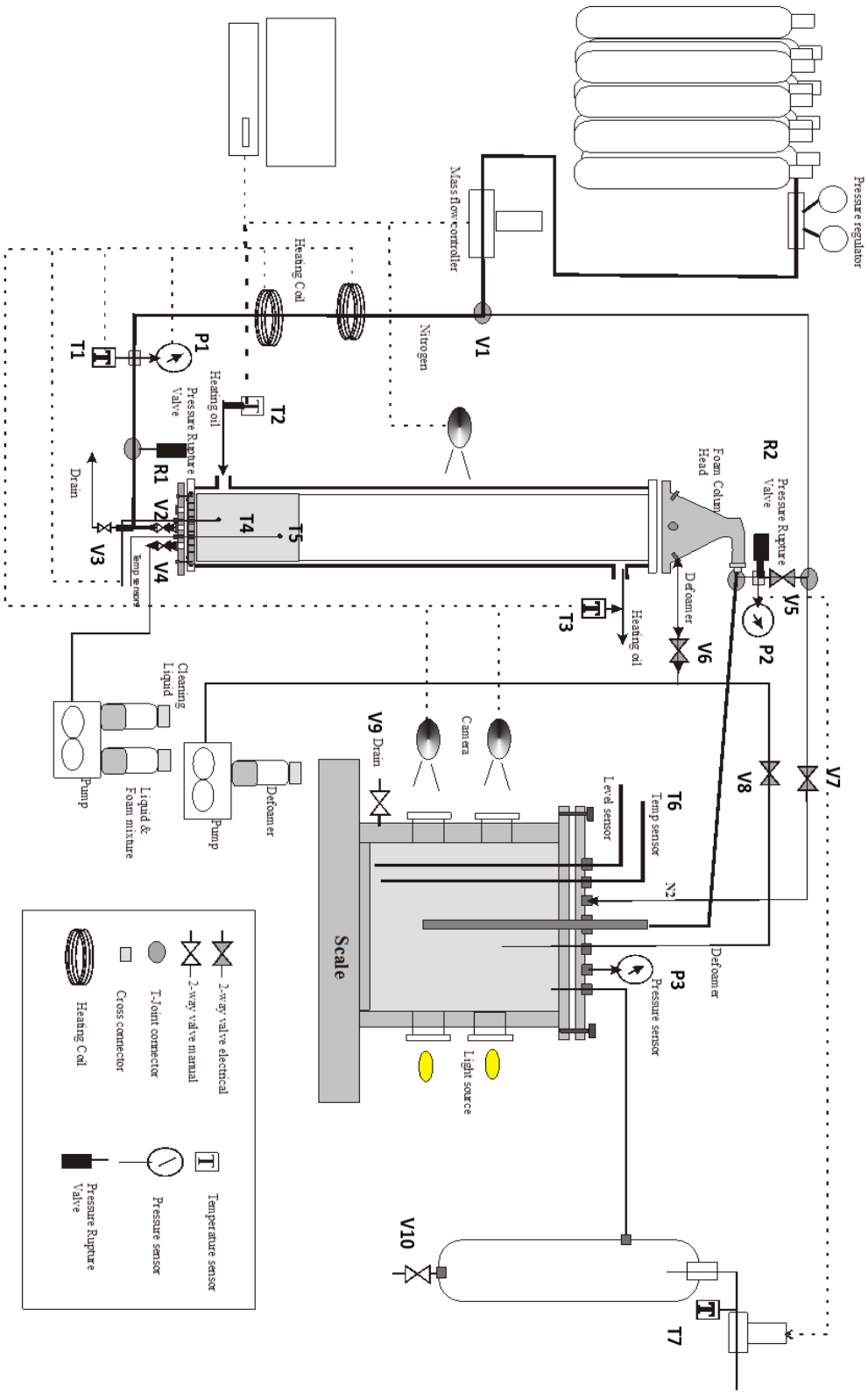

Figure 15: The schematic of the small scale sparger setup at TNO in Delft used in the present study.

Table 2: Setup specifications

$D_{test\ vessel}$	0.062		[m]
$H_{test\ vessel}$	0.5		[m]
$D_{carryover\ vessel}$	0.126		[m]
Parameters	**Min**	**Max**	**Units**
P	1	15	[bar]
T	25	150	[˚C]
Usg	0.01	0.3	[m/s]
Qg	1.09*	711**	[Nl/min]

* The minimum of gas flow rate corresponds to P = 1bar, T = 150 ˚C, Usg = 0.01 m/s

*** The flow rate corresponds to P = 15bar, T = 20 ˚C, Usg = 0.3 m/s is 711 Nl/min.

- The N_2 stream will be divided into two section downstream of the mass flow controller:
  - The top line (the line diverting upward from valve V1) is used for pressurizing the setup (bypass stream).
  - The bottom line (the line diverting upward from valve V1) is used to agitate foamers and it is injected through a sparger disk (main stream).
- The N_2 stream needs to be preheated to the required temperature. Preheating of the N_2 stream is done by using a gas heater unit. The N_2 temperature is monitored by a temperature sensor T1 just before it reaches the gas sparger and it is controlled by a thermostat at the outlet of the gas heater.
- Hot oil is injected and circulated outside the inner wall of the foamer test column and its temperature is monitored with temperature sensors.
- The top and bottom part of the foamer column are heated up by two heating elements.
- The temperature of the foamer test column is monitored by two temperature sensors which are mounted inside the vessel.
- Two pressure relief valves are used at the N_2 feed line and at the top of the foamer column for safety reasons.
- The pressure regulator is mounted at the top of carryover vessel. The pressure is measured by a pressure sensor mounted at the top of foamer column. Additional gas will be released to the outside to ensure the constant pressure during the test.

- A gas/liquid separator is installed upstream the pressure regulator to protect the pressure regulator from the possible liquid carry over to the regulator.
- For the carryover test, a flexible, high pressure hose is installed at the top of both vessels to connect the foamer test column to the carryover vessel. The pressure and temperature will be monitored at the top of the foamer column.
- The amount of carryover will be measured by using a scale.
- A camera is mounted outside of the foamer vessel to monitor the foam behaviour, specifically foam height.
- There are two drains at the bottom of both vessels which will be used during the cleaning cycles.

For every surfactant solution three tests are conducted namely: build-up, collapse and carryover test. A pictorial representation of the three tests can be seen in Figure 16. We start the test with 210 grams of surfactant solution inside the foam column and flow gas through it till the foam has developed to a certain height (approx. 30 cm). This can be seen in Figure 17 (a) where foam has reached the desired level marked in black. Once the build-up test is finished the gas flow is stopped and the foam is allowed to collapse as shown in Figure 17 (b). The collapse test is conducted till half of the foam collapses and is hence called half-life of foam. The last test i.e. the carry over test is then conducted by restarting the gas flow in the foam column and by letting the foam flow to the carryover vessel till the mass of liquid carried over becomes almost constant as shown in Figure 16. The various quantities used during the study such as foam density, build-up rate, collapse rate, etc. have been defined below in Table 3.

Table 3: Definition of quantities extracted from foam visualization.

Quantity	**Definition**
Build-up rate	$\frac{Buildup\ height}{Buildup\ time}$
Collapse rate	$\frac{Collapse\ height}{Collapse\ time}$
Carryover	Amount of liquid unloaded

Other than the above mentioned quantities we define foamability: this is simply the density of the foam that is produced in the foam setup. Foam density in the present experiment is given by the rate of liquid unloaded divided by volume flow rate of foam.

$$\rho_{foam} = \frac{w'_{carryover}}{v_{foam} \times A_{column}}$$

where, $w'_{carryover}$ is the rate of carryover in the linear region of the carryover curve as shown in Figure 16. We defined v_{foam} in two different ways, firstly as the build-up rate of foam and secondly as the superficial gas velocity. A_{column} is the cross-sectional area of the foam column.

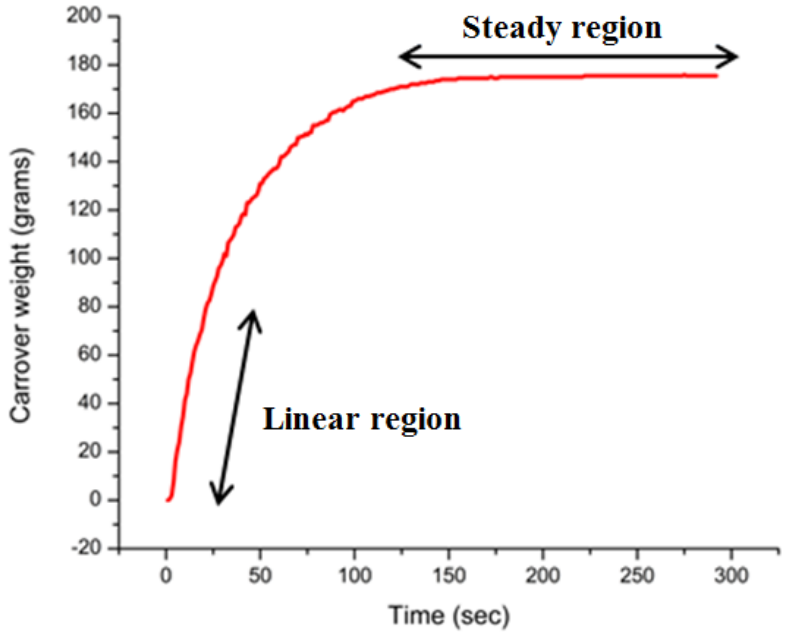

Figure 16: A typical carryover curve with linear and steady regions.

3.2 Sparger specification

The foam setup is equipped with a sparger which lets the gas pass through narrow pores leading to formation of gas bubbles when it enters the liquid. The sparger used in the setup is a SIKA-R 150 manufactured by Technische Handelsonderneming Nederland B.V. The specifications are mentioned in **Table 4**.

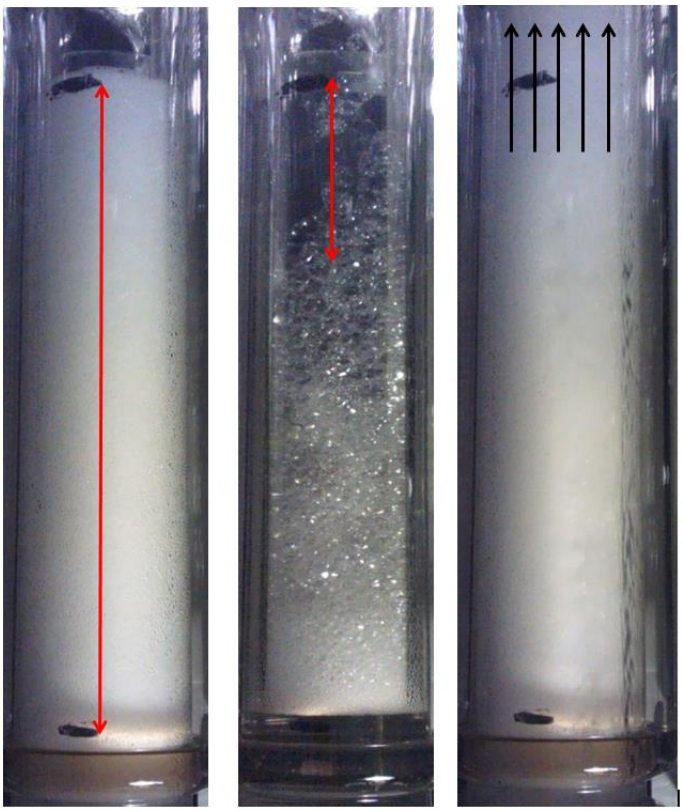

Figure 17: Pictorial representation of three tests namely: (a) Build-up tests, (b) Collapse test and (c) Carryover test.

Table 4: Sparger specification.

Parameter	**Value**	**Unit**
Avg. Pores size	150	μm
Sparger diameter	55	mm
Sparger thickness	3	mm
Permeability coefficient	117×10^{-12}	m^2
Material	Stainless steel	

3.3 Foam visualization

To capture the formation and collapse of the foam in order to extract the rates of formation and collapse we use a small camera (frequency 1 Hz). The pictures captured during the build and collapse test are then used extract various parameters such as foam density, collapse rate and build-up rate.

In addition, some high speed visualization experiments are carried out in order to capture the bubble flow through the liquid column in the foam setup. The setup with the camera is shown in Figure 18. The camera used in the study is an "Olympus i-speed" high speed camera. The camera specification is given in Table 5. In addition to the camera a 1000 W halogen lamp is used with a light diffuser sheet to avoid reflection. For the present study the camera is set at 500 fps with the shutter speed at 8 μs and is operated using dedicated software on a PC via ethernet link.

Table 5: High speed camera specification.

Parameter	**Value/Detail**
Resolution (full sensor)	800 x 600 pixels
Speed at full resolution	1000 fps
Maximum recording speed	33000 fps
Shutter	User adjustable up to 5 microseconds
Camera dimensions	115mm x 110mm x 233 mm
Camera weight	2 kg

Figure 18: Foam setup with high speed camera.

3.4 Maximum bubble pressure tensiometer

The dynamic surface tension measurements were carried out with commercially available tensiometer BP2 by KRUSS, GmbH (shown in Figure 19) at Materials department, TNO Eindhoven. The measurements were conducted on a range of concentrations varying from 50 ppm to 20000 ppm (by weight) of surfactant in deionize water.

A surfactant solution of a desired concentration is prepared and placed in a vessel, the vessel is then placed inside the setup and a capillary (diameter of capillary: 0.2 mm) is gently dipped into the solution. The depth of the capillary tip inside the surfactant solution in the vessel is set at 10 mm and the surface age is varied from 10 milliseconds to 50000 seconds for all the measurements.

The device is based on maximum bubble pressure method which uses the fact that while producing bubbles by blowing through a capillary, the maximum bubble pressure occurs when the bubble diameter is equal to the capillary diameter. In the process of bubble formation the minimum radius of curvature of the bubble occurs when the bubble radius is equal to the capillary radius i.e. r_3 as shown in Figure 20. The excess pressure inside a bubble is inversely proportional to the radius of the bubble; hence the maximum pressure occurs when the radius of the bubble is minimum and equal to the capillary radius. The following equation is then used to find the surface tension of the surface formed and the surface age is given by the time taken by the bubble to reach the radius equal to the capillary.

$$\sigma = \frac{(p_{max} - p_0).r}{2}$$

Figure 19: BP2 bubble pressure tensiometer by KRUSS, GmbH.

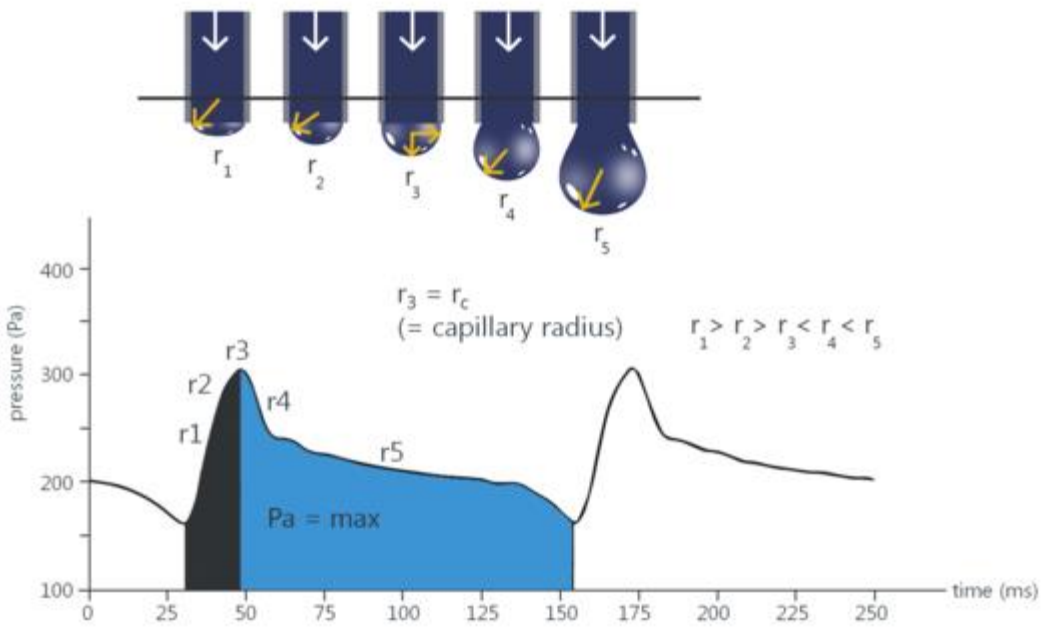

Figure 20: Maximum bubble pressure tensiometer working principal.

Chapter 4 Results and Discussion

This chapter will present the results obtained from the measurements and is divided into three sections. Two commercial surfactants were chosen for measurements which are: Foamatron and Trifoam Block 820. The first section discusses the results obtained for Foamatron in the small scale sparger setup. The second section discusses the result for Trifoam Block 820 in the small scale sparger setup and its comparison with Foamatron. In the final section we compare the results obtained for the two surfactants in the small scale sparger setup with the results from [39] conducted in the flow loop setup.

4.1 Foamatron results

Foamatron is a commercial surfactant used for deliquification in gas wells, the surfactant compositions and type is not reported by the manufacturer.

4.1.1 Dynamic surface tension for Foamatron

The dynamic surface tension (DST) results for Foamatron are presented in Figure 21. The surfactant concentration is varied from 50 ppm to 40000 ppm and the surface age is varied from 10 milliseconds to 50 seconds. The Rosen empirical equation for DST mentioned in section 2.1.3 is used to fit the dynamic surface tension curves for all concentrations. The fit parameters γ_m, t^* and n are obtained using custom fit option in MATLAB v2014b. The fit values are eventually used to calculate the rosen parameter for each concentration. The variation of the fit parameters and the rosen parameter with respect to concentration has been plotted in Figure 22. The critical micelle concentration seems to somewhere around 2000 ppm; the reduction in surface tension beyond this concentration is relatively slow.

4.1.2 Foam setup results for Foamatron

The small scale sparger setup used in the present thesis has been described in section 3.1. Here the effect of three parameters namely: gas velocity, pressure and surfactant concentration in the small scale sparger setup for Foamatron are discussed. The experiment matrix is shown in **Table 6**, where surfactant concentration, superficial gas velocity and pressure variations are reported. The present section describes the results of the three tests conducted for each experiment: build-up test, collapse test and the carryover test.

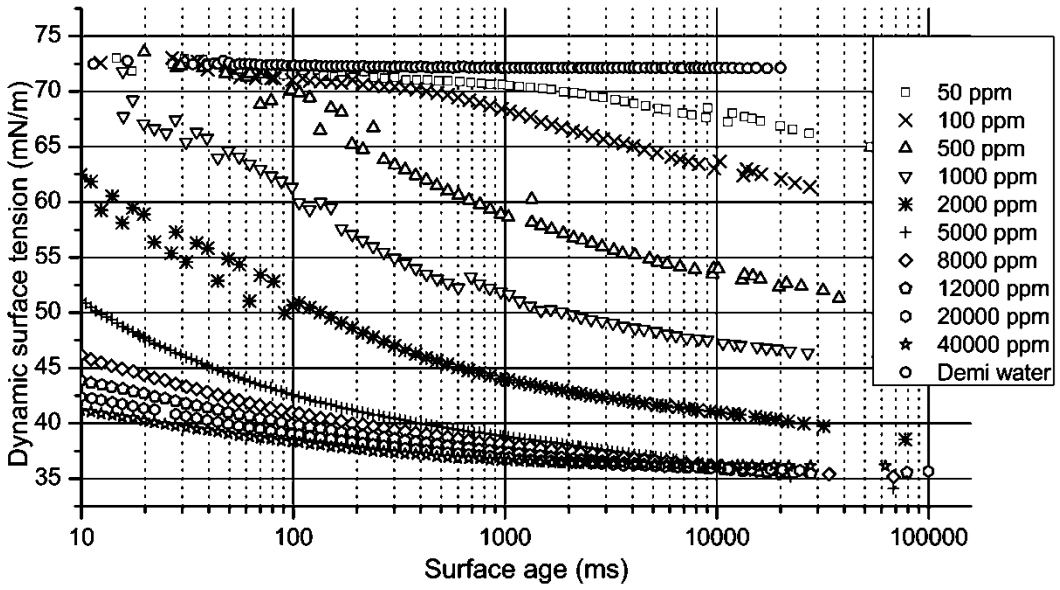

Figure 21: The graph shows the dynamics surface tension with respect to surface age for Foamatron at various concentrations at 22^0C.

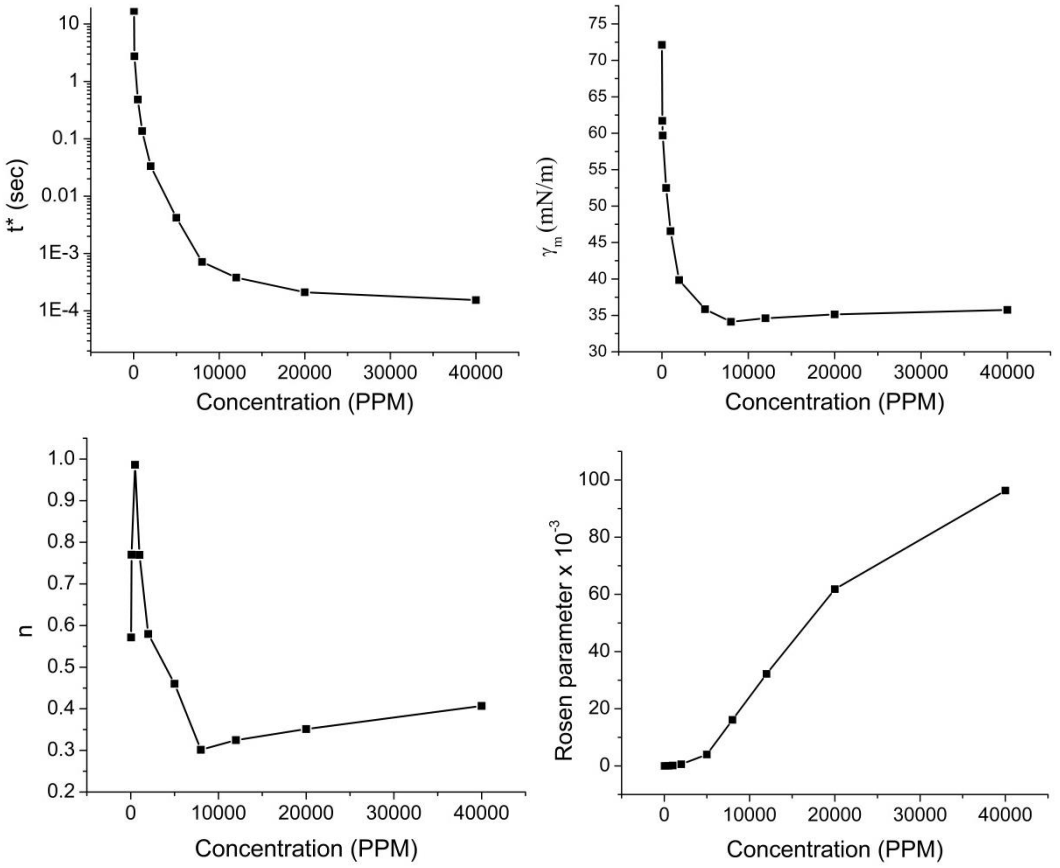

Figure 22: The figures show the variation of fit parameters γ_m, t^* and n with respect to concentration and the variation of rosen parameter with respect to concentration.

Table 6: Experiment matrix for foamatron, each column corresponds to superficial gas velocity and each row corresponds to surfactant concentration. Symbol ①, ⑤ and ⑩ refer to the gas pressure at which the experiment was conducted.

	0.01 m/s	0.02 m/s	0.05 m/s	0.1 m/s	0.15 m/s	0.2 m/s	0.3 m/s
100 ppm	①	①⑤	①⑤	①⑤			①
500 ppm	①	①	①	①			
1000 ppm	①	①⑤	①	①⑤	①	①	①⑤
2000 ppm	①⑤⑩	①⑤⑩	①⑤⑩		①	①	①
5000 ppm	①	①	①	①	①	①	①
8000 ppm	①	①	①	①			①

*The surfactant concentration given in the table is parts per million by weight. Solution is prepared with deionized water with pH level 4-4.5 pH was lowered by injecting CO_2 in the deionized water.

The effect of varying pressure and surfactant concentration on build up, collapse and carryover are shown in Figure 23, Figure 24 and Figure 25 respectively. The build-up rate (which corresponds to the foam formed per unit of time) is observed to have a linearly increasing trend with increasing gas velocity (up to 0.2 m/s) which is consistent with the expectation that a higher gas flow rate would lead to a larger foam production per unit time. It should be noted that the superficial gas velocity above 0.2 m/s leads to a decrease in build-up rate, which will be discussed in detail later. In general the collapse rate shows a decrease with increasing surfactant concentration. The increase in surfactant concentration leads to larger reduction in surface tension making the foam more stable. However, later we will see for Trifoam Block 820 that the reduction in surface tension is not the only important parameter. Increasing the gas velocity leads to relatively less stable foam as suggested by the trends. The carryover test results show

increasing trends with increasing velocity and concentration both. Although for low surfactant concentration the trends are not monotonous.

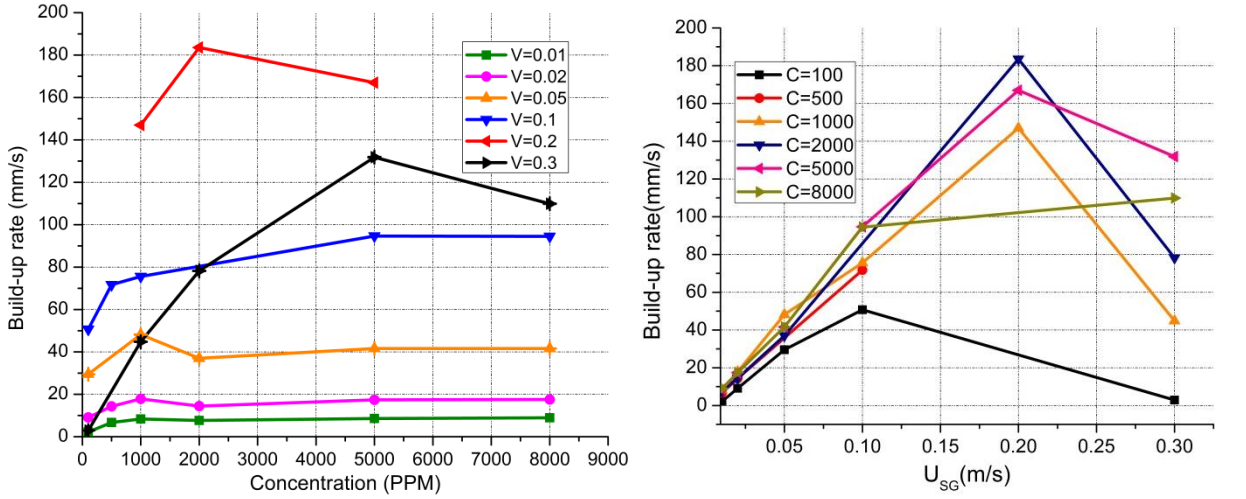

Figure 23: (a) Graph on left shows variation of build-up rate with respect to concentration. (b) Graph on right shows Build-up rate with respect to U_{SG} (superficial gas velocity).

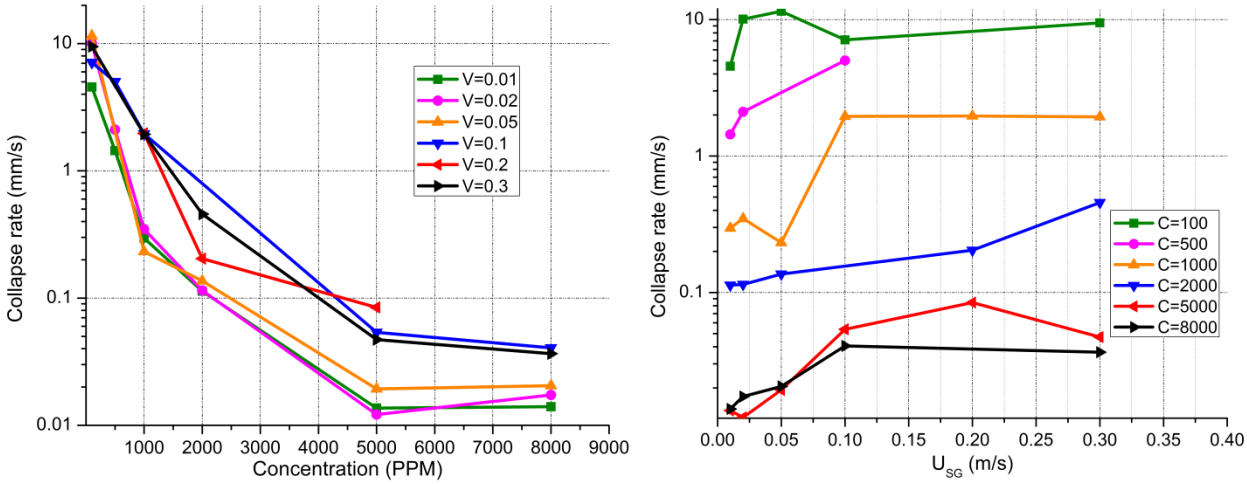

Figure 24: (a) Graph on left shows variation of collapse rate with respect to concentration. (b) Graph on right shows collapse rate with respect to U_{SG} (superficial gas velocity).

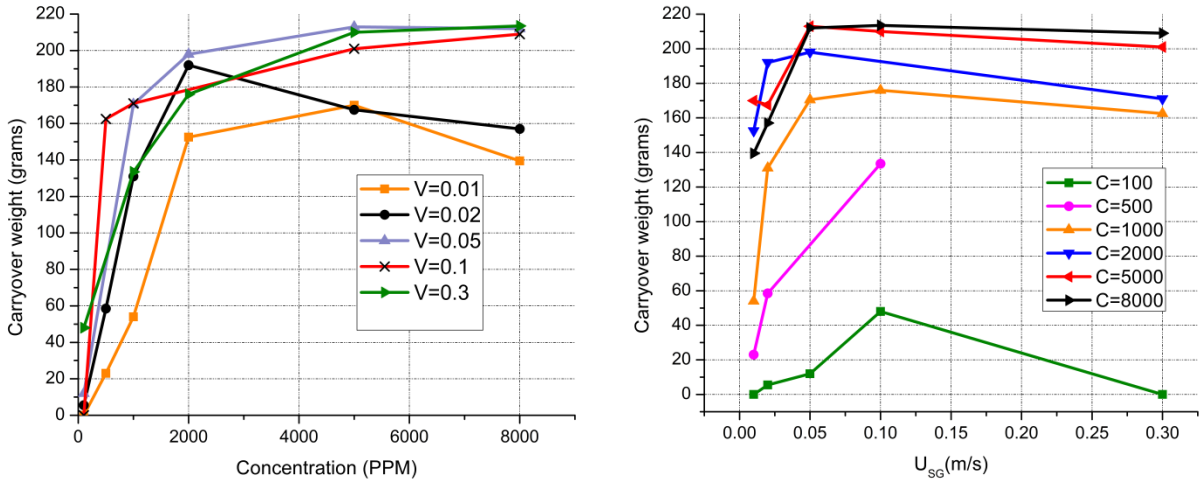

Figure 25: (a) Graph on left shows variation of carryover weight with respect to concentration. (b) Graph on right shows carryover weight with respect to U_{SG} (superficial gas velocity).

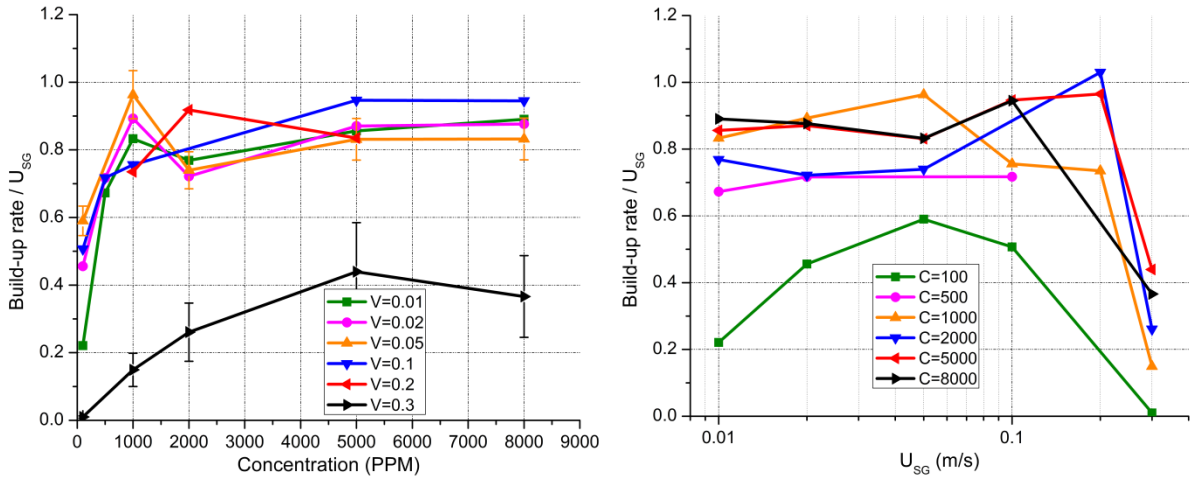

Figure 26: (a) Graphs shows build-up rate normalized with superficial gas velocity with respect to surfactant concentration (error bar shown), (b) Graphs shows build-up rate normalized with superficial gas velocity with respect to superficial gas velocity.

4.1.2.1 Effect of gas velocity and surfactant concentration on build-up rate

The build-up rate is an important parameter to quantify the amount of foam formed per unit of time. In the flow loop setup the amount of foam formed has a direct influence on the pressure drop as shown by [39]. However, the amount of foam formed differs for different surfactants and for different surfactant concentrations. Therefore, an estimate of the amount of foam formed in the gas well requires a characterisation of the foaming performance of a surfactant solution. Figure 23 (b) shows a linear increase in build-up rate with respect to superficial gas velocity up

to 0.2 m/s and an unexpected decrease then on. To understand such behaviour we normalize the build-up rate with the superficial gas velocity, see Figure 26. Ideally for stable foam the ratio of the build-up rate and the superficial gas velocity should be close to 1 (valid for dry foam because in wet foam the liquid content can have a significant contribution to the foam volume). The data points corresponding to surfactant concentration greater than 100 ppm and gas velocity less than 0.2 m/s in Figure 26 lie within the build-up rate to U_{SG} ratio of 0.8 to 1. Whereas the data points for 100 ppm in Figure 26 (a) and for U_{SG}=0.3 m/s in Figure 26 (b) correspond to a build-up rate to U_{SG} ratio much less than 0.6. The behaviour for surfactant concentration 100 ppm can be explained by the fact that the stability of the foam is low and hence the process of build-up is dominated by liquid drainage. For 100 ppm solution at low velocity the drainage rate is greater than the build-up rate; when increasing the gas velocity the build-up rate exceeds the drainage rate. However for U_{SG}=0.3 m/s the build-up rate is low even for higher concentrations. To explain this anomaly we look at the sequence of images from the build-up test. Figure 28 shows the build-up sequence for surfactant concentration 100 ppm and U_{SG}=0.05 m/s. The foam appears to build linearly with respect to time. This could be a result of bubbles stacking over each other in a regular fashion leading to a consistent build-up. However, it should be noted that the build-up to U_{SG} ratio is approximately 0.6, which is much less than expected. This could possibly be explained by the high collapse rate of foam at low concentration.

This hypothesis can be explained better using the Figure 27 which refers to a surfactant concentration of 100 ppm and U_{SG}=0.01 m/s. In this sequence the foam appears to build up consistently but the darker patches in the foam suggest that the collapse rate is significant and hence affects the build-up. To even strengthen the hypothesis, the collapse rate as read from Figure 24 (b) for 100 ppm solutions is of the order of 10 mm/s and U_{SG} = 0.01 m/s is of the same order. This would mean that at velocity close to the collapse rate, a significant effect of collapse can be observed during the build-up.

This explains the low build-up rates at low concentrations. However the low build up rate at U_{SG} = 0.3 m/s as seen in Figure 23 (b) is still not clear. For this we refer to the sequence of images in Figure 29. For U_{SG} = 0.3 m/s foam should ideally reach the top of the column within a second. We can observe that the foam build-up is not consistent and the foam behaves different at this velocity compared to the others (liquid splash can be observed in the images). The observation

and the data then suggest that there might possibly be a regime change which can cause such a behaviour. Further investigations were performed using high speed camera visualization which can be found in section 4.1.2.6.

4.1.2.2 Effect of gas velocity and surfactant concentration on collapse rate

The collapse test is important to understand the stability of the foam produced. The test results with respect to surfactant concentration and U_{SG} are presented in Figure 24 (a) and Figure 24 (b), respectively. The increase in surfactant concentration in general leads to decrease in collapse rate, i.e. to a more stable foam. We can observe a large change in the collapse rate from surfactant concentration 100 ppm to 5000 ppm but the change from 5000 ppm to 8000 ppm is relatively small. This could be attributed to the dynamic surface tension characteristic of the surfactant. From the dynamics surface tension curve given in Figure 21, it can be observed that the reduction of surface tension is significant between the curves for surfactant concentration up to 5000 ppm. However, the difference between the 5000 ppm and 8000 ppm is relatively small similar to the dynamic surface tension characteristic shown in Figure 21.

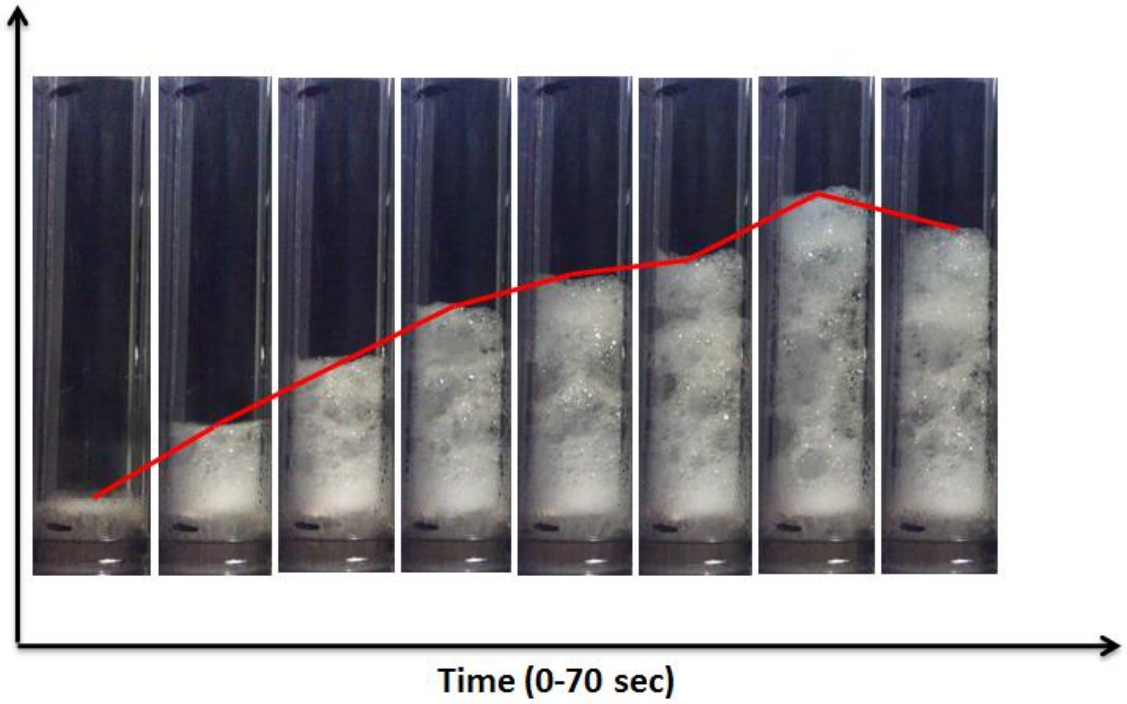

Figure 27: Image sequence from the build-up test for solution with surfactant concentration 100 ppm and U_{SG}=0.01 m/s (the first image refers to start of build-up test i.e. t=0 and the last image refers to t=70 seconds.

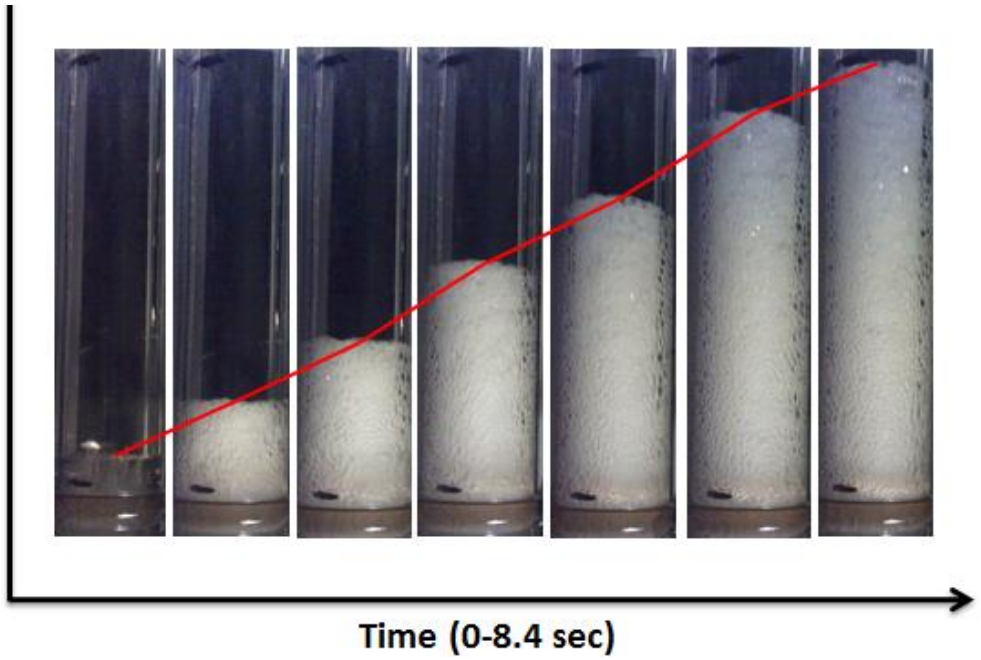

Figure 28: Image sequence from the build-up test for solution with surfactant concentration 100 ppm and U_{SG}=0.05 m/s (the first image refers to start of build-up test i.e. t=0 and the last image refers to t=8.4 seconds.

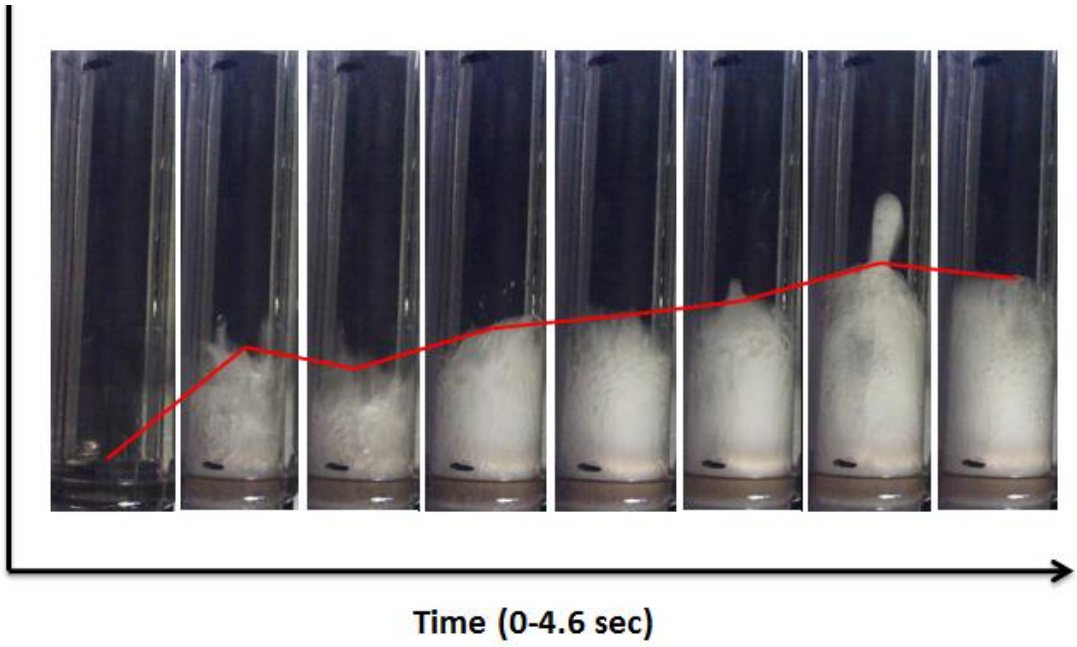

Figure 29: Image sequence from the build-up test for solution with surfactant concentration 100 ppm and U_{SG}=0.3 m/s (the first image refers to start of build-up test i.e. t=0 and the last image refers to t=4.6 seconds.

The increase in velocity in general leads to an increase in collapse rate i.e. less stable foam, larger velocity leads to larger bubble sizes which enhances the drainage rate and collapse. However, the increase occurs only up to U_{SG} = 0.1 m/s and thereafter the trend remains almost constant. As already mentioned, the results at high velocities suggest a regime change and hence the change in trend in collapse rate might be due to the same reason. At velocities less than 0.3 m/s, the increase in collapse rate with increasing velocity can be due to the fact that the surface tension of a bubble formed at higher velocities will be higher. At higher velocity the bubble formation time and the bubble rise time will be relatively lower. Therefore the surface age would be low, leading to formation of a bubble with higher surface tension.

4.1.2.3 Effect of gas velocity and surfactant concentration on carryover

One of the most important parameter to evaluate surfactant performance in deliquification is the amount of liquid the surfactant can remove from the well. The purpose of the carryover test is to understand the effect of different parameter such as gas velocity and surfactant concentration on how effectively the liquid can be unloaded. The results for carryover test are presented in Figure 30 (a) & (b) (carryover normalized is defined as the amount of carryover divided by the maximum liquid in the column i.e. 210 grams). An increase in velocity in general leads to an increase in the amount of liquid carried over. However this increase only occurs up to a certain velocity (approx. 0.1 m/s) and the deviation from that trend thereafter can be attributed to the possible change in flow regime at higher velocity. An increase in the velocity as shown in Figure 30 (b) from 0.01 up to 0.05 m/s increases the rate and the carryover weight by a significant amount. However, increasing the velocity beyond 0.05 m/s leads to a decrease in carryover for both concentrations. It should be noted that this has been a consistent trend when deviations are found for a higher velocity which is possibly due to a change in flow regime.

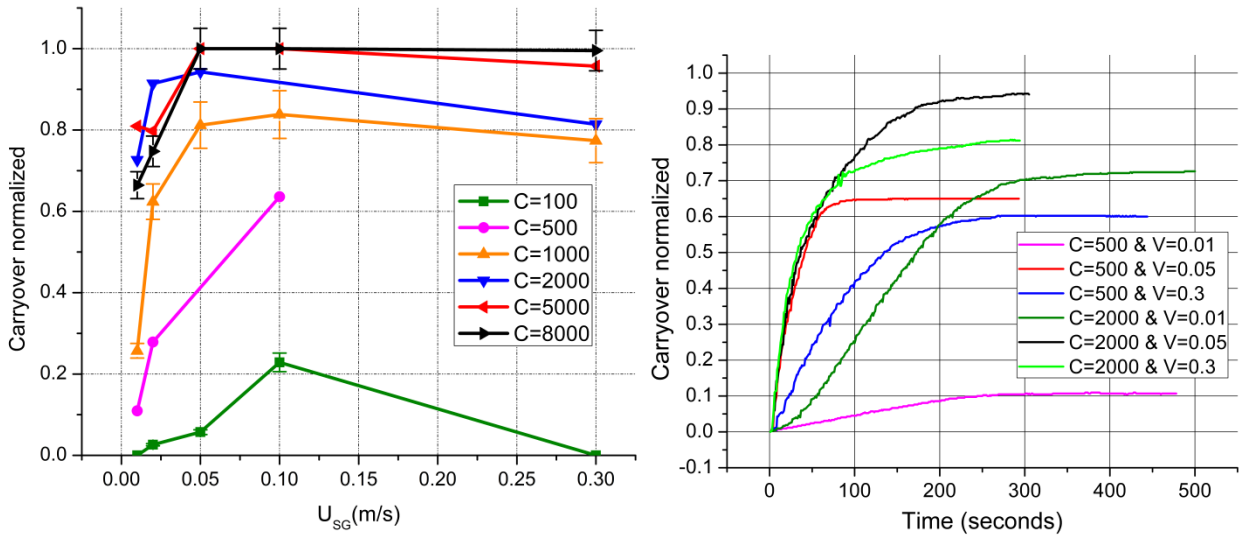

Figure 30: (a) The graph on the left shows the normalized carryover (carryover divided by total weight of solution used for the test i.e. 210 grams) with respect to U_{SG} with error bar, (b) the graph shows normalized carryover vs time for two concentrations: 500 and 2000 ppm and three velocities 0.01, 0.05 and 0.3 m/s.

The increase in concentration also leads to an increase in carryover. Increasing the concentration possibly has two effects. Firstly it leads to the formation of stable foam which could be unloaded without significant bubble break-up. This aspect leads to a better rate of carryover which is evident in Figure 30 (b) where for same velocity the rate of carryover is larger for larger concentration. Although this effect is significant for lower velocity (U_{SG}=0.01 m/s), it does not have a large effect for higher velocities since the time scale of collapse is much lower than the time scale of foam formation (build-up). Secondly the amount of surfactant molecules available for the foam creation increases with increasing concentration and hence depletion of surfactant from the solution takes a longer time leading to the formation of a larger volume of foam and consequently to larger carryover.

The carryover results and the above discussion suggest that the amount of carryover is dependent on the gas velocity unless the concentrations are low and liquid drainage has a significant effect. We found the buildup rate divided by collapse rate to have a significant correlation with the carryover weight. The amount of carryover does not only depend on the gas velocity but also on the concentration of the surfactant. As explained earlier for higher concentration, depletion of surfactant from the solution takes a longer time leading to more foam formation and carryover. Since the collapse rate shows high dependence on concentration hence normalizing build-up rate

with collapse rate takes into account both gas velocity and surfactant concentration. Thus a correlation between build-up rates/collapse rates to carryover weight is expected.

To find a correlation between the three measured quantities, we make use of certain observations. Firstly if the collapse rate is higher than the build-up rate, the carryover should be nearly zero since the foam collapses faster than it forms. Secondly if the build-up rate to collapse rate ratio is very large, the carryover should reach the maximum possible value (i.e. carryover normalized=1). This means that the fit curve should have two asymptotes: one along the minimum carryover weight of zero, corresponding to the case where the collapse rate is larger than build-up rate, and the other one along the maximum carryover which corresponds to a large ratio of the build-up rate to collapse rate. Using these conditions and with the help of some trial and error the following correlation between the two quantities is obtained:

$$w = w_{\max} - \frac{w_{\max}}{[1+(R/\mathrm{b})^{a}]}$$

Where w is the carryover weight, $w_{\max}$ is the maximum possible carryover i.e. 210 grams, R is the logarithm of the ratio of build-up rate to collapse rate, a and b are fit parameter. Here b would roughly be the value of R at which carryover is half of the maximum value and a dictates the slope of the curve.

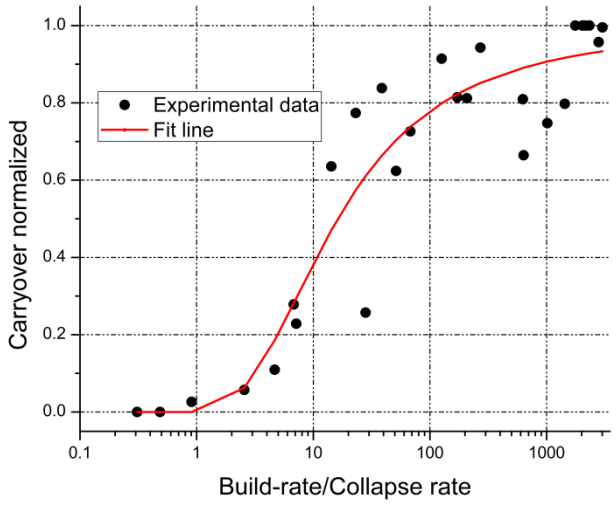

Figure 31: The graph shows the carryover vs build-up/collapse rate for Foamatron with a fit curve.

The fit equation is plotted along with the experiment data in Figure 31**: The graph** The fit parameters a and b for Foamatron are 2.508 and 1.211, respectively, and the fit has an R^2 value of 0.88. Although the correlation holds for Foamatron, in subsequent sections it will be checked whether the other surfactant would follow a similar correlation. Such a relation can possibly eliminate one of the three tests: most probably either the collapse or carryover test can be skipped and estimated using the correlation.

4.1.2.4 Effect of gas velocity and surfactant concentration on foamability

The definition of foamability should reflect the effectiveness with which liquid can be removed. Therefore we defined foamability in 3.1 as the density of the foam in two different ways, one based on superficial gas velocity and the other based on build-up rate.

The results of the foam density calculations are presented in Figure 32 and Figure 33. The definition of foam density based on U_{SG} represents the amount of liquid removed per unit of volume of gas that enters the system. However, this does not represent the density of the foam as not all gas that enters the system is encapsulated in the foam. We therefore define the foam density with the help of the build-up rate which is a better representation of the amount of liquid per unit volume of foam.

In general the foam density based on the build-up rate and on the gas velocity both show an increase with increasing concentration as shown in Figure 32 (a) and Figure 33 (a). This trend suggests that an increase in concentration leads to a larger liquid fraction in foam at the same gas velocity. The effect of the gas velocity on the foam density has a peculiar trend: the foam density for both definitions seems to have a maximum at around U_{SG}=0.02 m/s which occurs for all concentrations. To understand this we look at two effects. Firstly the increase in gas velocity leads to increase in gas momentum which enables the gas to take more liquid along with it. Secondly an increase in gas velocity leads to a decrease in liquid hold up (or increase in gas void fraction) up in the system. The two effects are opposing in context of the foam density: a higher gas velocity on one hand increases the amount of liquid carried along with the gas which increases the liquid content of the foam and hence it increases the foam density. On the other hand the increase in gas void fraction increases the gas content in the foam leading to a decrease in the foam density. We believe that these two counter acting effects are the reason for the occurrence of the maximum in the foam density at a certain velocity.

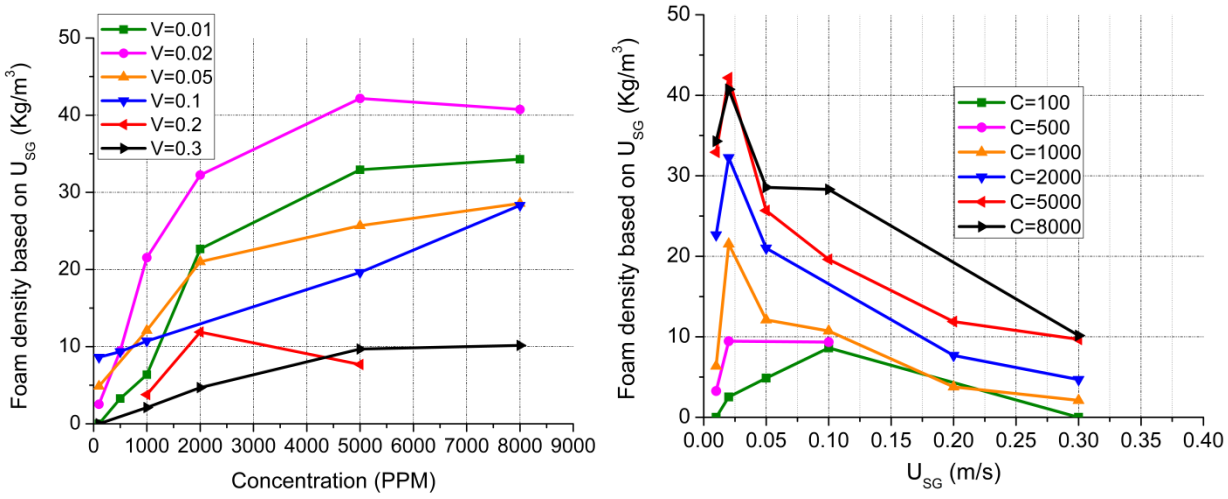

Figure 32: (a) Graph on left shows foam density (based on U_{SG}) with respect to surfactant concentration, (b) Graph on right shows foam density (based on U_{SG}) with respect to superficial gas velocity.

Increasing the gas velocity beyond the velocity where the maximum in the foam density occurs leads to a decrease in the foam density. However, for a foam density based on the build-up rate, the trend looks different at U_{SG}=0.3. The deviation from the regular trend has been a consistent behaviour at U_{SG}=0.3 for the previous results. It therefore becomes necessary to study the possible change in flow regime that leads to such deviations.

4.1.2.5 Regime change at higher gas velocity

Figure 13 in section 2.4 shows various flow regimes that can occur in a bubble column. The flow regime map is shown in Figure 34 where the red line represents the column diameter for the column used in the present thesis. The regime map suggests a regime change from bubble flow to slug flow at U_{SG}=0.06 m/s, however we observe all deviations in results after U_{SG}=0.2m/s. The flow regime map shown in Figure 34 is not a universal flow map and the exact regime transition velocity may differ under different conditions. Table 1 shows various parameters like surface tension, sparger size, etc. that can alter the velocity at which the regime changes occurs. To understand this better we conducted high speed visualization in order to capture the regime changes in the bubble column.

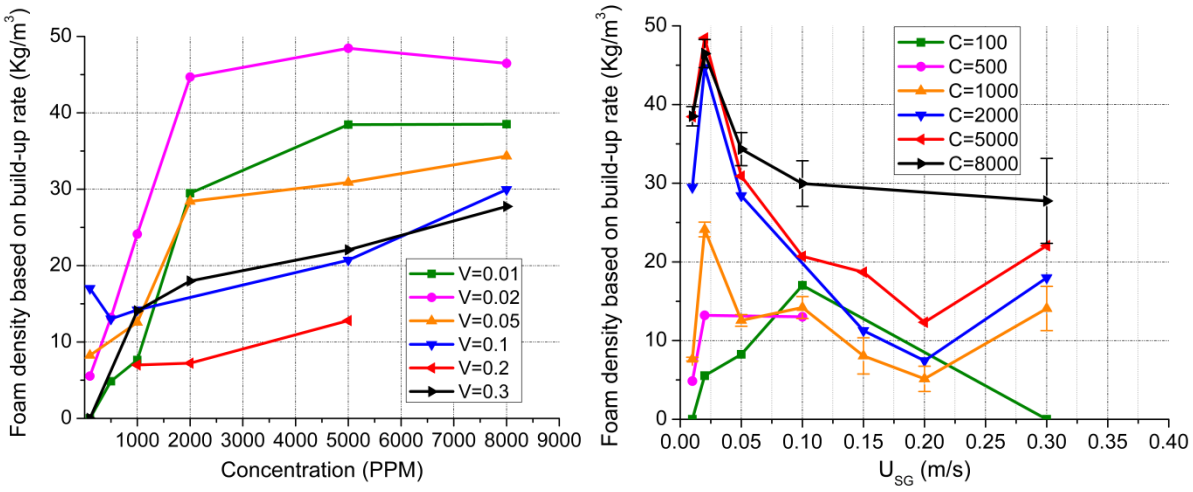

Figure 33: (a) Graph on left shows foam density (based on Build-up rate) with respect to surfactant concentration, (b) Graph on right shows foam density (based on Build-up rate) with respect to superficial gas velocity.

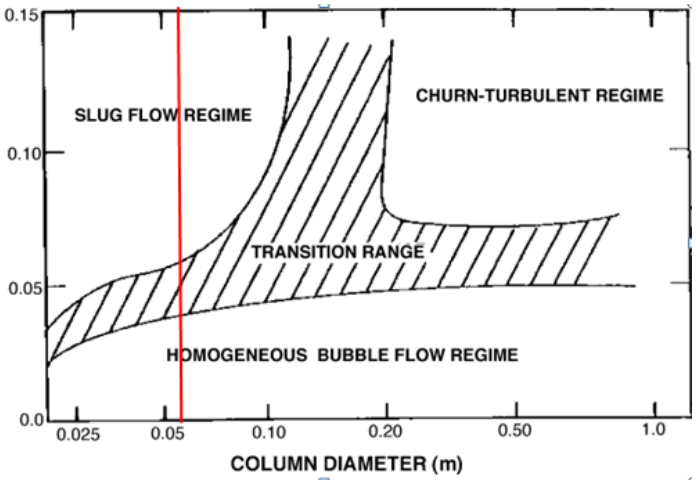

Figure 34: Flow regime map for bubble flow in a liquid column, the red line represents the column diameter for the Foam setup used in the study.

4.1.2.6 High speed visualization of bubble column

To understand the regime change in the bubble column we conduct a flow visualization at different superficial gas velocities for three solutions: deionized water, 500 ppm foamatron solution and 2000 ppm foamatron solution. The results of the visualization for deionized water are shown in Figure 35, where the bubble flow regime can be observed at U_{SG}=0.01 and 0.05 m/s. However after U_{SG}=0.05 m/s a significant coalescence in the bubbles can be observed leading to a larger bubble size. A large bubble can be observed at U_{SG}=0.2 and 0.3 m/s which

marks the end of the transition from bubble flow to slug flow. Hence a regime change for deionized water can be observed at around a superficial gas velocity of 0.15-0.2 m/s.

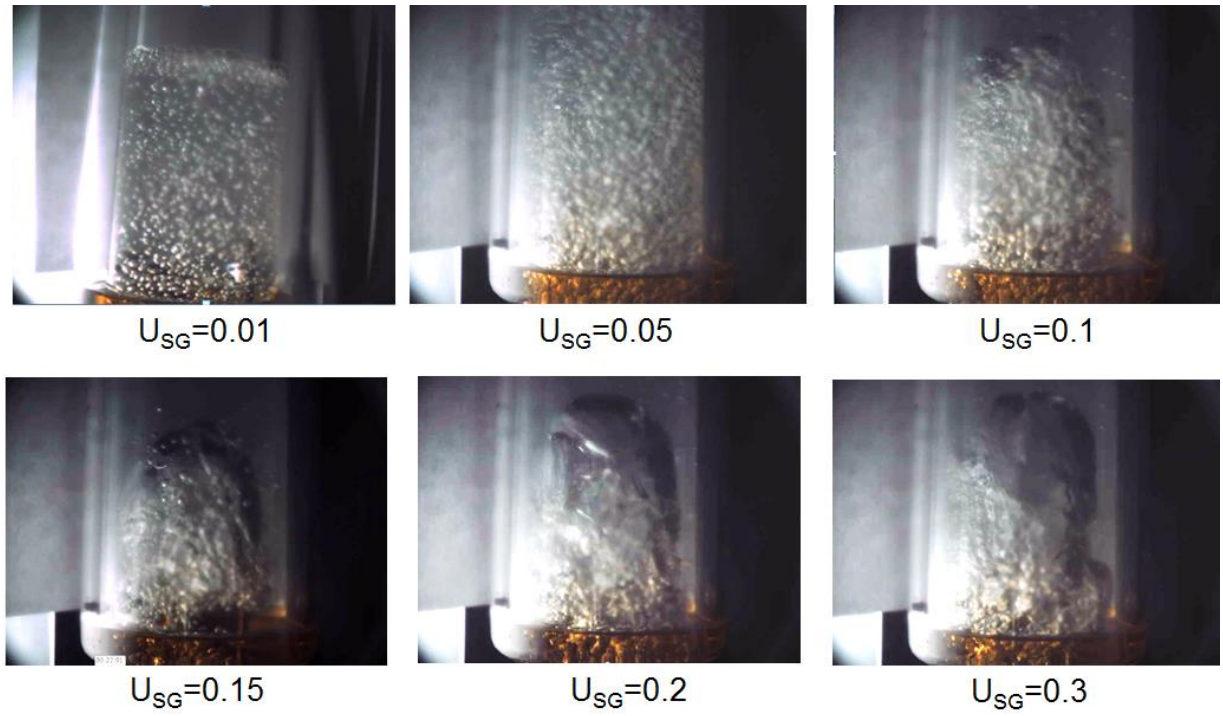

Figure 35: Snapshots of high speed flow visualization in the Foam setup for different superficial gas velocities.

The results for the flow visualization at different surfactant concentrations are shown in Figure 36. At U_{SG}=0.01 m/s a marked reduction in bubble sizes can be observed for increasing surfactant concentration. This adds to the explanation of a more stable foam at higher surfactant concentration solutions. It is not just the reduction in surface tension which makes the foam film more stable, also the reduction in bubble size due to an increase in concentration has a significant effect on the drainage and hence on the collapse rate (for details see appendix A). At U_{SG}=0.15 m/s, again a significant difference in bubble size is observed for increasing concentration. The large bubble appearing for deionized water does not appear for surfactant solutions. Although for U_{SG}=0.3 m/s a large bubble can be observed for all solutions. Hence the transition from bubble flow to slug flow happens somewhere between 0.15-0.3 m/s. It is evident that there exists a change in flow regime before U_{SG}=0.3 m/s where deviations were observed in previous results.

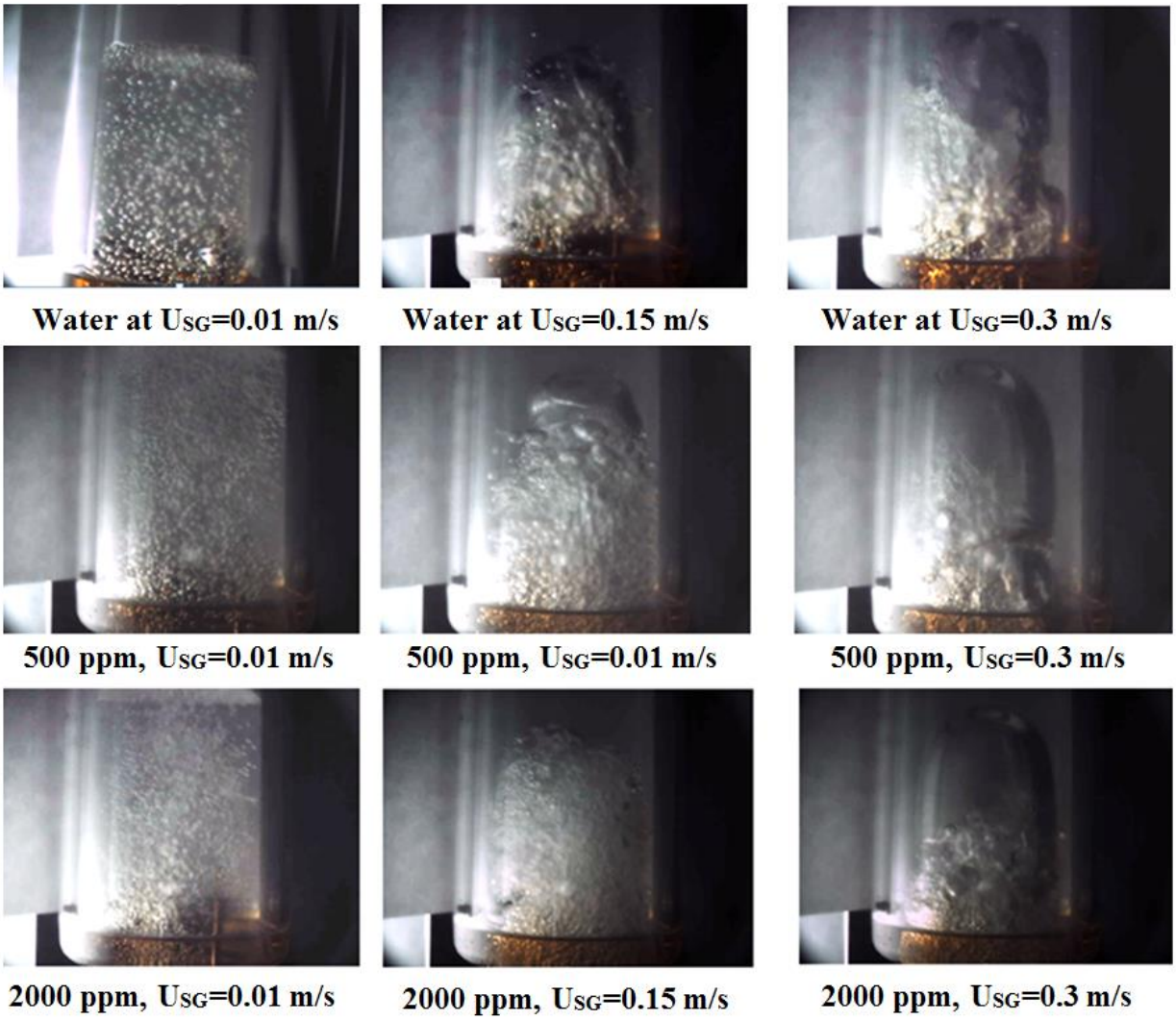

Figure 36: Snapshots of high speed visualization at different concentration and gas velocity, the top row shows the results for deionized water, the middle row shows results for 500 ppm solution and the bottom row show results for 2000 ppm solution.

An unexpected reduction in build-up rate, carryover and increase in foam density at U_{SG}=0.3 m/s were reported in earlier discussions. To understand why a change in flow regime can cause an unexpected change in build-up rate and an increase in foam density we visualized the surfactant solution-gas interface in the bubble column to observe the effect of flow regime transition on the foam formation. Sequences of images are reported in Figure 37 (for surfactant concentration 500 ppm) which shows a large bubble (at the start of flow inside the column) leaving the liquid-gas interface and the subsequent events that lead to foam formation.

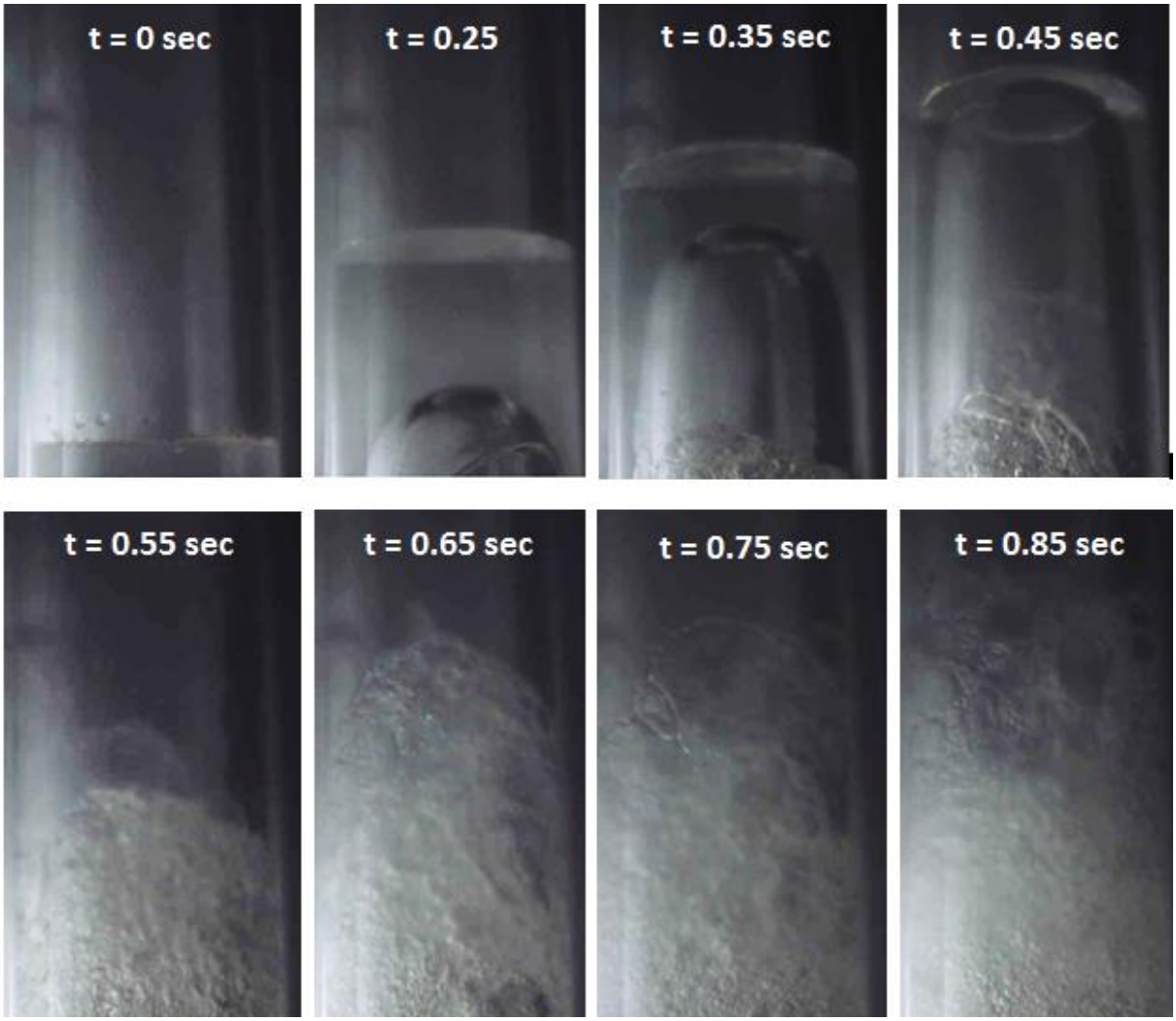

Figure 37: Sequence of images showing the Taylor bubble leave the liquid-gas interface and the subsequent foam formation.

The interface is visible at t=0 second at the bottom of the image; when the gas flows into the liquid column, the interface starts to rise. At t=0.25 seconds, the Taylor bubble is visible in the liquid column and approaches the interface. At t=0.45 seconds the bubble touches the interface and the liquid around the bubble flows down the periphery of the pipe. This downward flowing liquid falls on the rest of the liquid going upwards leading to the formation of foam due to mixing. The foam is then observed to rise upwards with a churning motion. This sequence of images show that the gas in the large bubble escapes as the bubble crosses the interface. This suggests that the amount of gas that enters the system and the amount of gas that is encapsulated inside the foam are significantly different (gas escapes the interface). Hence the foam does not build up with the same rate as the gas enters the system, which explains the low ratio of the

build-up rate to the superficial gas velocity ratio for high velocities. The formation of foam is partly a consequence of the liquid in the larger bubble falling on the rest of the liquid which seems similar to the foam formation in a shaker.

4.1.2.7 Effect of pressure on build-up rate, collapse rate and carryover

The present thesis includes a study of the effect of pressure on the three tests conducted in the small scale sparger setup. The pressure is varied from 1 bar to 10 bar. The gas velocity and surfactant concentrations for which the high pressure tests are conducted are given in **Table 6**.

The effect of the pressure on the build-up rate at a surfactant concentration of 100 ppm and 2000 ppm is presented in Figure 38 (a) and Figure 38 (b), respectively. The variation in pressure does not seem to have a significant effect on the build-up rate. The effect of pressure on the carryover weight for a surfactant concentration of 100 ppm and 2000 ppm is presented in Figure 39 (a) and Figure 39 (b), respectively. The variation in pressure does not seem to have any significant effect on the carryover weight.

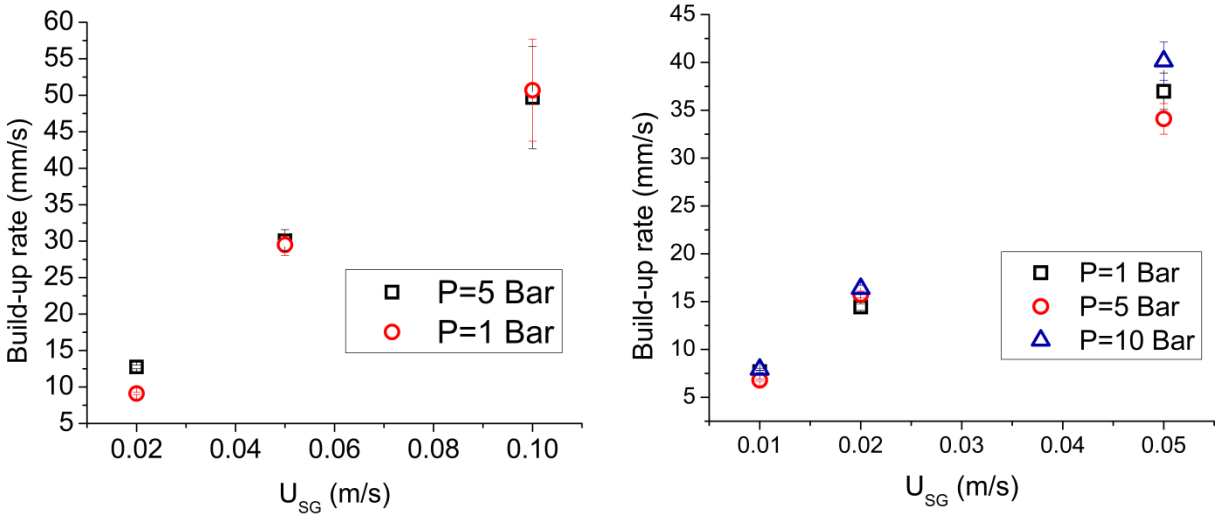

Figure 38: (a) Build-up rate with respect to U_{SG} for different pressures (1 and 5 bar) at surfactant concentration 100 ppm with error bars on left, (b) build-up rate with respect to U_{SG} for different pressures (1, 5 and 10 bar) at surfactant concentration 2000 ppm with error bars on right.

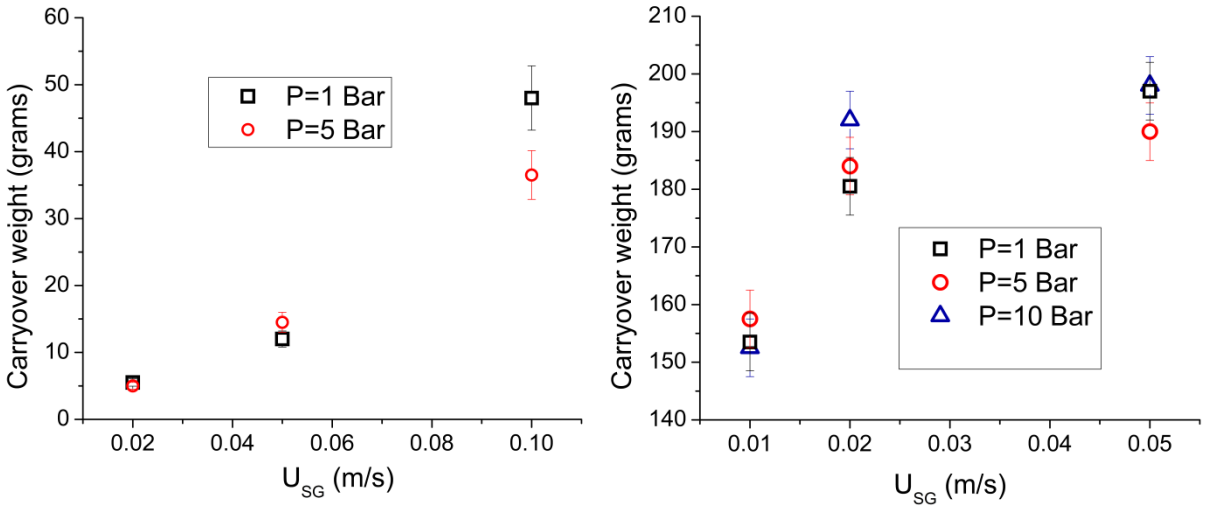

Figure 39: (a) Carryover weight with respect to U_{SG} for different pressures (1 and 5 bar) at surfactant concentration 100 ppm with error bars on left, (b) carryover weight with respect to U_{SG} for different pressures (1, 5 and 10 bar) at surfactant concentration 2000 ppm with error bars on right.

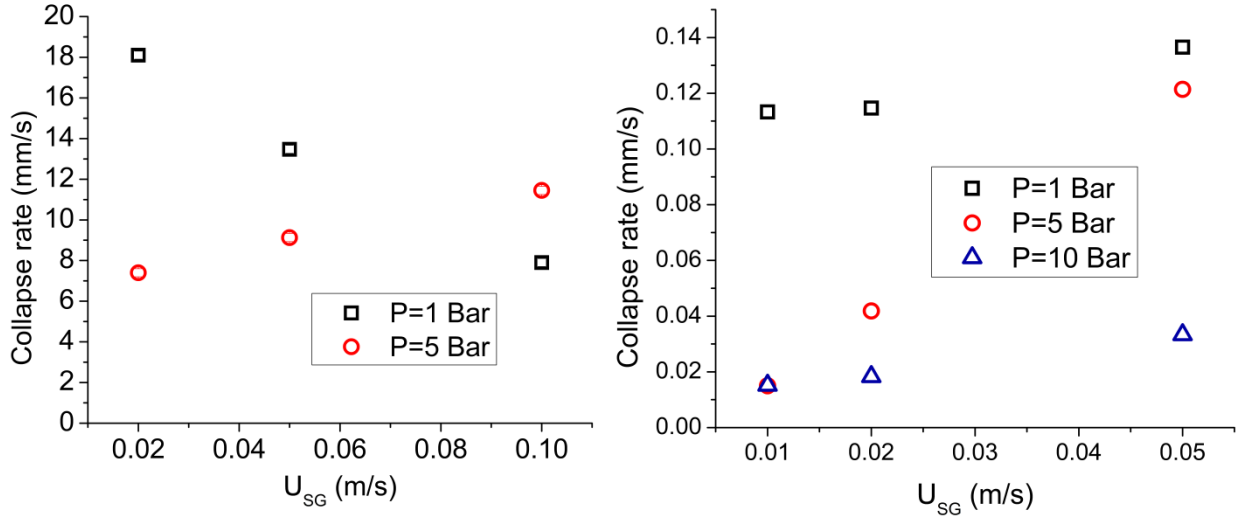

Figure 40: (a) Collapse rate with respect to U_{SG} for different pressures (1 and 5 bar) at surfactant concentration 100 ppm with error bars on left, (b) collapse rate with respect to U_{SG} for different pressures (1, 5 and 10 bar) at surfactant concentration 2000 ppm with error bars on right.

The effect of the pressure on the collapse rate for a surfactant concentration of 100 ppm and 2000 ppm is presented in Figure 40 (a) and Figure 40 (b), respectively. The collapse rate at 100 ppm seems to differ at the two pressures. The difference is significant but the collapse at low surfactant concentrations is quick and chaotic. This makes the repeatability of the collapse test

somewhat difficult for lower concentrations. Therefore the difference in collapse could be a result of the low repeatability.

However, the results of the collapse test at 2000 ppm for various pressures show a significant difference. The collapse rate of the foam has a direct dependence on the drainage rate which in turn depends on the size of the bubbles in the foam (see appendix A). To understand how an increase in pressure decreases the collapse rate with such a significant amount, we consider the coarsening property of foams. The coarsening in foam is due to the diffusion of gas from smaller bubbles that have a relatively high pressure to larger bubbles that have a lower pressure. The result is an increase in the average size of the bubbles in the foam; which in turn increases the drainage rate making the foam less stable. However if the pressure of the gas increases the diffusion coefficient of the gas reduces by the following relation as given in [57]:

$$\frac{D_{P1}}{D_{P2}} = \frac{\rho_{P2}}{\rho_{P1}}$$

- D_{P1} and ρ_{P1} are the diffusion coefficient and gas density at pressure P1
- D_{P2} and ρ_{P2} are the diffusion coefficient and gas density at pressure P2.

The relation above would suggest that increasing the pressure would lead to a reduction in the diffusion coefficient and hence it would slow down the coarsening rate. A slower coarsening rate would mean that the increase in the average bubble size would be delayed, leading to a relatively lower drainage rate and hence it would give a more stable foam. Images from the collapse tests are shown in Figure 41, Figure 42 and Figure 43 at U_{SG}=0.01, 0.02 and 0.05 m/s, respectively for a surfactant concentration of 2000 ppm at three different pressures (1, 5 and 10 bar). At U_{SG}=0.01 m/s (Figure 41) a clear effect of the pressure on the foam collapse can be observed. There seems to be a drastic difference between the collapse height and the quality of the foam when the pressure is increased from 1 bar to 5 bar which is also evident from Figure 40 (b). For U_{SG}=0.01 m/s, no significant difference is observed between 5 and 10 bar; because the foam is already quite stable at 5 bar, not much difference occurs for the foam stability when the pressure is increased. Similar results that show the better foam stability can be seen in Figure 42 and Figure 41.

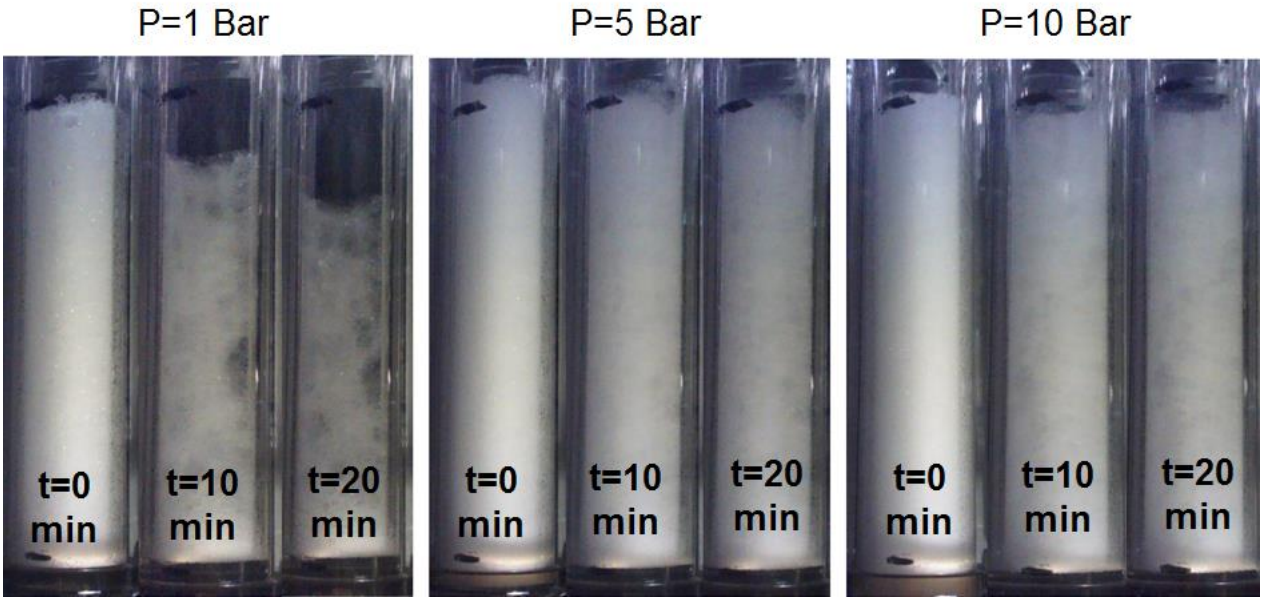

Figure 41: Images from collapse test at surfactant concentration 2000 ppm and U_{SG}=0.01 m/s for three pressures (1, 5, 10 bar) at t=0, 10 and 20 minutes.

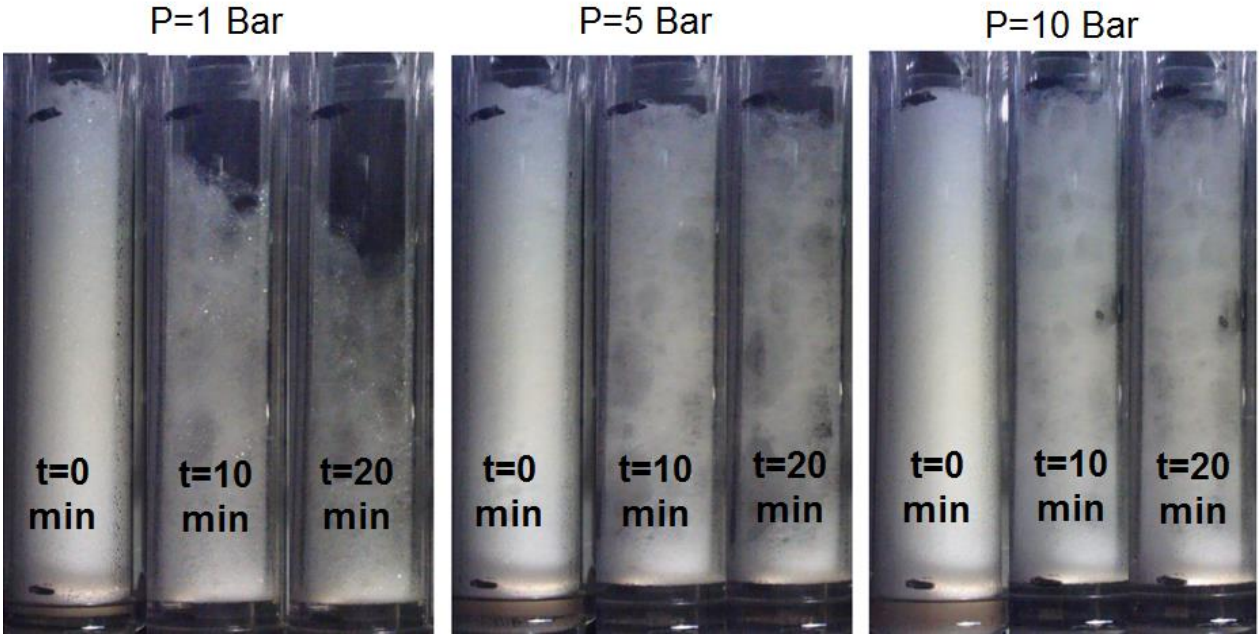

Figure 42: Images from collapse test at surfactant concentration 2000 ppm and U_{SG}=0.02 m/s for three pressures (1, 5, 10 bar) at t=0, 10 and 20 minutes.

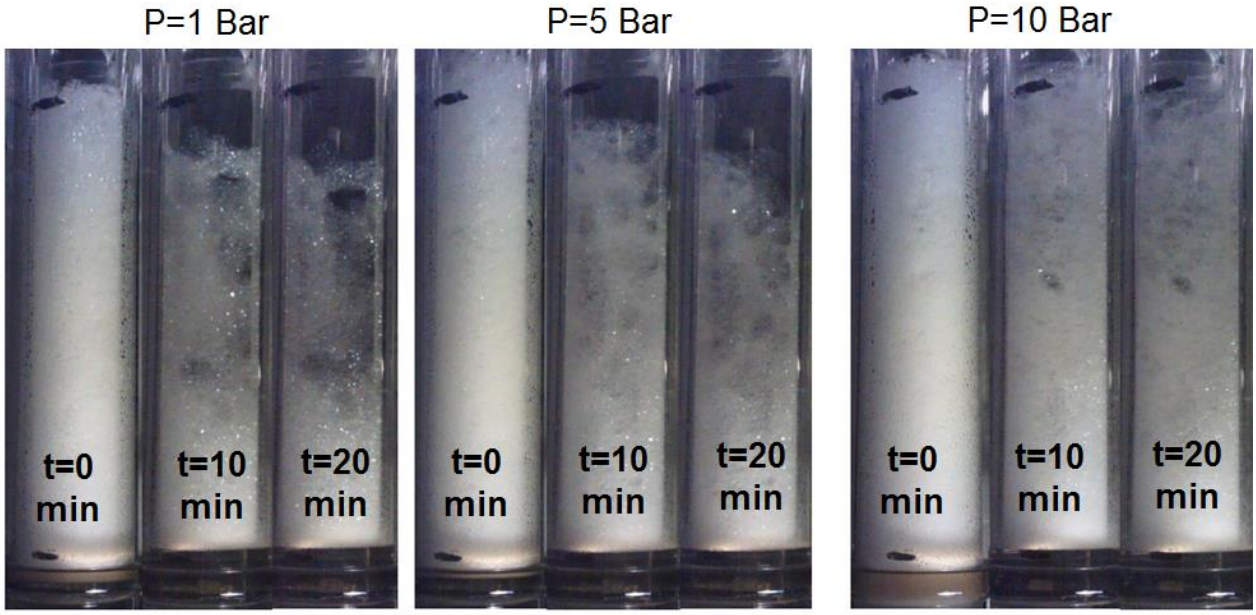

Figure 43: Images from collapse test at surfactant concentration 2000 ppm and U_{SG}=0.05 m/s for three pressures (1, 5, 10 bar) at t=0, 10 and 20 minutes.

4.2 Trifoam Block 820 results

Trifoam block 820 is another commercial surfactant used in this study. In this section we describe and discuss the results for Trifoam block 820 (TB820) and its comparison with Foamatron.

4.2.1. Dynamic surface tension for Trifoam Block 820

The dynamic surface tension results for Trifoam block 820 are presented in Figure 45. The surfactant concentration is varied from 100 ppm to 1500 ppm. The results for the dynamic surface for TB820 are obtained from [2]. The DST curve consists of two gradients separated by the red line.

The comparison between the two surfactants as shown in Figure 45 suggests that Foamatron has a lower surface tension compared to TB820 in the range of concentrations considered. However, the rate of the reduction of the surface tension could be larger for TB820 as compared to Foamatron depending on the surface age at which the rate is calculated.

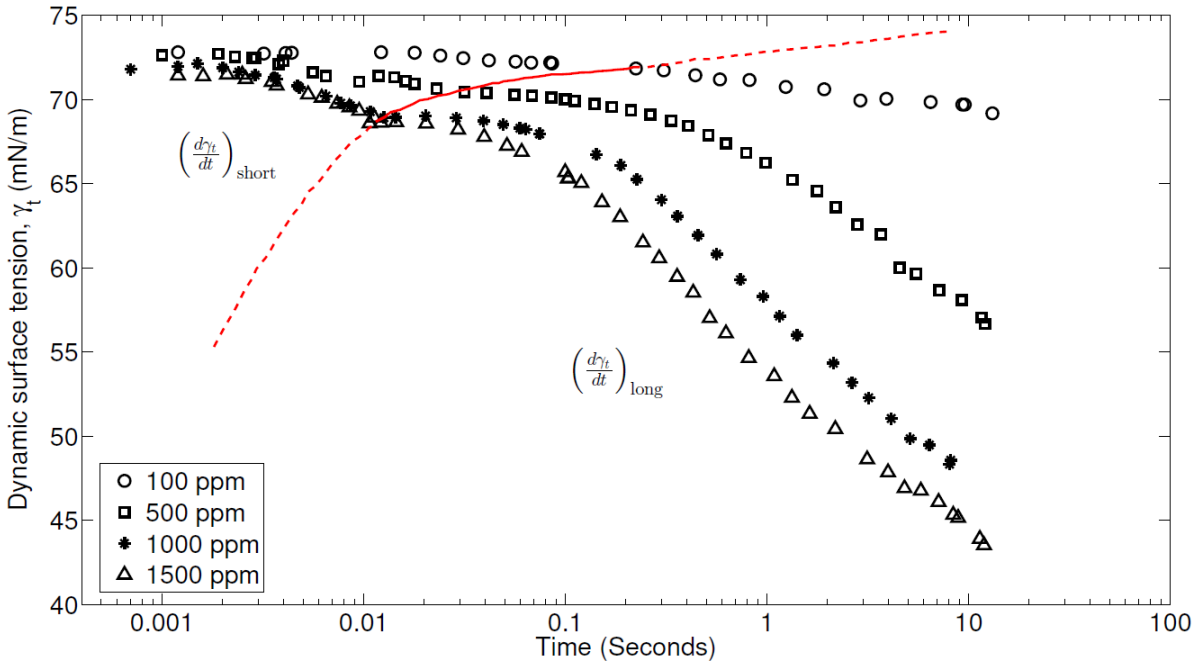

Figure 44: Dynamic surface tension curve for Trifoam Block 820 (source: [2]).

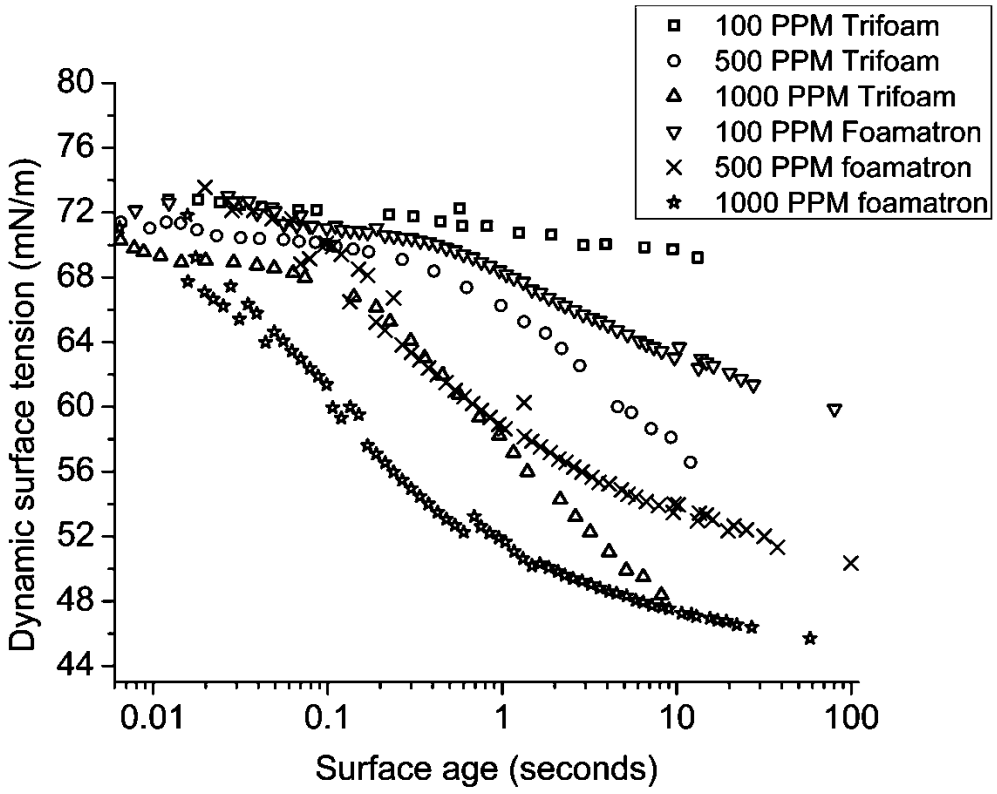

Figure 45: Dynamic surface tension curves for Trifoam Block 820 and Foamatron at a surfactant concentration of 100, 500 and 1000 ppm.

4.2.2. Foam setup results for Trifoam Block 820

We study the effect of the gas velocity and surfactant concentration on TB820 in the small scale sparger setup by conducting three tests: build-up test, collapse test and carryover test. The experiments are conducted for three superficial gas velocities: 0.01, 0.05 and 0.3 m/s. Three surfactant concentrations are used for each of the superficial gas velocities: 100, 500 and 1000 ppm. The pressure is maintained at atmospheric level and no variation with respect to the pressure is tested for TB820.

4.2.2.1 Effect of gas velocity and surfactant concentration on the build-up, carryover and collapse tests

The build-up rate and the carryover weight are shown in Figure 46 (b) and Figure 47, respectively; the results for both tests do not show large differences for the two surfactants. However, the difference in build-up rate and carryover weight for the two surfactants is more prominent for the lower velocity. This could be attributed to the fact that the collapse rates are significantly different for the two surfactants and at lower velocities the effect of collapse rate is relatively higher. Figure 46 (a) shows the variation of the collapse rate with respect to U_{SG} at surfactant concentrations of 100, 500 and 1000 ppm for TB820 and Foamatron. The variation for the collapse rate shows a similar trend as Foamatron, i.e. an increase in collapse rate with decreasing concentration. However, the collapse rates for TB820 are significantly lower than that of Foamatron. Considering that the surface tension is an important quantity in defining the foam stability, the lower collapse rate for TB820 is surprising since the surface tension of TB820 is larger than that of Foamatron for the same surface age. To understand this we consider the process of foam collapse: drainage of liquid through the plateau border is an important event when defining the foam collapse; a faster drainage would in general lead to a faster collapse. But drainage is not the only defining criterion, as was also mentioned in [33]. There exists a critical liquid fraction at which the foam collapses. Both parameters, the drainage rate and the critical liquid fraction, play a crucial role in defining the stability of the foam. Although we do not have the instruments to measure the liquid fraction (the critical liquid fraction is approximately 0.0001), we can roughly quantify the drainage based on the amount of free liquid present below the foam.

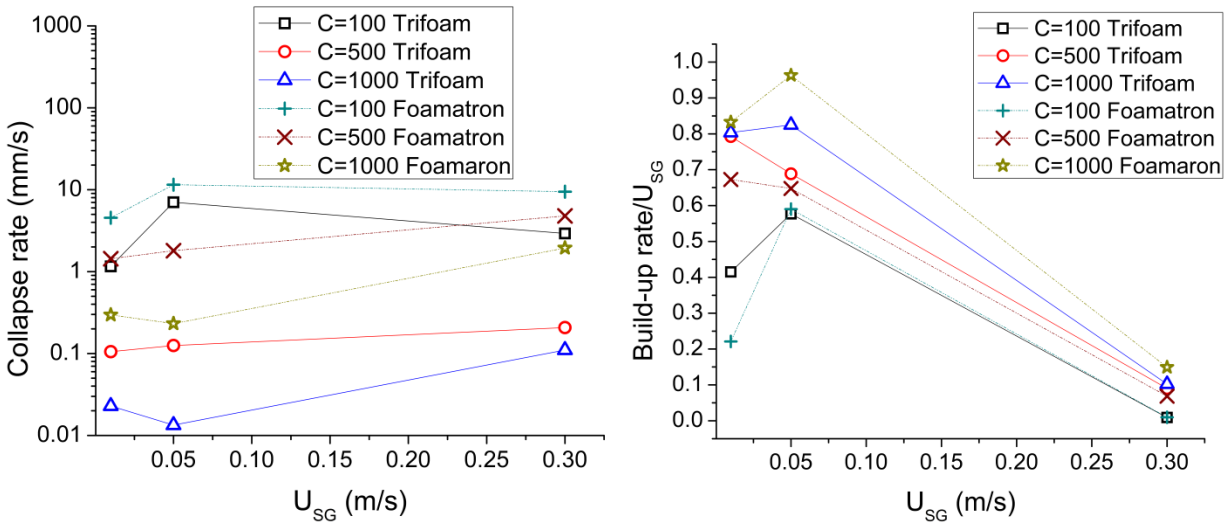

Figure 46: (a) Collapse rate with respect to U_{SG} for surfactant concentration 100, 500 and 1000 ppm for Foamatron and Trifoam Block 820 on left, (b) build-up rate with respect to U_{SG} for surfactant concentration 100, 500 and 1000 ppm for Foamatron and Trifoam Block 820 on right.

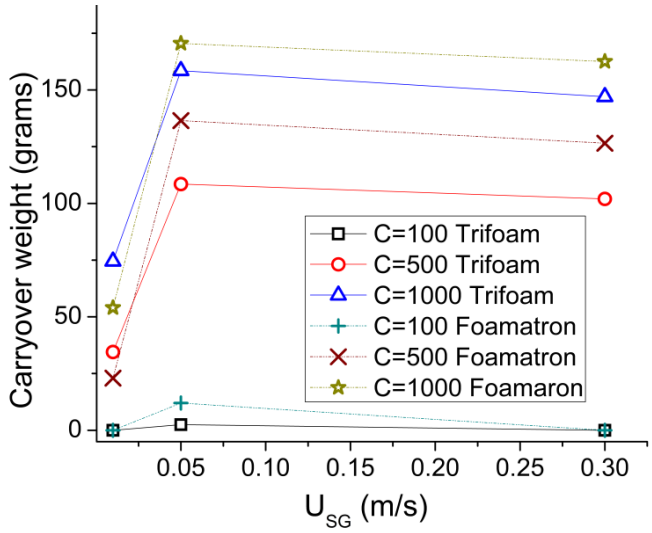

Figure 47: Carryover weight with respect to U_{SG} for surfactant concentration 100, 500 and 1000 ppm for Foamatron and Trifoam Block 820.

After the completion of the build-up test and the start of the collapse test, the foam starts to drain and the interface between the free liquid and foam starts to rise. This interface rise is captured using image processing technique in MATLAB v2014b and the results for Foamatron and TB820 at surfactant concentration 500 ppm and 1000 ppm are presented in Figure 48 (a) and (b), respectively. It can be observed that the two surfactants lead to nearly the same interface rise with respect to time for 500 ppm, and TB820 drains faster than Foamatron for 1000 ppm

solution. This would suggest that the drainage rate of TB820 is either the same or larger than that of Foamatron depending on the conditions. However, the data for the collapse rate and Figure 49 clearly show that the collapse rate for TB820 is much lower than that for Foamatron. The drainage rate in foam has a direct and significant influence on the collapse of foam; a foam with faster draining is supposed to collapse faster, which is contrary to what we observe.

One would expect that a foam showing larger drainage and better stability would have a lower critical liquid fraction at which the bubbles break. As described in [33], the critical liquid fraction of foam is a function of the nature of the surfactant and of its concentration. It could be postulated that Trifoam has a smaller critical liquid fraction compared to Foamatron. Since we do not know the precise composition of the surfactant that we use, it is difficult to find out why the two surfactants might have a different critical liquid fraction. The whole argument of the existence of a critical liquid fraction revolves around the T1 & T2 rearrangement that occurs in foam as given in [34]. These T1 & T2 events are related to the rearrangement and reconfiguration of bubbles in foam. The empirical formulae suggested in [34] for the critical liquid fraction has an inverse relationship with the time scale of these events. Hence a study of these events and of their time scales for different surfactant may help to understand why foam stability differs for different surfactants at the same conditions.

4.2.2.2 Relation between build-up rate, collapse rate and carryover

Finally we consider the ratio of the build-up rate and the collapse rate with respect to the carryover weight for both surfactants according to the following equation in Figure 50:

$$w = w_{\max} - \frac{w_{\max}}{[1+(R/\mathrm{b})^{a}]}$$

The fit parameters a and b are found to be 3.469 and 2.428 respectively and the R^2 value for the fit is 0.8624. The fit parameters for TB820 are very different from the fit parameters for Foamatron and thus the fit seems to be surfactant dependent.

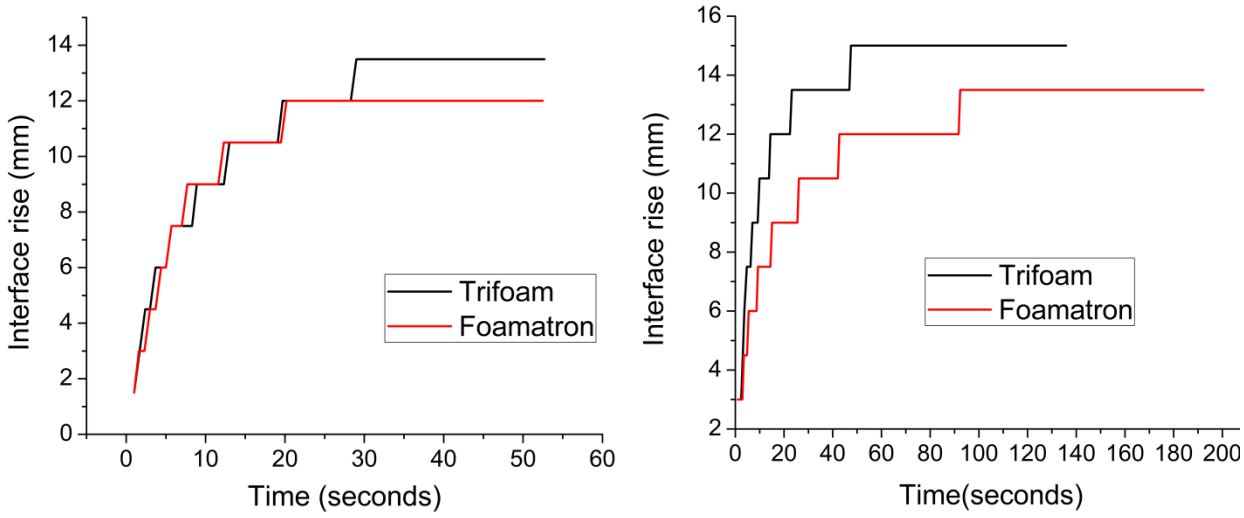

Figure 48: (a) Interface (foam-free liquid) rise with respect to time for Foamatron and TB820 at 500 ppm on left, (b) for Foamatron and TB820 at 1000 ppm on right.

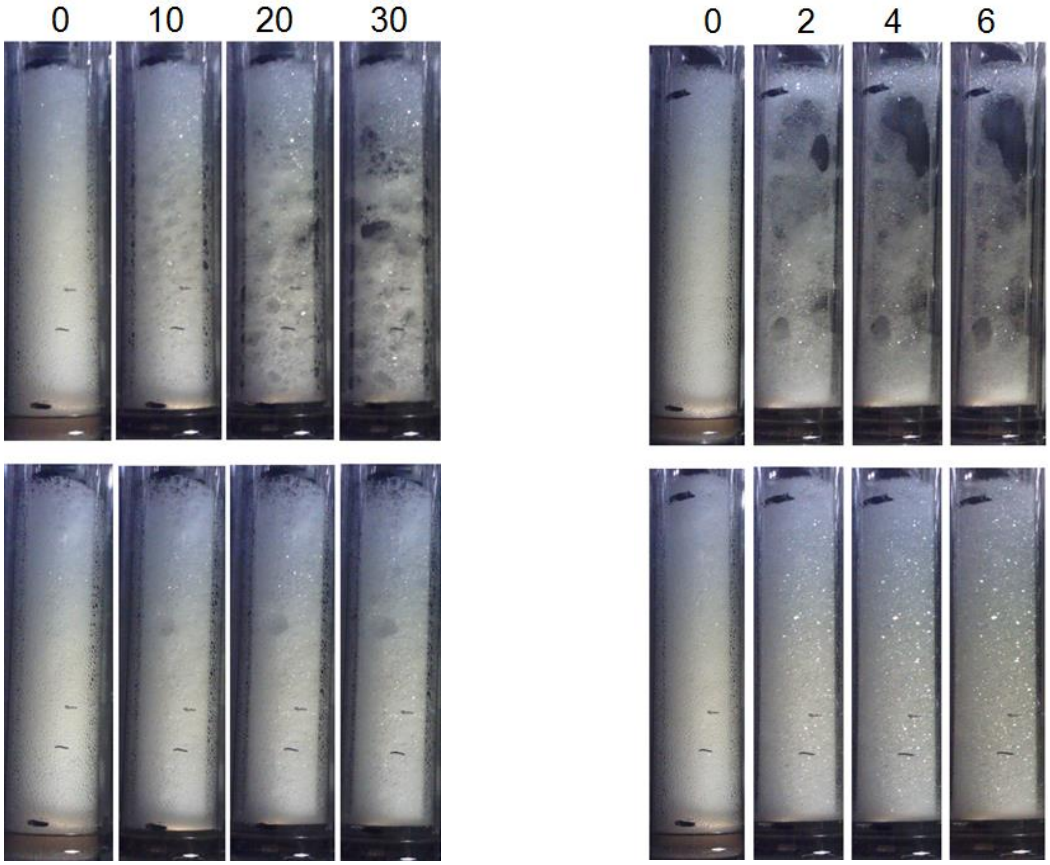

Figure 49: (a) The set of pictures on the left are from collapse test at 500 ppm, the images on top are for Foamatron and the bottom are for TB820, number on the top represents time in seconds, (b) The set of pictures on the right are from collapse test at 1000 ppm, images on top are for Foamatron and the bottom are for TB820, number on the top represents time in minutes.

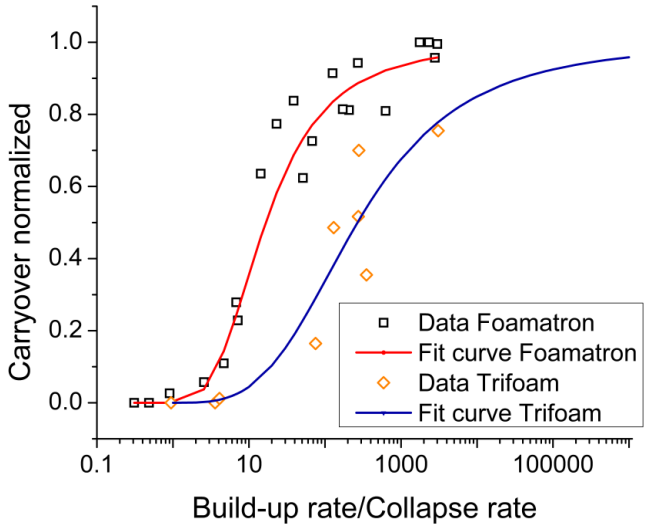

Figure 50: Fitted curve for relation between carryover and build-up rate/collapse rate for TB820 and Foamatron.

4.3 Overall comparison of small scale sparger test and flow loop setup

Through conducting various measurements with the small scale setup, we have obtained insight into the effect of parameters like gas velocity, surfactant concentration and pressure on the foam formation and stability. However there has been some debate as to whether the sparging setup properly represents the foam behaviour at the large scale of the well in operation (or the flow loop setup, i.e. the intermediate scale) and whether it thus can be used to make a good selection of a foamer for field operation. In this section we will compare the insights from the small scale sparger setup with the results from the flow loop measurements [39]. We will try to answer whether a small scale sparger setup is a suitable device for selecting foamers for field operation.

In gas wells, the onset of liquid loading starts with the transition from annular flow to churn flow when the gas velocity has become insufficient to lift the liquid film and liquid droplets to maintain the annular flow regime. The surfactant solution should in principle only be used once the flow regime transition to churn flow occurs, as the use of a foamer in the annular flow regimes leads to an unnecessary increase in pressure drop. The basic outcome of using foamers in the churn flow regime (or even in the slug flow regime) should be a transition back to the annular flow regime, which mitigates liquid loading. Such a transition was studied in a flow loop setup in [39] and the results are shown in Figure 51 and in Figure 52. The flow pattern transitions suggest that the use of a surfactant reduces the superficial gas velocity at which the transition from annular flow to churn flow occurs. More importantly increasing the surfactant

concentration decreases the superficial gas velocity at which the transition occurs. This observation can be made for both flow maps in Figure 51 and Figure 52 at superficial liquid velocity of 2 mm/s and 50 mm/s, respectively. The change of flow regime from slug flow, to churn flow, and to annular flow should also include a consistent decrease in the liquid hold-up in the system. In other words, when using different surfactant concentration at the same gas and liquid superficial velocities, the concentration that shows a lower liquid holdup should be considered more effective in unloading liquid from the well. Figure 53 clearly shows that the liquid hold-up for the same superficial liquid and gas velocities is lower for higher surfactant concentration. A similar effect can be observed in the small scale sparger setup used in the present study; increasing the concentration increases the carryover weight of the liquid as shown in Figure 54 (b). The increase in carryover in the small scale setup represents the ability of the surfactant to foam and to unload more liquid, which is similar to the effect of the increasing concentration in the flow loop setup, where the decrease in liquid hold-up also represents the ability of the surfactant to carry more liquid to the top.

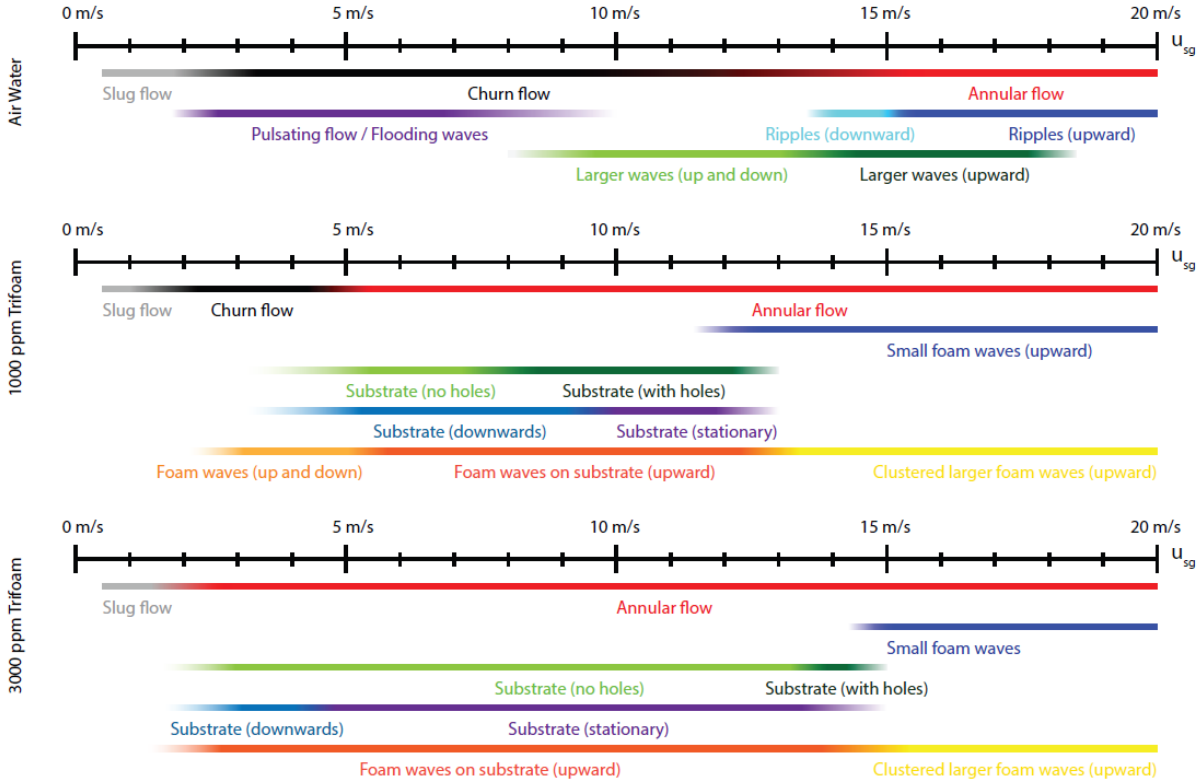

Figure 51: Schematic indicating the flow pattern transitions and the morphological features of the flow patterns at a superficial liquid velocity of 2 mm/s (source: [39]).

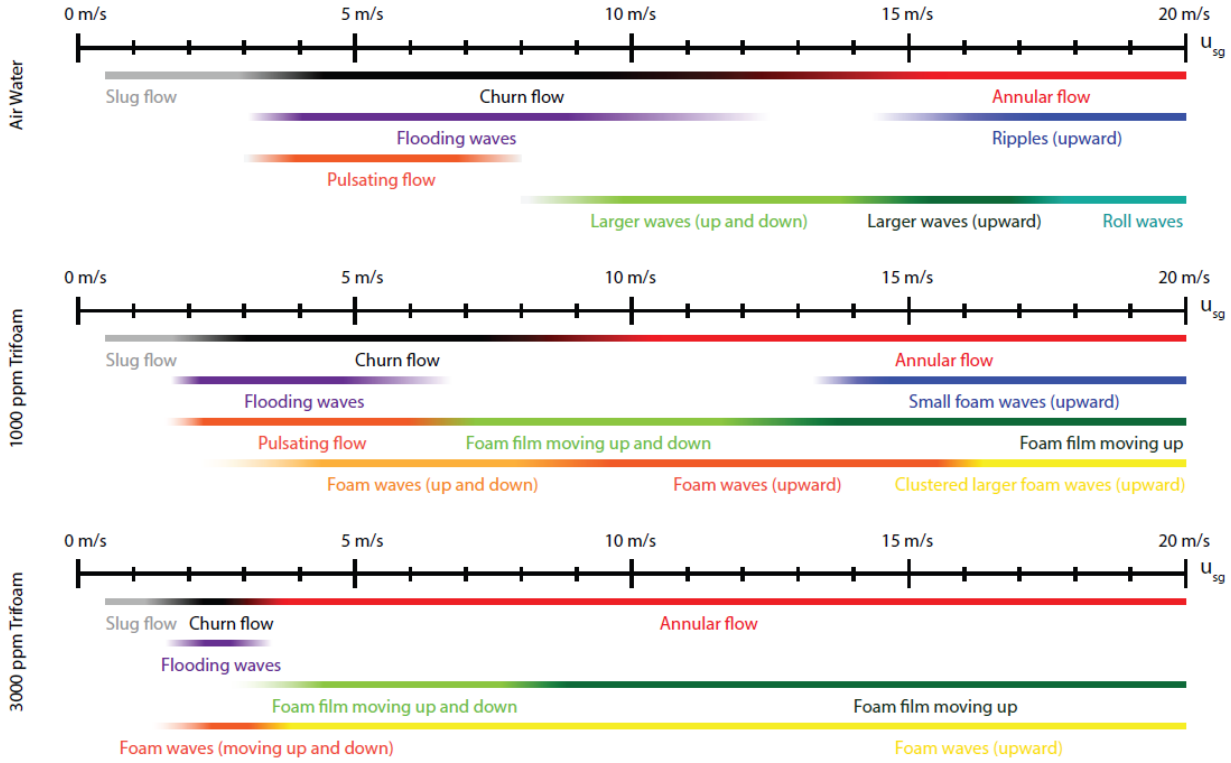

Figure 52: Schematic indicating the flow pattern transitions and the morphological features of the flow patterns at superficial liquid velocity 50 mm/s (source: [39]).

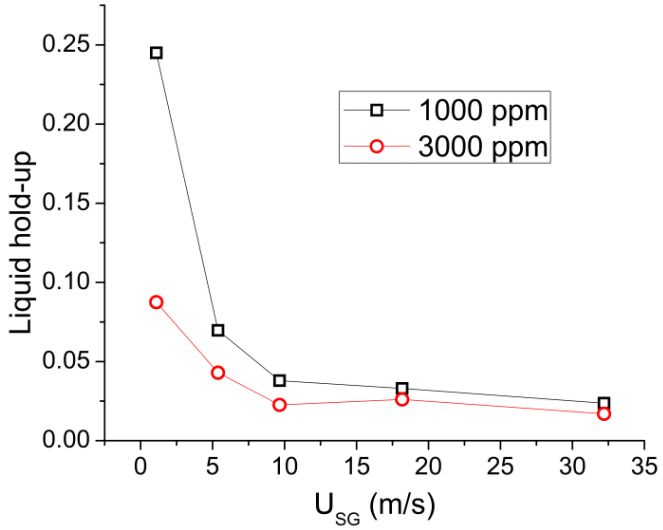

Figure 53: Liquid hold-up with respect to the superficial gas velocity for Trifoam Block 820 at two different concentrations in the flow loop setup at superficial liquid velocity 10 mm/s (data source: [39]).

The above discussion suggests that using different concentrations of the solution affects the ability of the gas to carry more liquid in both the small scale sparger setup and in the flow loop setup. The effect of using different concentrations of the surfactant on the carryover test can be

observed in the small scale setup similar to the way that is found in the flow loop setup in context of liquid unloading. However the carryover test in the small scale sparger setup gives two important quantities: the rate of carryover and the weight of carryover. We will discuss the importance of these two quantities in the foamer selection. We find that the rate of carryover (in the linear region of the carryover curve) is largely dependent on the build-up rate (all points in the Figure 54 (a) can be fitted with a single line) and it has a weak correlation with the concentration as seen in Figure 54 (a). However the carryover weight in Figure 54 (b) shows a significant increase with increasing concentration. It is expected that the ability of the surfactant to unload more liquid should increase significantly as we increase the surfactant concentration (a similar trend is noticed for flow loop setup). But at higher build-up rates the amount of liquid unloaded becomes less dependent on the concentration as the limit of carryover is reached (the maximum amount of carryover possible). We can observe that the carryover weight represents the effect of a surfactant better than the carryover rate and hence should be a more appropriate criterion for selecting foamers. However it is still not clear as to what gas velocity should the carryover test should be conducted in the small scale sparger test to produce results more representative of the conditions at the large scale. It can be argued that the flow pattern at U_{SG}=0.3 with surfactant as shown in Figure 37 is a churning motion which closely represents the flow hydrodynamics at the large scale (the onset of liquid loading happens in the churn flow regime at large scale). However it should be noted that the carryover at higher velocity (or build-up rates), as shown in Figure 54(b), generally reaches the maximum possible carryover, which makes it difficult to differentiate the effect of the concentration. Hence conducting a carryover test at lower gas velocities would be a better way to select foamers, although the downside is the difference in the flow morphology as compared to the flow loop setup. Considering that the flow morphology at U_{SG}=0.3 is close to what is seen in the flow loop setup, it would be beneficial to find a way to conduct the test at higher velocities without reaching the maximum of the carryover weight i.e. the interpretation of results are not affected by the limit of carryover. One possible way could be to increase the height of the sparger setup. With the above discussion we suggest that the carryover test might represents the ability of the surfactant in unloading the liquid and it shows similar trends as the flow loop setup in context of liquid unloading.

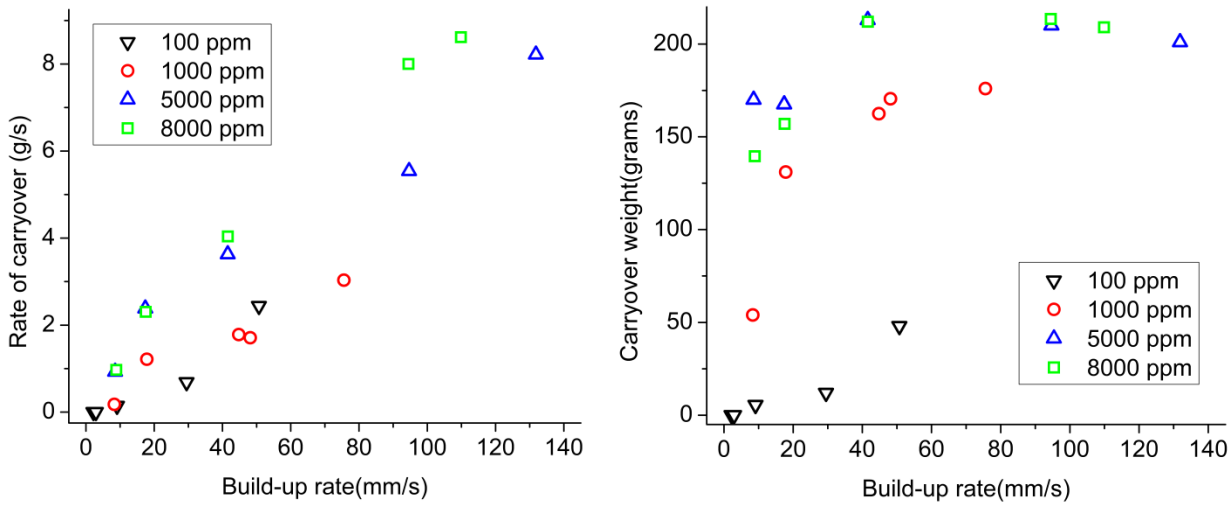

Figure 54: (a) Rate of carryover with respect to build-up rate for different surfactant concentrations for Foamatron on left, (b) Weight of carryover with respect to build-up rate for different surfactant concentrations for Foamatron on right.

But the authors in [39] suggested that the sparger setup is not a good predictor of the foaming behaviour in the flow loop setup. Hence it would be wise to consider and analyse the reasoning given in [39] as well. Two reasons are given why the sparger setup is not a good predictor given in [39] are:

1) "The hydrodynamics of the foam formation are very gentle, leading to relatively large bubbles of equal size that rise slowly to the liquid-foam interface. Therefore, all bubbles are incorporated into a stable foam, and the volume of the created foam is determined only by the surfactant depletion. Because of the relatively large bubble size, already at relatively low surfactant concentrations all the liquid is incorporated into the foam. It is therefore difficult to characterise the surfactants by the volume of foam created in this test".
2) "For low concentrations, the water content of the foam increases with increasing concentration, while at high concentrations, the water content of the foam decreases with increasing concentration in the small scale setup. Such non-monotonic behaviour is not observed in the flow loop".

The first reason states that it is difficult to characterize the surfactant on the basis of the volume of foam created per unit liquid. As shown previously, we found that the carryover test results might be used to characterize foamers and possibly make a selection. Although it should be

noticed that the objective of [39] was to use the amount of foam formed as an input to a mechanistic model for predicting the pressure drop whereas we are interested in a standardized test to qualitatively select foamers. The foamer selection should not only be based on the ability of the surfactant to unload the liquid but also on the effect of the surfactant on pressure drop. The pressure drop model suggested in [39] takes the amount of foam formed per unit liquid as an input. The amount of foam formed per unit liquid can also be defined as the reciprocal of the foam density. In flow loop setup, the foam density decreases on increasing concentration whereas in case of small scale sparger setup the foam density increases on increasing concentration. This suggests that the results from small scale sparger setup might not be useful in predicting pressure drop. However, it should be noted that the foam densities in [39] are unusually high.

We observe that the small scale sparer setup can be used as a measure of the ability of surfactant in unloading liquid but might not be a good predictor for pressure drop. The selection of a foamer should depend on two criteria's: the ability of the surfactant to unload liquid and the pressure drop due to foaming. Increasing concentration might have a positive effect on liquid unloading but can cause increase in pressure drop in the flow loop setup after a certain concentration. Hence it is observed in the flow loop setup [39] that there exists an optimal concentration at which both the liquid unloading and pressure drop are within acceptable range. This optimal concentration cannot be directly predicted using the small scale sparger setup as the setup is not appropriate for predicting pressure drop. However, it could be possible to set a surfactant concentration cut-off criterion such that the concentration we select using the small scale test is close to the optimal concentration in the flow loop setup. However, this would require significant data from both the small scale and flow loop setup in order to set such a criterion.

The second reason states that in the small scale setup used by [2] for SDS (Sodium dodecyl sulfate), the water content (foam density) of the foam increases with increasing concentration for low concentration and decreases with increasing concentration for higher concentration as shown in Figure 55. It is also mentioned that such non-monotonous behaviour is not observed in the flow loop experiments [39]. However it should be noted that the maximum concentration of SDS used in the flow loop setup [39] is 790 ppm (or 2.74 mM/L) and that the decrease in foam

density on increasing the concentration is observed for much higher concentration (~1500 ppm) for the small scale setup as shown in Figure 55. Hence the reasoning that a non-monotonous behaviour in observed in the small scale but not the flow loop setup is probably not definitive unless the range of concentration are similar for the two tests.

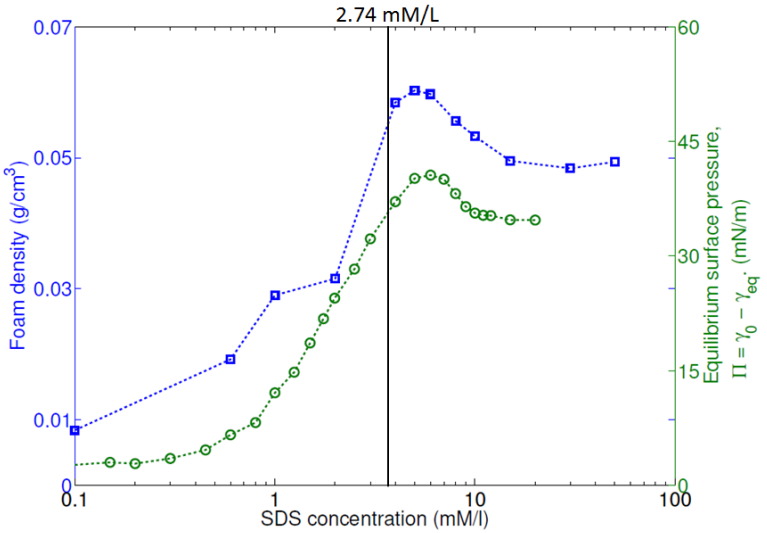

Figure 55: Variation of foam density (in blue) with respect to surfactant (SDS) concentration for small scale sparger setup used by [2]. The vertical black line shows the maximum concentration of SDS for which test was conducted in the flow loop setup as reported in [39] (reproduced from [2]).

To summarize the comparison between the small scale sparger test and the flow loop test, we postulate that the amount of liquid carryover might represent the characteristics of the unloading behaviour in the flow loop setup but the small scale sparger setup does not show promise in context of pressure drop prediction. We also considered and analysed the reasoning given in [39] as to why the sparger setup is not a good predictor of the foaming behaviour in the flow loop setup. We find that the reasons given in [39] partly suggest that the sparger setup cannot be used for pressure drop predictions. However, the sparger setup can represent the ability of the surfactant to unload liquid and additional work is required to understand how to select an optimal concentration from the small scale test.

Chapter 5 Conclusions and Recommendations

5.1 Conclusions

The motivation of the present work was towards standardizing surfactant evaluation in small scale sparger setup by understanding the effect of certain parameters like gas velocity, surfactant concentration and pressure. The study brings new insights on the foam behaviour in a small scale sparger setup. The effect of varying the surfactant concentration has been studied by a number of authors in the past. The present research makes an important step in understanding the effect of three parameters: surfactant concentration, gas velocity and pressure in a small scale sparger setup. We finally use the insights to make recommendations for better evaluation of foamers for gas well deliquification.

The amount of foam formed per unit time (or build-up rate) is found to scale with the gas velocity. Unless the foamer concentration is low, the amount of foam has a strong dependence on the gas velocity and a weak dependence on the surfactant concentration (as observed in build-up test results). However, there seems to be a deviation at higher velocities because of the bubble-slug flow regime transition. The visualization with the high speed camera indicates that the N_2-water system shows the slug flow regime at higher velocities. Foam formation for surfactant solutions at high velocities is partly due to the intermixing between the gas and the slugs; this foam exhibits a churning type motion.

The collapse tests for one of the surfactants (Foamatron) suggest that increasing the concentration increases the stability of the foam because of two reasons. Firstly the reduction of the surface tension with increasing concentration makes the film more stable. Secondly the decrease in bubble size with increasing concentration reduces the drainage rate and hence it improves the foam stability. However the experiments with the second surfactant (Trifoam Block 820) suggest that the stability comparison between two surfactants on basis of the surface tension yields contrary results. Even though the surface tension and drainage rate for Trifoam Block 820 are higher than that of Foamatron, Trifoam Block 820 shows a better stability. We postulate that the difference in stability is due to a possible difference in the critical liquid fraction (at which bubbles break) of the two surfactants.

The pressure and temperature inside the gas wells are relatively high; in the present study we investigate the effect of pressure on the foam behaviour. The build-up rate and the carryover results do not seem to be affected by the pressure variation. This should in principle suggest that

the ability of the surfactant to unload liquid is not directly affected by pressure variations. However the collapse rates suggest that the foam stability increases with increasing pressure due to the decrease in the diffusion coefficient of the gas. The lower diffusion coefficient reduces the coarsening rate of the foam leading to a lower average bubble size with respect to time. This decreases the drainage rate and improves the foam stability. Hence a foam deliquification process that is effective at atmospheric pressure, as suggested by the results, should also be effective for higher pressures.

Finally we attempted to understand whether the sparger test setup is useful in qualitative selection of foamers for field operations. We found that the carryover test can represent the ability of the surfactant to unload liquid similar to the trends for the flow loop setup. To represent the flow hydrodynamics closely, it would be beneficial to conduct the test at a relatively higher velocity (slug flow regime) where the foam behaviour is similar to that in the flow loop setup. However at higher velocities and for high concentrations the amount of carryover reaches the maximum possible value and hence it should be made sure that the interpretation of the test results is not affected by the limit set to the maximum carryover. Moreover, we find that the sparger test might not be an appropriate test for predicting pressure drop which is important in selecting foamers (and foamer concentrations) to be used for field operations.

5.2 Recommendations

One of the important conclusions is the difference in stability of surfactants based on the critical liquid fraction. To understand this better, it is required to conduct a systematic study of different surfactants to identify the difference in critical liquid fraction using either a conductivity measurement or any other suitable technique. The mechanisms behind the existence of a critical liquid fraction as mentioned in the literature are the T1, T2 events that occur during foam collapse. Hence a detailed study of the mechanisms would help to obtain a better understanding of how one surfactant is more stable than the other, even when the dynamic surface tension does not suggest so.

The effect of physical parameters such as the foam column height and the sparger size could affect the test results significantly. A study of the effect of these physical parameters on foam behaviour would help in standardizing the test equipment. Moreover, the height of the foam column can have an effect on the concentrations at which the maximum carryover can be achieved. If increasing the height of the column can increase the concentration at which the

maximum carryover is achieved, we might be able to conduct tests in the slug flow regime in the small scale setup (more representative of large scale) without the limit of carryover affecting the test results.

The amount of foam that is formed in the small scale setup scales directly with the velocity as most of the gas is encapsulated in the foam for the bubble flow regime. However we still do not know the exact mechanism of entrainment of gas into liquid at higher gas velocities (churn flow and annular flow). The quantification of the entrainment in such regimes can be helpful in comparing and scaling the foam generated in the small scale setup to the foam generated in the flow loop setup.

Acknowledgement

I would like to express my special appreciation and thanks to my TNO supervisor Ir. Pejman Shoeibi Omrani for his consistent support throughout the project. You have been a tremendously good mentor for me. I would also like to thank my University supervisor Prof. dr. ir. R.A.W.M. Henkes for finding time for progress meetings and for guiding me whenever required. Special thanks are due to dr. ir. Dries van Nimwegen for being involved in the project: your expertise and experience in the subject was a great help.

The dynamic surface tension measurements conducted at TNO in Eindhoven would not have been possible without the support of dr. Marielle Wouters and dr. Daniel Turkenburg. Thanks to them the measurements went smooth and easy. The high speed camera visualization gave us significant insights and I would like to thank Ir. Andries van Wijhe for helping with setting up the camera. I would also like to thank the project group at TNO: dr. ir. Jos van't Westende, ir. Erik Nennie and ir. Ram Shukla and the support staff at TNO in the Leeghwaterstraat in Delft. Special thanks are due to my family. Words cannot express how grateful I am to my mother and father for all of the sacrifices that you have made for me. I would also like to thank all of my friends Bart, Rohith, Vaidas and Hassam who supported me during the project at TNO.

Bibliography

[1] J. F. Lea, H. Nickens and M. Wells, Gas well deliquification, Gulf Professional Publishing, 2008.

[2] D. Kawale, "Influence of dynamic surface tension on foams: Application in gas well deliquification," MSc thesis, Delft University of Technology, 2012.

[3] D. Weaire and S. Hutzler, The Physics of Foams, Oxford University Press, 2001.

[4] K. Lunkenheimer, G. Czichocki, R. Hirte and W. Barzyk, "Novel results on the adsorption of ionic surfactants at the air/water interface–sodium-n-alkyl sulphates," *Colloids and Surfaces A: Physicochemical and Engineering Aspects,* vol. 101, no. 2-3, p. 187–197, 1995.

[5] R. J. Pugh, "Foaming, foam films, antifoaming and defoaming," *Advances in Colloid and Interface Science,* Vols. 67-142, p. 64, 1996.

[6] J. Gibbs, "Scientific Papers of J. Willard Gibbs," *Thermodynamics,* vol. 1, 1906.

[7] M. J. Rosen and X. Y. Hua, "Dynamic surface tension of aqueous surfactant solutions. 1. basic parameters," *Journal of Colloid and Interface Science,* vol. 124, no. 2, pp. 652-658, 1988.

[8] M. J. Rosen and T. Gao, "Dynamic surface tension of aqueous surfactant solutions. 5. mixtures of different charge type surfactants," *Journal of Colloid and Interface Science,* vol. 173, no. 1, pp. 42-48, 1995.

[9] M. J. Rosen and L. D. Song, "Dynamic surface tension of aqueous surfactant solutions. 8. effect of spacer on dynamic properties of gemini surfactant solutions," *Journal of Colloid and Interface Science,* vol. 179, no. 1, pp. 261-268, 1996.

[10] M. J. Rosen and Y. H. Xi, "Dynamic surface tension of aqueous surfactant solutions. 2. parameters at 1-s and at mesoequilibrium.," *Journal of Colloid and Interface Science,* vol. 139, no. 2, pp. 397-407, 1990.

[11] M. J. Rosen and Y. H. Xi, "Dynamic surface tension of aqueous surfactant solutions. 3. some effects of molecular-structure and environment.," *Journal of Colloid and Interface Science,* vol. 141, no. 1, pp. 180-190, 1991.

[12] M. Rosen, X. Hua and Z. Zhu, "Dynamic surface tension of aqueous surfactant solutions: Iv relationship to foaming," *Surfactants in solution,* vol. 11, pp. 315-327, 1991.

[13] M. J. Rosen and T. Gao, "Dynamic surface tension of aqueous surfactant solutions. . compounds

containing 2 hydrophilic head groups and 2 or 3 hydrophobic groups and their mixture with other surfactants," *Journal of the American Oil Chemists Society,* vol. 71, no. 7, pp. 771-776, 1994.

[14] M. J. Rosen and T. Gao, "Dynamic surface tension of aqueous surfactant solutions. 7. physical significance of dynamic parameters and the induction period," *Journal of Colloid and Interface Science,* vol. 172, no. 1, pp. 242-248, 1995.

[15] D. T. Nguyen, "Fundamental surfactant properties of foamers for increasing gas production," *Petroleum Science and Technology,* vol. 27, no. 7, pp. 733-745, 2009.

[16] T. Tamura, Y. Kaneko and M. Ohyama, "Dynamic surface tension and foaming properties of aqueous polyoxyethylene n-dodecyl ether solutions," *Journal of Colloid and Interface Science,* vol. 173, no. 2, pp. 493-499, 1995.

[17] P. Stevenson, Foam Enginnering: Fundamentals and Applications, John Wliey and Sons, 2012.

[18] J. Plateau, Statique Experimentale et theorique des Liquides soumis aux seules Forces Moleculaires, Paris: Gauthier-Villars, 1873.

[19] M. Durand and D. Langevin, "Physicochemical approach to the theory of foam drainage," *The European physical Journal E,* vol. 7, pp. 35-44, 2002.

[20] R. Leonard and R. Lemlich, "A study of interstitial liquid flow in foam, part 1," *AIChE Journal,* vol. 11, pp. 18-24, 1965.

[21] A. Kraynik, Foam Drainage, Sandia Report SAND, 1983.

[22] D. Weaire, S. Hutzler, G. Verbist and E. Peters, "A Review of Foam Drainage," *Adv. Chem. Phys.,* vol. 102, pp. 315-374, 1997.

[23] S. A. Koehler, S. Hilgenfeldt and H. A. Stone, "A Generalized View of Foam Drainage: Experiment and Theory," *Langmuir,* vol. 16, pp. 6327-6341, 2000.

[24] P. Rand and A. Kraynik, "Drainage of Aqueous Foams: Generation-Pressure and Cell-Size Effects," *SPEJ,* pp. 152-154, 1983.

[25] D. S. R. Sarma and K. C. Khilar, "Effects of initial gas volume fraction on stability of aqueous air foams," *Ind. Eng. Chem. Res.,* vol. 27, no. 5, pp. 892-894, 1990.

[26] J. v. Neumann, "Discussion - shape of metal grains," *Metal InterfacesASM,* pp. 108-110, 1952.

[27] R. M. Pherson and D. Srolovitz, "An exact generalization to higher dimensions of von Neumann's theory of two-dimensional grain growth," *Nature,* vol. 446, pp. 1053-1055, 2007.

[28] J. Lambert, R. Mokso, I. Cantat, P. Cloetens, J. Glazier, F. Graner and R. Delannay, "Coarsening foams robustly reach a self similar growth regime," *Phys. Rev. Lett. ,* vol. 104, 2010.

[29] J. Lambert, I. Cantat, R. Delannay, R. Mokso, P. Cloetens, J. Glazier and F. Graner, "Experimental growth law for bubbles in a moderately "wet" 3D liquid foam," *Phys. Rev. Lett.,* vol. 99, 2007.

[30] D. Durian, D. Weitz and D. Pine, "Scaling behaviour in shaving cream," *Phys. Rev. A,* vol. 44, pp. R7902-5, 1991.

[31] S. Magrabi, B. Dlugogorski and G. Jameson, "Bubble size distribution and coarsening of aqueous foams," *Chemical Engineering Science,* vol. 54, no. 16, pp. 4007-4022, 1999.

[32] A. Saint-Jalmes, M. Peugeot, H. Ferraz and D. Langevin, " Differences between protein and surfactant foams: Microscopic properties, stability and coarsening," *Colloids and Surfaces A,* vol. 263, pp. 219-225, 2005.

[33] V. Carrier and A. Colin, "Coalescence in draining foams," *Langmuir,* vol. 19, no. 11, pp. 4535-4538, 2003.

[34] A.-L. Biance, A. Delbos and O. Pitois, "How Topological Rearrangements and Liquid Fraction Control Liquid Foam Stability," *Physical Review Letters,* vol. 106, pp. 068301-4, 2011.

[35] S. Saleh and M. Al-Jamae'y, "Foam-assisted liquid lifting in low pressure gas wells," in *SPE Production Operations Symposium*, 1997.

[36] T. Duangprasert, A. Sirivat, K. Siemanond and J. O.Wilkes, "Vertical two-phase flow regimes and pressure gradients under the influence of sds surfactant," *Experimental Thermal and Fluid Science,* vol. 32, pp. 808-817, 2008.

[37] T. Sawai, M. Kaji and T. Urago, "Effect of surfactant additives on pressure drop reduction in vertical upward two-phase flow," in *5th International Conference on*, Yokohama,Japan, 2004.

[38] R. Rozenblit, M. Gurevich, Y. Lengel and G. Hetsroni, "Flow patterns and heat transfer in vertical upward air-water flow with surfactant," *International Journal of Multiphase Flow,* vol. 32, no. 8, pp. 889-901, 2006.

[39] D. v. Nimwegen, "The Effect of Surfactants on Gas-Liquid Pipe Flows," PhD thesis, Delft University of Technology, 2015.

[40] T. Engels, W. v. Rybinski and P. Schmiedel, "Structure and dynamics of surfactant based foams," *Progress in Colloid and Polymer Science,* vol. 111, pp. 117-126, 1998.

[41] R. Varadaraj, J. Bock, P. V. Jr., S. Zushma and N. Brons, "Relationship between fundamental

interfacial properties and foaming in linear and branched sulphate, ethoxysulphate and ethoxylate surfactants," *Journal of Colloid and Interface Science,* vol. 140, no. 1, pp. 31-34, 1990.

[42] N. Kantarcia, F. Borakb and K. O. Ulgena, "Review: Bubble column reactors," *Process Biochemistry,* vol. 40, pp. 2263-2283, 2005.

[43] D. WD, L. Y, Z. A and R. M, "Hydrodynamic properties of the Fisher-Tropsch slurry process," *Industrial and Engineering Chemistry Process Design and Development,* vol. 19, pp. 699-708, 1980.

[44] A. Shaikh and M. H. Al-Dahhan, "A Review on Flow Regime Transition in," *International Journal of Chemical Reactor Engineering,* vol. 5, 2007.

[45] R. Krishna, P. M. Wilkinson and L. L. Van Dierendonck, "A model for gas holdup in bubble columns incorporating the influence of gas density on flow regime transitions," *Chemical Engineering Science,* vol. 46, no. 10, pp. 2491-2496, 1991.

[46] P. M. Wilkinson, A. P. Spek and L. L. Van Dierendonck, "Design parameters estimation for scale-up of high-pressure bubble columns," *AIChE Journal,* vol. 38, no. 4, pp. 544-554, 1992.

[47] I. G. Reilly, D. S. Scott, T. J. W. De Bruijn and D. MacIntyre, "The role of gas phase momentum in determining gas holdup and hydrodynamic flow regimes in bubble column operations," *Canadian Journal of Chemical Engineering,* vol. 72, no. 1, pp. 3-12, 1994.

[48] T.-J. Lin, K. Tsuchiya and L.-S. Fan, "On the measurements of regime transition in high-pressure bubble columns," *Canadian Journal of Chemical Engineering,* vol. 77, no. 2, pp. 370-374, 1999.

[49] A. Shaikh and M. Al-Dahhan, "Characterization of the hydrodynamic flow regime in bubble columns via computed tomography," *Flow Measurement and Instrumentation,* vol. 16, no. 2-3, pp. 91-98, 2005.

[50] D. B. Bukur, D. Petrovic and J. G. Daly, "Flow regime transitions in a bubble column with a paraffin wax as the liquid medium," *Industrial & Engineering Chemistry Research,* vol. 26, no. 6, pp. 1087-1092, 1987.

[51] P. Wilkinson, "Physical Aspects and Scale-up of High Pressure Bubble Columns," Ph.D. Thesis, University of Groningen, 1991.

[52] M. C. Ruzicka, J. Drahos, P. C. Mena and J. A. Teixeira, "Effect of viscosity on homogeneous-heterogeneous flow regime transition in bubble columns," *Chemical Engineering Journal,* vol. 96, no. 1-3, pp. 15-22, 2003.

[53] M. Urseanu, "Scaling up bubble column reactors," Ph.D. Thesis, University of Amsterdam, 2000.

[54] A. Sarrafi, M. Jamialahmadi, H. Muller-Steinhagen and J. M. Smith, "Gas holdup in homogeneous and heterogeneous gas-liquid bubble column reactors," *Canadian Journal of Chemical Engineering,* vol. 77, no. 1, pp. 11-21, 1999.

[55] M. Jamialahmadi, H. Muller-Steinhagen, A. Sarrafi and J. M. Smith, "Studies of gas holdup in bubble column reactors," *Chemical Engineering & Technology,* vol. 23, no. 10, pp. 919-921, 2000.

[56] M. C. Ruzicka, J. Drahos, M. Fialova and N. H. Thomas, "Effect of bubble column dimensions on flow regime transition," *Chemical Engineering Science,* vol. 56, no. 21-22, pp. 6117-6124, 2001.

[57] E. Cussler, Diffusion Mass Transfer in Fluid Systems (2nd edition), New York: Cambridge University Press, 1997.

[58] S. Neethling, H. Lee and J. Cilliers, "A foam drainage equation generalized for all liquid contents," *Journal of Physics: Condensed Matter,* vol. 14, pp. 331-342, 2002.

Appendix A: Drainage model

The drainage of the liquid through foam is an important criterion that affects the stability of foams. A number of parameters affect the drainage of liquid through the foam and it is important to understand the degree of influence of these parameters to interpret the results. [58] gives the drainage equation that considers pressure losses through both the plateau border and the vertices. The pressure drop due to viscous losses in a single plateau border was described as follows:

$$\Delta P_{PB} = \frac{C_{PB}\upsilon_P \mu (L - k_1 r)}{r^2}$$

where υ_P is the average velocity of liquid through the Plateau border, k_1 is the constant relating size of vertex to radius of curvature, L is the length of the plateau border, μ is the liquid viscosity and C_{PB} is the plateau border loss ('drag') coefficient.

The pressure drop in a vertex is approximated by the following:

$$\Delta P_V = \frac{C_V \upsilon_P \mu}{r}$$

where C_V is the vertex loss ('drag') coefficient.

The total pressure loss is estimated using the addition of the two pressure drops, this pressure drop in the flowing liquid can then be equated to the hydrostatic and capillary pressure to obtain the following drainage equation.

$$\frac{\partial \varepsilon}{\partial t} - \nabla\left(\frac{\varepsilon \rho g}{k(r,\varepsilon,r_b)\mu}\right) - \nabla\left(\frac{\varepsilon \nabla(\rho g \int_y^{h_f} \varepsilon dy - \frac{\gamma}{r})}{k(r,\varepsilon,r_b)\mu}\right) = 0$$

where ε is the liquid volume fraction in the foam, ρ is the density of liquid, g is acceleration due to gravity, r_b is the effective radius of gas (radius of bubble – thickness of liquid film), γ is the surface tension, h_f is the total height of foam and k is given by the following relation:

$$k(r,\varepsilon,r_b) = \left(\frac{3C_{PB}}{r^2} + \frac{4.178(C_V - 0.418C_{PB})}{r r_b}(1-\varepsilon)^{1/3} + \frac{6.806(C_V - 1.588C_{PB})}{r_b^2}(1-\varepsilon)^{2/3}\right)$$

The use of the drainage model in the present thesis is only meant to understand the effect of the bubble radius on the foam drainage. We therefore do not validate the model to fit the equation to the surfactant we use but rather use the same coefficient as given in [58]. We numerically solved the drainage equation using MATLAB v2014b and radius of bubbles at liquid volume fraction 0.15. The liquid volume fraction distribution contours are shown in the figure below.

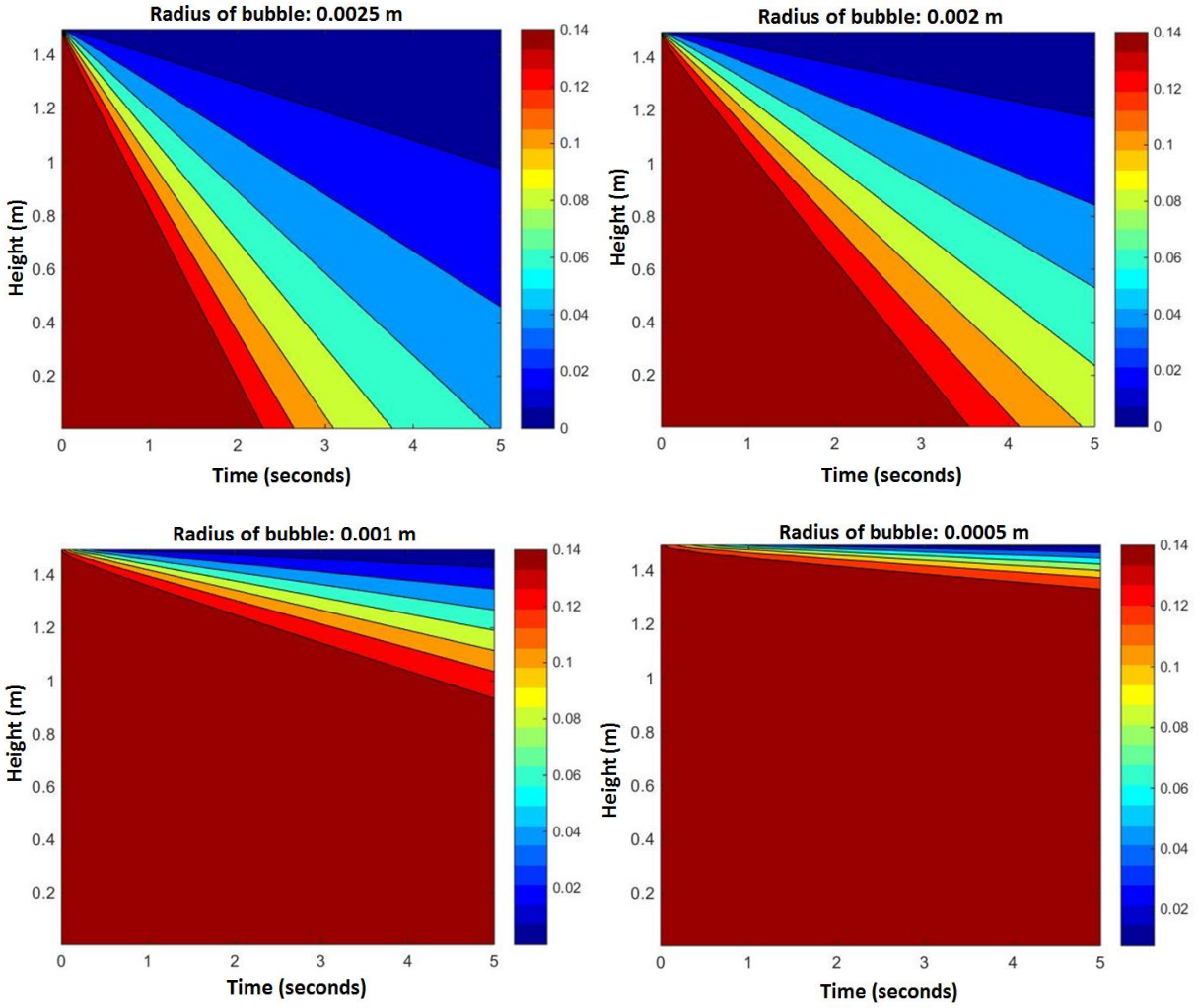

The total height of the foam is 1.4 m; the y-axis represents the height along the foam where bottom of foam is 0 m and the top of foam is 1.4 m and the x-axis is the time in seconds. The radius of the bubble at which the numerical calculation is carried out is givem on top of each contour. The contours clearly show the effect of the bubble radius on the drainage in foams: decreasing the bubble radius from 2.5 mm to 0.5 mm decreases the drainage rate by almost 20 times.